Aus dem Institut für Pharmakologie
der Medizinischen Fakultät Charité – Universitätsmedizin Berlin

DISSERTATION

Influence of Adipose tissue-specific Adipose Triglyceride Lipase on the Development of Heart Failure

zur Erlangung des akademischen Grades
Doctor medicinae (Dr. med.)

vorgelegt der Medizinischen Fakultät
Charité – Universitätsmedizin Berlin

von
Janek Salatzki
aus Bad-Saarow

Datum der Promotion: 02.03.2018

Table of contents

List of figures

List of tables

Abbreviations

A-Fabp	adipocytes-type Fatty Acid-binding Protein
ACC	acetyl-CoA-carboxylase
acetyl-CoA	acetyl-coenzym A
Adipoq-AAKO	adipoq-promoter adipocyte-specific ATGL-KO mouse
AMPK	AMP-activated protein kinase
ANF	atrial natriurec factor
ANOVA	analysis of variance
aP2	adipose Protein 2
apo-B…	apolipoprotein-B
Asp	aspartic acid
atATGL-KO	adipose tissue-specific ATGL-KO
ATGL	adipose triglyceride lipase
ATP	adenosie triphosphate
AUC	area under the Curve
BAT	brown adipose tissue
BEL	Belgium
BNP	brain natriuretic peptide
bp	base pairs
BP	blood pressure
BW	body weight
Ca^{2+}	calcium
CAD	coronary artery disease
cAMP	cyclic adenosine monophosphate
CAN	Canada
CGI-58	comparative gene identification-58
cGMP	cyclic guanosine monophosphate
CHE	Switzerland
CNP	c-type natriuretic peptide
CO	cardiac output
CO_2	carbon dioxide
CPT-1	carnitine palmitoyltransferase I
CTGF	connective tissue growth factor
DAG	diacylglycerol
DHF	diastolic heart failure
DNA	deoxyribonucleic acid
EAT	epididymal adipose tissue
ECM	excessive extracellular matrix
EDV	end-diastolic volume
EE	energy expenditure
EF%	ejection fraction
ESC	european society of cardiology
FA	fatty acids
FABP	plasma membrane fatty acid binding protein
FABP4	fatty acid binding protein 4
FACS	fatty-acyl-CoA-synthase
$FADH_2$	flavin adenine dinucleotide
FAO	free fatty acid oxidation
Fat	fat mass
FAT/CD36	fatty acid translocase

FATP	fatty acids transport protein
FFA	free fatty acids
FGFs	fibroblast growth factors
FIN	Finland
FoxO	forkhead box protein O
FPG	fasting plasma glucose
FS%	fractional shortening
FSP27	fat-specific Protein 27
G0S2	G_0/G_1 switch gene 2
GBR	Great Britain
gDNA	genomic DNA
GER	Germany
GFR	glomerular filtration rate
GLUT	glucose transporter
GPIHBP1	glycosyl-phosphatidylinositol-anchored high-density lipoprotein-binding protein 1
GTT	glucose tolerance test
HDL	high-density lipoprotein cholesterol
HE	hematoxylin-eosin
HF	heart failure
HFD	high-fat diet
HFpEF	heart failure with preserved ejection fraction
HFrEF	heart failure with reduced ejection fraction
HPLC	high-performance liquid chromatography
HSL	hormone-sensible lipase
HW	heart weight
IDF	international diabetes federation
IL-…	Interleukin
ip	intraperitoneal
ISV	interventricular septum thickness
ITT	insulin tolerance test
kD	kilo Dalton
KO	knock-out
LC	liquid chromatography
LPL	lipoprotein lipase
LV	left ventricle
LVH	left ventriular hypertrophy
LVID, diastole	end-diastolic left ventricular internal diameter
LVID, systole	end-systolic left ventricular internal diameter
LVM	left ventricular mass
LVPW	left ventricular posterior wall
LVvol, diastole	end-diastolic left ventricular volume
LVvol, systole	end-systolic left ventricular volume
MAC…	macrophage-specific marker
MAG	monoacylglycerol
MAP	mean arterial pressure
MGL	monoacylglycerol lipase
MI	myocardial infarction
mmHg	millimeter of mercury
MMPs	matrix metalloproteases

MS	mass spectrometer
mTORC1	mammalian target of rapamycin complex 1
NaCl	sodium chloride
NADH	nicotinamide adenine dinucleotide
NED	Nederlands
NF-kappaB	nuclear factor-kappaB
NLSD	neutral lipid storage disease
NMR	nuclear magnetic resonance
NPR-…	natriuretic peptide receptor
NYHA	New York Heart Association (NYHA) Functional Classification
O_2	oxygen
Pa	pascal
PAT	perirenal adipose tissue
PBS	phosphate buffered saline
PCR	polymerase chain reaction
PDGFs	platelet-derived growth factors
PDH	pyruvate dehydrogenase
PKA	protein kinase A
PKG	protein kinase G
PLs	phospholipids
PNPLA2	patatin-like phospholipase domain containing 2
PPAR-…	peroxisome proliferator-activated receptor…
qRT-PCR	quantitative real-time PCR
rpm	revolutions per minute
RQ	respiratory quotient
RT	room temperature
sc	subcutaneous
SEM	standard error of the mean
Ser	serine residues
SHF	systolic heart failure
SNS	sympathetic nervous system
SV	stroke volume
TAC	transverse aortic constriction
TAE	tris-acetate-EDTA
TAG	triacylglycerol
TGF-β	transforming growth factor beta
TL	tibia length
TNF-α	transforming growth factor alpha
UCP1	uncoupling protein 1
v	velocity
VLDL	very-low-density lipoproteins
vol	volume
WAT	white adipose tissue
WT	wild type
β-MyHC	β-Myosin Heavy Chain
Δp	pressure difference
ρ	density

Abstract in English

Influence of Adipose tissue-specific Adipose Triglyceride Lipase on the Development of Heart Failure

Introduction

Cardiac metabolism undergoes changes in response to pathological left ventricular hypertrophy (LVH) and heart failure (HF), characterized by increased reliance on glycolysis, decreased fatty acid (FA) oxidation and a loss of metabolic flexibility. In addition to the heart, non-cardiac organs are involved in these metabolic changes. In this context, the influence of white adipose tissue (WAT) and its release of FA on the development of LVH and HF are not well investigated. The aim of this study was to investigate the effect of Adipose Triglyceride Lipase (ATGL) in WAT on the development of LVH and HF in a pressure overload-induced cardiac hypertrophy model in mice.

Methods

Male adipose tissue-specific ATGL knock-out (atATGL-KO) and wild-type mice (WT) underwent transverse aortic constriction (TAC-surgery) or sham-surgery. Echocardiography 1 week before, 5 and 11 weeks after Sham/TAC-surgery were performed to evaluate wall thickness, left ventricular mass (LVM) and cardiac function.

In addition, histological and gene expression analysis of hearts were performed. Insulin sensitivity, body composition, glucose tolerance and FA serum levels were measured to investigate metabolic changes.

Results

TAC-surgery caused a significant increase in LVM compared to Sham-surgery in atATGL-KO and WT mice 5 weeks post-surgery. However, there were no significant differences in LVM between atATGL-KO and WT mice.

11 weeks after TAC-surgery, LVM in WT was significantly larger compared to atATGL-KO (LVM [mg] WT-TAC: 211.16±19.73; atATGL-KO-TAC: 124.32±9.06; $p<0.0001$). Also, LVM to tibia length ratio (LVM/TL) and LVM to body weight ratio (LVM/BW) confirmed this result. The larger LVM in WT mice was associated with a larger left ventricular chamber diameter and reduced cardiac function compared to atATGL-KO after TAC-surgery (EF [%] WT-TAC: 23.84±1.78 atATGL-KO-TAC: 40.72±1.34; $p<0.0001$). Histological analysis confirmed a larger cardiac cross-section and slightly more cardiac fibrosis in WT mice compared to atATGL-KO after TAC-surgery. Markers for cardiac hypertrophy were elevated in both genotypes.

Metabolic tests revealed that atATGL-KO mice after TAC-surgery had an improved glucose tolerance and insulin sensitivity, and significant lower serum levels of specific FFA.

Conclusion

The present study demonstrates that atATGL is a crucial determinant for the development of pressure overload-induced HF. The lack of ATGL in WAT, the associated reduction of FA release may lead to subsequent switches in cardiac energy substrates from FA to glucose. In addition, the reduced FFA serum levels might be directly linked to the improvement of LV-function.

Zusammenfassung auf Deutsch

Einfluss der fettgewebsspezifischen Adipozyten Triglycerid Lipase auf die Entwicklung der Herzinsuffizienz

Einleitung
Der kardiale Metabolismus ändert sich während der Entwicklung einer linksventrikulären Hypertrophie (LVH) und einer Herzinsuffizienz (HF), welche gekennzeichnet ist durch eine erhöhte Abhängigkeit von Glykolyse, einer erniedrigten Oxidation von Fettsäuren (FA) und einem Verlust der metabolischen Flexibilität. Neben dem Herzen sind auch nicht-kardiale Organe von diesen metabolischen Veränderungen betroffen. In diesem Zusammenhang ist der Einfluss von weißen Fettgewebe (WAT) und seiner Freisetzung von FA auf die Entwicklung der LVH und HF wenig untersucht. Das Ziel dieser Studie war es, den Effekt von Adipozyten Triglycerid Lipase (ATGL) im WAT auf die Entwicklung einer LVH und HF in einem Model der druckinduzierenten kardialen Hypertrophie in der Maus zu untersuchen.

Methoden
Männliche fettgewebsspezifische ATGL knock-out (atATGL-KO) und Wildtyp Mäuse (WT) wurden einer transversen Aortenkonstriktion (TAC-OP) oder Scheinoperation (Sham-OP) unterzogen. 1 Woche vor, 5 und 11 Wochen nach der Sham/TAC-OP wurde die linksventrikuläre Masse (LVM) und die kardiale Funktion echokardiographisch untersucht.
Zusätzlich wurden histologische und Genexpressions-Analysen der Herzen durchgeführt. Die Insulinsensitivität, Glukosetoleranz, Körperzusammensetzung und FA-Serumspiegel wurden gemessen, um metabolische Veränderungen zu untersuchen.

Ergebnisse
Die TAC-OP resultierte in einer signifikanten Zunahme der LVM im Vergleich zur Sham-OP bei atATGL-KO und WT Mäusen 5 Wochen nach OP. Es lagen jedoch keine signifikanten Unterschiede in der LVM zwischen atATGL-KO und WT Mäusen vor.
11 Wochen nach TAC-OP, LVM in WT war signifikant größer im Vergleich zu atATGL-KO (LVM [mg] WT-TAC: 211,16±19,73; atATGL-KO-TAC: 124,32±9,06; $p<0,0001$). Dieses Ergebniss konnte auch mit dem Verhältnis von LVM zur Tibialänge (LVM/TL) und Körpergewicht (LVM/BW) bestätigt werden. Die größere LVM in WT Mäusen war assoziert mit einem größeren linksventrikulären Kammerdurchmesser und einer reduzierten kardialen Funkion im Vergleich zu atATGL-KO nach TAC-OP (EF [%] WT-TAC: 23,84±1,78 atATGL-KO-TAC: 40,72±1,34; $p<0,0001$). Histologische Untersuchugen konnten einen größeren kardialen Durchmesser bestätigen und zeigten geringfügig mehr kardiale Fibrose in WT Mäusen im Vergleich zu atATGL-KO nach TAC-OP. Marker für kardiale Hypertrophy waren in beiden Genotypen erhöht.
Metabolische Untersuchungen zeigten, dass atATGL-KO Mäuse nach TAC-OP eine verbesserte Glukosetoleranz und Insulinsensitivität entwickelten, sowie signifikant geringere Serumspiegel von spezifischen FA auswiesen.

Zusammenfassung
Die vorliegende Studie zeigt, dass atATGL ein wichtiger Faktor für die Entwicklung der druckinduzierten HF ist. Das Fehlen von ATGL im WAT und die damit assoziierte Reduktion der FA Freisetzung könnte zu einem Wechsel der kardialen Energiesubstratverwertung von FFA zu Glukose führen. Weiterhin könnte die Reduktion der FFA-Serumspiegel direkt mit der Verbesserung der LV-Funktion in Verbindung stehen.

1 Introduction

1.1 Adipose Tissue

Adipose tissue can be subdivided into White Adipose Tissue (WAT), Brown Adipose Tissue (BAT) (myofibroblasts Cinti, 2011) and newly identified Brite/Beige Adipose Tissue (Ishibashi and Seale, 2010; Petrovic et al., 2010), all described to have different functions. WAT can be characterized by its location in visceral WAT and subcutaneous WAT. The important features of WAT and BAT are described below.

1.1.1 White Adipose Tissue

The primary purpose of WAT is to store fatty acids (FA) and release them in times of prolonged fasting and when glucose is limited (Rosen and Spiegelman, 2006). Morphologically, white adipocytes are filled with unilocular cytoplasmic lipid droplets, which squeeze the nucleus. An increase or decrease of adipose tissue mass is mainly due to a change in size (hypertrophy) of the adipocytes and not a change in the number of adipocytes (Lüllmann-Rauch and Paulsen, 2012). Adipose tissue can be divided into visceral or central WAT, which is located around mesenteric vessels in the abdomen, and subcutaneous WAT, which is found in abdominal, gluteal and femoral depots (White and Tchoukalova, 2014). There is also a functional difference between visceral and subcutaneous WAT.

Increased central WAT depot is associated with a greater risk of cardiovascular diseases and metabolic disorders, such as dyslipidemia and type 2 diabetes mellitus, compared to subcutaneous WAT (Fox et al., 2007). Furthermore, peripheral subcutaneous WAT is related with improved insulin sensitivity and lower risk of type 2 diabetes mellitus and atherosclerosis (Misra et al., 1997; Snijder et al., 2003; Tanko et al., 2003). Subcutaneous adipose tissue distribution is more common in women, while central distribution is more common in men (Lafontan and Langin, 2009). In rodents, subcutaneous WAT is located cervical, interscapular, subscapular, axilla-thoracic, inguinal and gluteal. In contrast, central WAT is found in the mediastinum, around mesenteric arteries and organs in the abdomen and perirenal (Cinti, 2011). Also, pro-inflammatory cytokines seem to be more secreted into the blood circulation from central WAT compared to subcutaneous WAT (Bluher, 2008). Importantly, central WAT has a larger supply of nerves and vessels and shows a higher density of lipolytic β2-adrenergic and a reduced density of anti-lipolytic α2-adrenergic receptors than subcutaneous WAT (Lafontan and Langin, 2009; Mauriege et al., 1999).

1.1.2 Brown Adipose Tissue

BAT is regulated by the sympathetic nervous system and is mainly used to regulate body temperature when the body is exposed to coldness (Contreras et al., 2015; Himms-Hagen, 1986). Morphologically, brown adipocytes consist of multilocular cytoplasmic lipid droplets instead of unilocular lipid droplets like in WAT. The rich vascularity and the numerous mitochondria are the reason for the brown color of BAT. The mitochondria are more spherical than in other cell types and contain more laminar cristae, which increase the surface area resulting in faster FA β-oxidation using uncoupling protein (UCP1) (Rial and Gonzalez-Barroso, 2001). UCP1 uncouples oxidative phosphorylation, resulting in protons to flow across the inner mitochondrial membrane without being used for adenosine triphosphate (ATP) synthesis, but instead for heat production (Cinti et al., 1989). In human infants, BAT is mainly located around the heart, aorta and great vessels (Smorlesi et al., 2012). Importantly, BAT mass is markedly reduced in adults. However, rodents have distinct BAT pads interscapular (Rosen and Spiegelman, 2006). Cold exposure and physical exercise in mice can result in a transformation of WAT into BAT, so-called browning (Nedergaard et al., 2007). In addition, Adipose Triglyceride Lipase (ATGL) seems to be crucial for the thermogenesis in BAT, as adipose tissue-specific ATGL knock-out (KO) in mice results in a conversion of BAT into WAT-like tissue (Ahmadian et al., 2011).

1.1.3 Consequences of central obesity

It has been known for quite some time that large accumulation of central WAT (abdominal obesity) is associated with a higher incidence of type 2 diabetes mellitus, hypertension, and cardiovascular diseases compared to the accumulation of subcutaneous WAT (Bjorntorp, 1992). In a clinical setting, obesity is defined as a body-mass-index (BMI – weight in kilograms divided by the square of the height in meters) of 30.0 or above (Berrington de Gonzalez et al., 2010). Current data from the German Health Interview and Examination Survey for Adults revealed that 23.3% of men and 23.9% of women are obese and that the prevalence is increasing (Mensink et al., 2013). Obesity could be linked to the development of atherosclerosis, coronary artery disease (CAD), heart failure (HF) and atrial fibrillation (Mandviwala et al., 2016).

In context, central obesity could be identified as leading risk factor for HF, CAD, stroke, arrhythmias and sudden cardiac death (Chrostowska et al., 2013; Poirier et al., 2006). Central obesity is often measured using the waist circumference (Alberti et al., 2005).

Waist circumferences of above 88 cm in women and 102 cm in men are found to be sensitive thresholds for an increase in cardiometabolic disorders such as high blood pressure, elevated triacylglycerols (TAG), low HDL and high fasting glucose (Mason and Katzmarzyk, 2010). A comprehensive meta-regression analysis revealed that a 1 cm increase in waist circumference is associated with a 2% increase in CAD risk in the future (de Koning et al., 2007). Excess central WAT causes metabolic abnormalities such as hypertriglyceridemia, inflammation, insulin resistance, hyperinsulinemia, glucose intolerance and endothelial dysfunction, which increase the risk for CAD (Despres, 2012). However, one single mechanism that relates obesity to cardiovascular disease remains unknown (Chrostowska et al., 2013). This study focussed on the effect of fatty acids released from white adipose tissue on the development of heart failure.

1.1.4 Absorption and storage of lipids

FA are important energy substrates, components of the cell membrane and signaling molecules in all organisms (Young and Zechner, 2013). Below, the absorption of lipids and in particular FA is described as well as the processes of storing and releasing FA from WAT.

Digestion of lipids is a process including lipases secreted by glands in the tongue, gastric enzymes in the stomach, pancreatic lipases and bile salts secreted from the gall bladder. Dietary absorption of lipids occurs inside the small intestinal lumen through enterocytes. The main lipids taken up by the intestines are TAGs, phospholipids (PLs) and cholesterol (Iqbal and Hussain, 2009). TAG is an ester derived from three long-chain FAs, which are esterified to the trivalent alcohol glycerol (Young and Zechner, 2013). Pancreatic enzymes digest TAG in monoacylglycerol (MAG) and FAs. MAG and FAs are absorbed from the small intestine into the enterocytes, using specific protein-independent and protein-dependent transporters (such as FAT/CD36) on the apical side of enterocytes. Inside the cytoplasm of the enterocytes, FAs and MAG are transported to the endoplasmic reticulum by fatty acid-binding proteins (FABP). MAG and FAs are used for TAG biosynthesis catalyzed by monoacylglycerol and diacylglycerol acyltransferase (Iqbal and Hussain, 2009). Afterward, the initiation of chylomicrons with lipidation of apolipoprotein-B48 (apo-B48) is initiated inside the enterocytes (Hassing et al., 2012). Chylomicrons are the primary lipoprotein from the intestine released into the lymphatic circulation. They are transported to the liver, where TAG and apo-B100 are used to produce very-low-density lipoproteins (VLDL). Lipoproteins contain hydrophobic

TAG, cholesteryl esters and fat-soluble vitamins in their core and are surrounded by polar phospholipids and apolipoproteins (apo-B48 or apo-B100). VLDL redistribute TAG to muscles, heart and adipose tissue (Young and Zechner, 2013).

TAG-rich lipoproteins are a source of energy and frequently used for storage, such as in adipose tissue. The absorption of VLDL and chylomicrons into the adipose tissue is regulated by lipoprotein lipase (LPL), which is synthesized in adipocytes and transported to the endothelial cell surface (Hassing et al., 2012). LPL is a homodimer formed by endoplasmic reticulum and binds to glycosyl-phosphatidylinositol-anchored high-density lipoprotein-binding protein 1 (GPIHBP1) on the capillary lumen side (Beigneux et al., 2008). Interestingly, the expression of LPL is upregulated by insulin and glucocorticoids. LPL hydrolyzes TAG into FAs and glycerol and hence performs intravasal lipolysis. While glycerol is transported to the liver, while FAs and MAG are taken up inside the adipocytes (**Figure 1.1**). Here FAs and MAGs are re-esterified to TAG and stored in lipid droplets (Young and Zechner, 2013). The excess formation of lipid droplets inside the cells can cause a toxic effect called “lipotoxicity” (Greenberg et al., 2011).

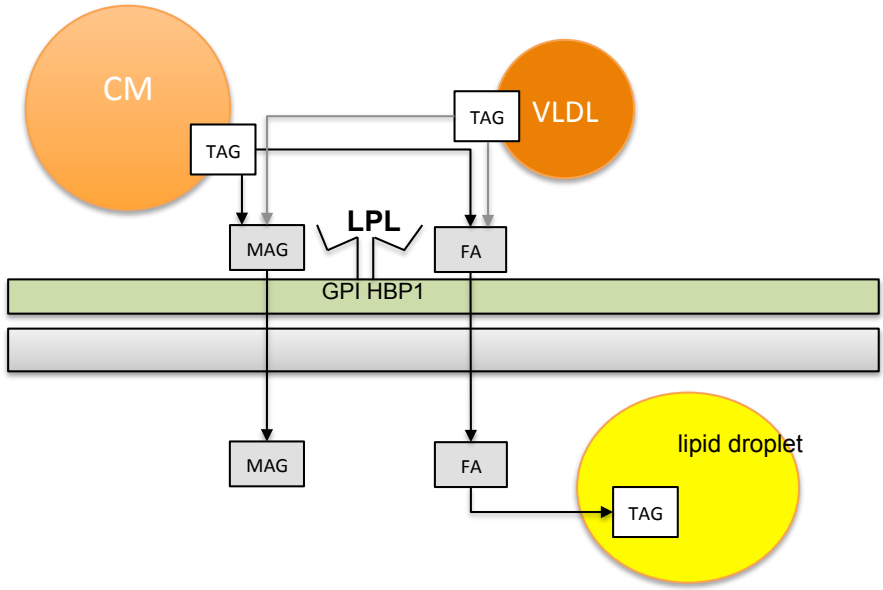

Figure 1.1 Overview of intravascular lipolysis

Lipoprotein lipase (LPL) hydrolyzes triacylglycerol (TAG) in chylomicrons (CM) and very-low-density lipoproteins (VLDL) on the luminal surface of the capillary endothelium. LPL binds to glycosyl-phosphatidylinositol-anchored high-density lipoprotein-binding protein 1 (GPIHBP1). LPL forms TAG into monoacylglycerol (MAG) and fatty acids (FA), which are taken up through the plasma membrane of adipocytes. MAG are generated further into FAs and glycerol, while FAs are re-esterified intracellular into TAG and stored in intracellular lipid droplets (adapted from Young and Zechner, 2013).

1.1.5 Function and regulation of lipolysis in white adipose tissue

In adipocytes, lipid droplets store TAG and cholesterol. WAT can release FAs and glycerol during fasting, which is unique. Organs, such as heart or skeletal muscles use FAs and glycerol of TAG upon fasting to generate energy through mitochondrial β-oxidation (Iqbal and Hussain, 2009). FAs are liberated from WAT by three main enzymes, identified over the last years in the process of sequential hydrolysis of TAG (Young and Zechner, 2013), defined as lipolysis (Bolsoni-Lopes and Alonso-Vale, 2015) (**Figure 1.2**). WAT-derived FAs are transported with the blood and eventually delivered into other organs (heart and skeletal muscle) for mitochondrial β-oxidation. The first step of lipolysis is the hydrolysis of TAG to diacylglycerol (DAG) and one FA molecule, catalyzed by Adipose Triglyceride Lipase (ATGL) (Zechner et al., 2012). The second step is hydrolysis of DAG to MAG and one additional FA molecule, which is catalyzed by hormone-sensitive lipase (HSL) (Fruhbeck et al., 2014). The final step is the hydrolysis of the last FA and one glycerol molecule from MAG. In this step monoacylglycerol lipase (MGL) is the primary enzyme (Douglass et al., 2015). Hence, lipolysis produces three FFA and one glycerol molecule out of TAG (**Figure 1.2**).

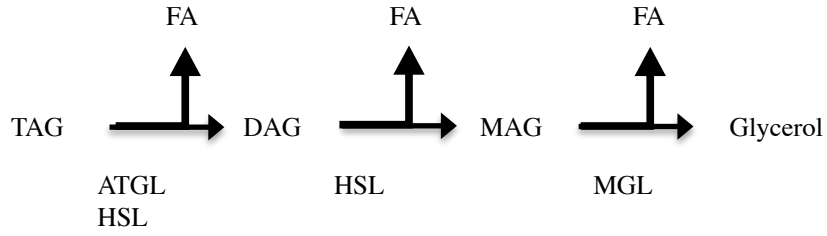

Figure 1.2 Lipolysis of triacylglycerol

Triacylglycerol (TAG) is hydrolyzed to diacylglycerol (DAG) and one FA molecule by Adipose Triglyceride Lipase (ATGL) and partly by Hormone-Sensitive Lipase (HSL). DAG is hydrolyzed to monoacylglycerol (MAG) and one FA molecule by HSL. The final step is the hydrolysis of MAG to one last FA molecule and glycerol molecule from MAG by monoacylglycerol lipase (MGL) (adapted from Bolsoni-Lopes and Alonso-Vale, 2015).

While ATGL is the first step of lipolysis, HSL was long considered to be the only lipase responsible for hydrolysis of TAG. Below, HSL and MGL are shortly described while ATGL is explained in more detail.

1.2 Hormone-sensitive lipase

Hormone-sensitive lipase (HSL) was first described in 1964 and is more responsible for DAG than for TAG hydrolysis (Osuga et al., 2000). Furthermore, HSL is involved in the hydrolysis of cholesterol ester, retinyl ester and to a smaller extent of TAG (Lass et al., 2011). HSL is expressed in WAT, BAT and non-adipose tissues such as testis. HSL-deficiency causes an accumulation of DAG and reduces circulating FFAs in mice (Haemmerle et al., 2002). Catecholamines, atrial natriuretic factor (ANF) (Sengenes et al., 2003) and growth hormones (Dietz and Schwartz, 1991) stimulate the expression of HSL, while insulin is its main inhibitor (Engfeldt et al., 1988). Catecholamines bind to β-adrenergic receptors on the membrane of adipocytes. Activated β-adrenergic receptors stimulate G proteins, resulting in increased levels of cyclic adenosine monophosphate (cAMP) (Wang et al., 2008). cAMP activates Protein Kinase A (PKA), which phosphorylates HSL (Anthonsen et al., 1998) (further details see below). HSL requires phosphorylated perilipin-1, mediated via PKA, for its translocation to the lipid droplets and its lipolytic activity (Lass et al., 2011; Wang et al., 2009a) (**Figure 1.3**). Insulin decreases cAMP concentration by activating phosphodiesterase, resulting in reduced HSL activity (Bolsoni-Lopes and Alonso-Vale, 2015; Degerman et al., 1990).

1.3 Monoacylglycerol lipase

Monoacylglycerol lipase (MGL) is the primary lipase responsible for hydrolysis of MAG and 2-arachidonoyl-glycerol, which is a ligand for cannabinoid receptors in the brain (Schlosburg et al., 2010). It is expressed in multiple organs, such as WAT, brain, liver, kidneys, testicles and heart (Bolsoni-Lopes and Alonso-Vale, 2015). Taschler and colleagues demonstrated that MGL-deficiency in mice results in reduced plasma FA and glycerol levels. However, the MGL-deficiency is partially compensated by HSL and the mice show only moderate defects of lipolysis. Also, MGL-deficient mice show improved glucose tolerance and insulin sensitivity, but regular food intake and fat mass (Taschler et al., 2011). The endocannabinoid system might regulate the expression of MGL, but the exact mechanism of regulation is still unclear (Bolsoni-Lopes and Alonso-Vale, 2015; Taschler et al., 2011).

1.4 Adipose Triglyceride Lipase

It was long believed that HSL is the only main enzyme involved in lipolysis of TAG in WAT. However, since the discovery of ATGL in 2004 it has been shown that ATGL is the rate-limiting enzyme regulating lipolysis (Schweiger et al., 2006). ATGL prefers TAG substrates with long-chain fatty acid esters (mainly palmitoleic, palmitic and stearic acid) (Young and Zechner, 2013). Three groups described ATGL simultaneously as Adipose Triglyceride Lipase (Zimmermann et al., 2004), desnutrin (Villena et al., 2004) and phospholipase A2-ζ (Jenkins et al., 2004).

1.4.1 ATGL – structure of gene

Murine ATGL gene consists of a 486-amino acid protein and a calculated molecular mass of 54kD (Zimmermann et al., 2004). However, the human ATGL gene encodes a 504-amino acid protein and is to 86% identical to the mouse protein (Zimmermann et al., 2004). Wilson and colleagues indicated that ATGL belongs to a gene family called patatin-like phospholipase domain-containing protein A1 to A9 (PNPLA1-9). In this family, ATGL has been identified as being PNPLA2 (Wilson et al., 2006). Typical in this gene family is the patatin domain-containing N-terminal region (Rydel et al., 2003; Villena et al., 2004). Patatin domain-containing proteins can be found in animals, plants, fungi and bacteria (Banerji and Flieger, 2004; Young and Zechner, 2013). Within the patatin domain is the catalytic center of ATGL located. The catalytic center is found to be a dyad composed of Ser47 and Asp166 (Duncan et al., 2010; Lass et al., 2011). Besides, the dyad within the patatin-like domain is responsible for protein-protein interaction between ATGL and its regulatory enzymes CGI-58 and G0S1 (see 1.4.4 and 1.4.5) (Cornaciu et al., 2011).

Furthermore, it is presumed that the C-Terminus of ATGL consists of α-helical and loop regions with hydrophobic regions. Those regions are considered to bind to lipid droplets in the cytoplasm (Kobayashi et al., 2008; Schweiger et al., 2008). ATGL is highly expressed in WAT and BAT, while its expression in cardiac muscle, skeletal muscle and testis is much lower (Zimmermann et al., 2004).

1.4.2 Regulation of ATGL

ATGL mRNA expression levels are reported to be elevated by glucocorticoids and fasting. Furthermore, the expression of ATGL is reduced by insulin and food intake (Zechner et al., 2012). In addition, its mRNA expression level is reduced by mammalian target of rapamycin complex 1 (mTORC1), an important energy and nutrient sensor in

the cell and linked to insulin pathway (Chakrabarti et al., 2010). In adipocytes, ATGL is a target for the transcriptional regulation by Peroxisome proliferator-activated receptor gamma (PPAR-γ) (Kim et al., 2006) and Forkhead box protein O1 (FoxO1) (Lettieri Barbato et al., 2014).

1.4.3 ATGL as nutrient-sensing enzyme

FoxO1 is a nutrient-sensing protein, which binds to ATGL-promoter in a starvation state and causes its upregulation. Hyperinsulinemia causes reduced expression of ATGL by the detachment of FoxO1 (Chakrabarti and Kandror, 2009). Lipolysis was demonstrated to be critical for maintaining energy homeostasis during starvation, similar to autophagy, regulation of intracellular breakdown of cellular components utilized as an alternative energy source (Singh et al., 2009). Autophagy of lipids is a lysosomal degradation, called lipophagy. “Lipa” is one of the controlling enzymes in the lipophagy pathway, which is upregulated by lower nutrient levels. High Lipa expression is associated with an upregulation of ATGL (Lettieri Barbato et al., 2014).

1.4.4 Co-activator of ATGL

Its vesicular transportation to lipid droplets regulates ATGL posttranscriptionally (Guo et al., 2008). It is highly regulated by its co-activator comparative gene identification-58 (CGI-58), also called α/β-hydrolase domain-containing 5 (Abhd5) (Lass et al., 2006). CGI-58 is found on the surface of the lipid droplets (Girousse and Langin, 2012). Under basal conditions CGI-58 binds to Perilipin-1, which limits the hydrolytic activity of ATGL (Lafontan and Langin, 2009). If Perilipin-1 is phosphorylated, CGI-58 is released and binds to ATGL. Together they form an active complex, which increases lipolysis (Ahmadian et al., 2010; Bolsoni-Lopes and Alonso-Vale, 2015) (**Figure 1.3**). Mutations of CGI-58 in humans cause a rare neutral lipid storage disease called Chanarin-Dorfman syndrome, which is characterized by TAG accumulation in most non-adipose tissues and ichthyosis (Lefevre et al., 2001).

Recently, adipocytes-type Fatty Acid-binding Protein (A-Fabp) could be found to interact with CGI-58 and promotes ATGL-mediated TAG lipolysis (Hofer et al., 2015). It has also been shown that ATGL is hormone-sensitive. Perilipin-1 can be phosphorylated through β-adrenergic stimulated PKA. Activated PKA releases CGI-58, which then binds to ATGL, causing its activation (Granneman et al., 2007). PKA-mediated phosphorylation of ATGL on Ser406 suggests a moderate increase of ATGL lipolytic activity, mediated by β-adrenergic stimulation (Pagnon et al., 2012). The concept of β-adrenergic and

catecholamine stimulated lipolysis has already been previously described for HSL (Anthonsen et al., 1998; Bolsoni-Lopes and Alonso-Vale, 2015).

ATGL is also phosphorylated by AMP-activated protein kinase (AMPK) on two serine residues in mice (Ser406 and Ser430) (Bartz et al., 2007; Zimmermann et al., 2004). AMPK-mediated ATGL phosphorylation increases lipolysis in adipocytes in vivo in mice, FA oxidation and UCP-1 induction of thermogenesis (Ahmadian et al., 2011).

1.4.5 Inhibitor of ATGL

G0S2, a protein encoded by G_0/G_1 switch gene 2, has been identified as a significant inhibitor of ATGL (Yang et al., 2010). It acts in the transition from G0 to G1 in the cell cycle (Russell and Forsdyke, 1991). G0S2 binds to ATGL and causes the inhibition of its basal and stimulated lipolytic activity (Yang et al., 2010) (**Figure 1.3**). In lipid droplets, G0S1 directly interacts with ATGL on its patatin-like domain, independent of CGI-58 co-expression (Lu et al., 2010; Papackova and Cahova, 2015).

Furthermore, fat-specific Protein 27 (FSP27) could recently be identified to interact with ATGL and decrease its lipolytic activity (Grahn et al., 2014). FSP27 is a differentiation-regulated protein in adipocytes. Its depletion in murine WAT adipocytes causes increased lipolysis, decreased TAG storage and smaller lipid droplets (Nishino et al., 2008). Additionally, the ADP-ribosylation factor 1 (Arf1), Golgi Brefeldin A Resistance Factor (GBF1) and coat protein complex I (COPI) have been identified to regulate the transportation of ATGL from the endoplasmic reticulum to lipid droplets (Ellong et al., 2011; Soni et al., 2009).

In summary, ATGL activation and inhibition is regulated by various mechanisms. However, CGI-58-dependent activation of ATGL seems to be the most important regulatory mechanism (Lass et al., 2006; Young and Zechner, 2013) (**Figure 1.3**).

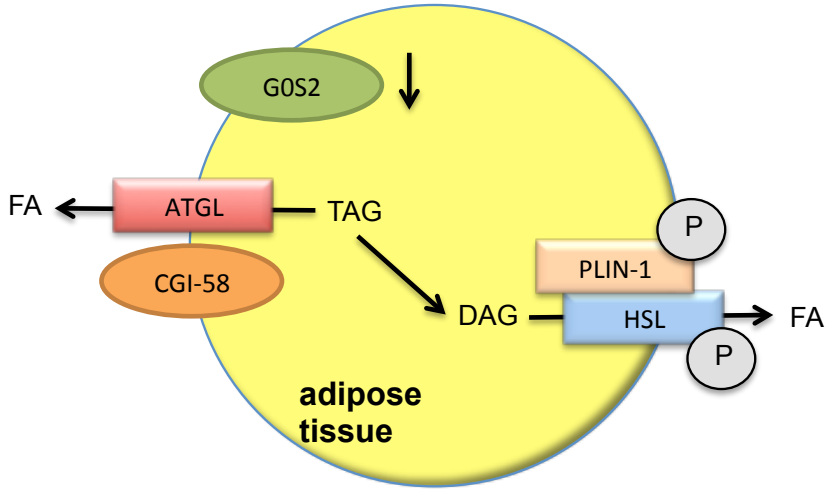

Figure 1.3 Regulation of ATGL and HSL in adipose tissue

Adipose Triglyceride Lipase (ATGL) binds to lipid droplets and hydrolyze triacylglycerol (TAG) to diacylglycerol (DAG) and one fatty acid (FA) molecule. ATGL is upregulated by its co-activator comparative gene identification-58 (CGI-58) and downregulated by its inhibitor G_0/G_1 switch gene 2 (G0S2). Activated Protein Kinase A (PKA) phosphorylates (P) Perilipin-1 (PLIN-1) and Hormone-Sensitive Lipase (HSL). HSL hydrolyze diacylglycerol (DAG) to monoacylglycerol and FA (adapted from Zechner et. al, 2012).

1.4.6 Function of Adipose Triglyceride Lipase

ATGL is expressed ubiquitously in the body, making it essential for most organs. Global ATGL-deficient mice showed a decline of the basal and stimulated lipolysis (Bezaire et al., 2009; Haemmerle et al., 2006; Kershaw et al., 2006). Haemmerle and colleagues observed in adipocytes of gonadal WAT isolated from ATGL-deficient mice (ex-vivo-lipolysis) a 75% reduction in FA and glycerol release. Moreover, in global ATGL-KO mice, the whole body fat mass is enlarged due to an increase in gonadal and inguinal WAT depots. TAG accumulation in global ATGL-KO mice occurs mainly in WAT, but also ectopic fat accumulation was observed in heart, skeletal muscle, kidney, testis, and liver (Haemmerle et al., 2006). In addition, severe cardiac and skeletal myopathies and premature death are reported in global ATGL-KO mice (Bezaire and Langin, 2009; Haemmerle et al., 2006), with a reduction of FA release into the blood circulation (Huijsman et al., 2009; Miyoshi et al., 2008). Furthermore, global ATGL-KO mice feature reduced TAG, β-hidroxybutirate, total cholesterol, VLDL and HDL levels (Bezaire and Langin, 2009; Bolsoni-Lopes and Alonso-Vale, 2015). On a gene expression level, ATGL-deficiency is associated with decreased expression of genes necessary for lipid metabolism in BAT and the heart. Also, genes for ATP biosynthesis in cardiac and skeletal muscle are downregulated (Pinent et al., 2008).

Furthermore, severe hypothermia was observed in animals lacking ATGL when exposed to coldness (Haemmerle et al., 2006). This can be explained by the reduction

of FA-delivery to the mitochondria and reduced mitochondrial respiration rate (Cannon and Nedergaard, 2004). However, ATGL-deficiency is not associated with reduced food consumption, O_2 consumption, CO_2 production or physical activity (Haemmerle et al., 2006; Schoiswohl et al., 2010).

There are also numerous metabolic changes described in global ATGL-deficient mice. For instance, global ATGL-KO mice have a reduced ability to adequately switch from glucose metabolism to free fatty acids (FFA) metabolism during fasting (Huijsman et al., 2009). Also, the global ATGL-deficiency causes an increased glucose tolerance and higher insulin sensitivity compared to wild-type mice (WT) (Haemmerle et al., 2006). Interestingly, in ATGL-KO mice insulin signaling was increased in skeletal muscle, unchanged or slightly increased in adipose tissue and reduced in liver (Kienesberger et al., 2009). It remains complicated to connect global ATGL-KO to insulin sensitivity in mice. Therefore, additional studies in adipose tissue-specific ATGL-KO mice were used to investigate this relationship in detail.

Different groups used an aP2-Cre-recombinase adipose tissue-specific ATGL-KO mouse model (atATGL-KO) to study the connection between adipocyte ATGL and systemic insulin sensitivity. In this atATGL-KO mice in vivo lipolysis was noticeably reduced, adipose tissue mass was increased, and insulin tolerance tests (ITT) revealed an improvement in insulin sensitivity. Furthermore, the groups demonstrated an improved hepatic insulin response (Ahmadian et al., 2011; Wu et al., 2012). Recently, adiponectin-driven Cre expression was used to create an alternative adipocyte-specific ATGL-KO mouse (Adipoq-atATGL-KO) (Schoiswohl et al., 2015). Schoiswohl and colleagues also demonstrated reduced FA circulation, improved systemic insulin tolerance and better hepatic insulin signaling in Adipoq-atATGL-KO mice (Schoiswohl et al., 2015).

ATGL has also been studied in liver-specific KO mouse models. Liver-specific ATGL-KO mice developed a larger liver mass, hepatic steatosis and reduced liver β-oxidation (Ong et al., 2011; Wu et al., 2011). In hepatic ATGL-KO mice mRNA expression levels of PPAR-α and CPT-1α were reduced in hepatocytes, which however did not result in a reduction of FA oxidation (FAO) (Wu et al., 2011).

1.4.7 Adipose Triglyceride Lipase in the heart

Using KO- and overexpression-models in rodents, different groups have investigated the influence of ATGL in the heart. Global ATGL-KO causes massive lipid accumulation in cardiomyocytes, leading to increasing cardiac fibrosis and severe cardiac dysfunction (Haemmerle et al., 2006). In addition, Haemmerle and colleagues revealed a reduction of ejection fraction, an increased thickness of the interventricular septum and the posterior wall thickness of the left ventricle in global ATGL-KO mice. Cardiac dysfunction due to global ATGL-KO leads to a premature death in male and female mice. In particular, male ATGL-KO mice suffer from dilatation of the right and left ventricle (Haemmerle et al., 2006). Results by Schoiswohl and colleagues confirmed that global ATGL-deficiency causes severe cardiac lipid accumulation in mice hearts, cardiac insufficiency and eventually earlier death (Schoiswohl et al., 2010). Cardiomyocyte-specific ATGL-KO mice develop cardiac fibrosis, pathological hypertrophy and a diminished cardiac FAO (Kienesberger et al., 2013). Also in rats, cardiomyocyte-specific ATGL-deficiency leads to cardiac hypertrophy and ATGL-overexpression prevents hypertrophy, induced by phenylephrine (Gao et al., 2015). Interestingly, Gao and colleagues suggest, that cardiomyocyte-specific ATGL-deficiency results in decreased PPAR-α binding activity, which causes a reduced β-oxidation capacity and increased intracellular FFA and ceramide accumulation in cardiomyocytes resulting in cardiac hypertrophy (Gao et al., 2015). In addition, global ATGL-deficiency is associated with perivascular inflammation and endothelial dysfunction, which is suggested to be linked to severe cardiac dysfunction in mice (Schrammel et al., 2014).

Humans suffering from mutations in the ATGL gene develop neutral lipid storage disease (NLSD) (Fischer et al., 2007; Hirano et al., 2008). NLSD can cause TAG accumulation in skeletal muscle, liver and heart, which is similar to the severity in ATGL-KO mice. Patients with NLSD suffer from muscle weakness in adolescence. In older patients, cardiac steatosis and dilated cardiomyopathy occurs, which often result in heart transplantation (Hirano et al., 2008).

Importantly, the results of cardiomyocyte-specific ATGL overexpression models are consistent with studies performed on global ATGL-KO animals. Kienesberger and colleagues demonstrated in mice with cardiomyocyte-specific ATGL overexpression, lower cardiac lipid accumulation, reduced cardiac fibrosis and protected cardiac function in a pressure-overload induced Transverse Aortic Constriction (TAC) model (Kienesberger et al., 2012). Interestingly, cardiomyocyte-specific ATGL overexpression

in mice is characterized by decreased rates of FAO, reduced FA uptake and increased glucose oxidation, when compared to control group. Interestingly, the total production of acetyl-CoA in cardiomyocytes remained similar to WT mice, causing no impairment of ATP production (Kienesberger et al., 2012).

Huijmann and colleagues studied metabolic changes in global ATGL-KO mice after running exercise. The group revealed that global ATGL-KO mice have increased muscle and liver glycogen exhaustion and glucose utilization, but reduced FFA availability and lipolysis during forced exercise on a treadmill (Huijsman et al., 2009). In addition, Schoiswohl and colleagues confirmed that mice with global ATGL-deficiency except in cardiac muscle (global knock-out, cardiac knock-in) show attenuated increase of FA during exercise and hypoglycemia (Schoiswohl et al., 2010). A recent study of our group investigating the physiological hypertrophy revealed that atATGL-KO mice after chronic exercise on treadmill developed reduced left-ventricular mass increase compared to WT mice (Foryst-Ludwig et al., 2015). We could confirm that atATGL-KO had a reduced FA release into the blood circulation from WAT and a reduced myocardial uptake of FFA. Furthermore, we demonstrated that the FA palmitoleic acid C16:1 is a co-mediator responsible for cardiac hypertrophy in mice (Foryst-Ludwig et al., 2015).

Collectively, several KO and overexpression studies in rodents and clinical observations in humans reveal ATGL as being a crucial enzyme for the lipid metabolism in influencing the function of multiple organs. While the role of ATGL in the development of physiological cardiac hypertrophy has been evaluated, the importance for the pathological cardiac hypertrophy and heart failure is a primary aim of this study.

1.5 Left ventricular hypertrophy

Left-ventricular hypertrophy (LVH) is defined as an increase in left ventricular muscle mass (LVM). It is an adaptive mechanism to pressure or volume overload. On a cellular level cardiac hypertrophy includes the increased size of cardiomyocytes, vascular cells and higher production of extracellular matrix (Cacciapuoti, 2011; Grossman et al., 1975). In general, pathological LVH and physiological LVH are distinguished. Physiological LVH is considered as a beneficial adaptation postnatal growth induced by pregnancy or chronic physical training. Physiological LVH is characterized by an increase of LVM, accompaniment by an increase in ventricular chamber diameter with an improved cardiac function (Bernardo et al., 2010; Foryst-Ludwig and Kintscher, 2013).

On the other side, pathological LVH can be induced by pressure or volume overload. Chronic pressure overload occurs due to hypertension and obstruction of the LV or aortic outflow tract (Peterson, 2002). Also, myocardial infarction, CAD and different types of cardiomyopathies lead to the development of pathological LVH (Bernardo et al., 2010). Pathological LVH is associated with a significant increase in LVM, cardiac dysfunction, fibrosis and eventually cell death, which can cause heart failure (HF) (Broberg and Burchill, 2015).

Depending on the type of hypertrophy, the heart shape varies (**Figure 1.4**). Pressure overload results in concentric hypertrophy, which is characterized by an increase of cardiomyocytes in width due to sarcomeres added in parallel. Concentric hypertrophy causes wall thickening of the LV and a decrease of the LV chamber diameter. In contrast, volume overload results in eccentric hypertrophy, which refers to an increase in LVM with normal or even decreased wall thickness and a dilated LV chamber. Eccentric hypertrophy is caused by an addition of sarcomeres in series resulting in an increase in cardiomyocyte length (Grossman et al., 1975; Johnson et al., 2015) (**Figure 1.4**). Leading causes of eccentric hypertrophy are aortic regurgitation regarding valve disease and endurance training (e.g. long distance running) (Bernardo et al., 2010; Pluim et al., 2000). Concentric hypertrophy is caused by hypertension and aortic constriction, but also by resistance strength training (e.g. weight lifting) (Pluim et al., 2000). Pathological LVH increases the risk of HF, death following myocardial infarction, ventricular arrhythmias and decreased LV ejection fraction (Lavie et al., 2014; Verdecchia et al., 2001).

In addition, cardiac fibrosis is a process observed in pressure and volume overload LVH (Kong et al., 2014). Cardiac fibrosis, the accumulation of excessive extracellular matrix, increases the risk of arrhythmia and sudden cardiac death (Wu et al., 2008). For cardiac fibrosis to occur, fibroblasts proliferate and differentiate into myofibroblasts in response to pathological stress (Pichler et al., 2012). Several molecular signals are involved in the proliferation of fibroblasts into myofibroblasts and hence the development of cardiac fibrosis such as Transforming Growth Factor beta (TGF-β) (Dobaczewski et al., 2010), Platelet-Derived Growth Factors (PDGFs), Fibroblast Growth Factors (FGFs) and pro-inflammatory factors such as Interleukin-1β (IL-1β) and IL-6 (Kong et al., 2014). Also, other organs, such as epicardial adipose tissue, contribute to cardiac fibrosis, leading to atrial fibrillation (Hatem et al., 2016). While adipocytes release inflammatory cytokines and growth factors, a study from Wang and colleagues performed in rats demonstrated that FAs themselves induce the release of connective tissue growth factor (CTGF), which can accelerate the development of cardiac fibrosis (Wang et al., 2009b).

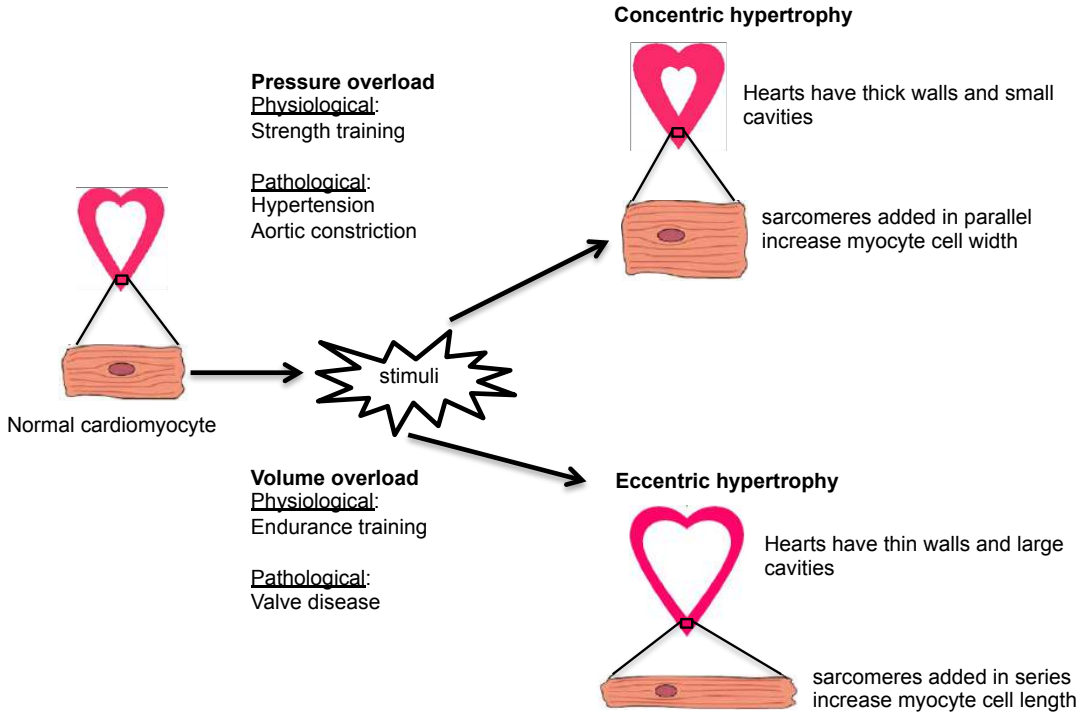

Figure 1.4 Different stimuli induce concentric and eccentric hypertrophy

Pressure overload results in thickening of left ventricular walls and small cavities with sarcomeres added in parallel and cardiomyocytes increase in cell width. Volume overload results in a thin left ventricular wall and large cavities with sarcomeres added in series and cardiomyocytes increase in cell length (adapted from Bernardo et. al, 2010).

1.6 Heart Failure

Heart failure (HF) is a progressive condition in which the heart is unable to pump blood in response to systemic demands (AHA, 2015; Heineke and Molkentin, 2006). Importantly, cardiovascular disease was the leading cause of death worldwide in the past years (Mozaffarian et al., 2015). An estimated number of 1.8 million people in Germany (Zugck, 2013) and 5.7 million in the USA suffered from HF (Mozaffarian et al., 2015). In 2013, HF was the third most common cause of death in Germany with 29973 women and 15842 men (Bundesamt, 2014). In 2012, the costs for HF treatment were estimated to be $30.1 billion in the USA alone (Heidenreich PA, 2013). Despite high costs for treatment, more innovative therapies and intensified research, HF remains one of the leading causes of morbidity and mortality worldwide.

1.6.1 Classification of Heart Failure

HF can be differentiated between chronic and acute. Chronic HF is referred to patients who have suffered from HF for some time, while acute HF describes the rapid onset or worsening of symptoms/signs of HF (see below) (Ponikowski et al., 2016). Here we focus primarily on chronic HF.

Chronic HF is defined as an impaired function of the heart resulting in two syndromes, initially called systolic heart failure (SHF) and diastolic heart failure (DHF) and originally described in Fishberg´s textbook of 1937 (Fishberg, 1937). SHF is defined as the inability of the ventricle with a normal end-diastolic volume (EDV) to eject a normal stroke volume (SV). DHF, on the other hand, occurs, when the ventricle with a normal EDV is incapable of accepting venous blood return to the heart (Fishberg, 1937; Katz and Rolett, 2016). However, recently the European Society of Cardiology (ESC) has redefined HF. According to the 2016 ESC guidelines, HF is defined as a “symptomatic syndrome graded by the New York Heart Association (NYHA) functional classification” (Ponikowski et al., 2016). The NYHA functional classification (**Figure 1.5**), which was revised last in 1994, is currently the most widely used method to grade the severity of HF in a clinical and outpatient setting (Dolgin, 1994; Ponikowski et al., 2016).

Class I	No limitation of physical activity. Ordinary physical activity does not cause undue breathlessness, fatigue, or palpitations.
Class II	Slight limitation of physical activity. Comfortable at rest, but ordinary physical activity results in undue breathlessness, fatigue, or palpitations.
Class III	Marked limitation of physical activity. Comfortable at rest, but less than ordinary physical activity results in undue breathlessness, fatigue, or palpitations.
Class IV	Unable to carry on any physical activity without discomfort. Symptoms at rest can be present. If any physical activity is undertaken, discomfort is increased.

Figure 1.5 New York Heart Association (NYHA) functional classification for symptomatic Heart Failure

(adapted from Ponikowski et al., 2016)

NYHA classification is based on the HF-symptoms and the degree of physical activity. Hence, to diagnose HF, clinical presentation is very relevant. Typical clinical symptoms for HF are breathlessness, orthopnoea, paroxysmal nocturnal dyspnoea, reduced exercise tolerance, fatigue, tiredness, and ankle swelling. There are also less typical symptoms of HF such as a nocturnal cough, sleeping difficulties, wheezing, loss of appetite, confusion, palpitations and syncopes (Ponikowski et al., 2016) (**Figure 1.6**).
The term “stable chronic HF” is used for patients, who have had unchanged symptoms for at least one month. The new ESC guidelines differentiate between patients with “heart failure with preserved ejection fraction” (HFpEF) (EF ≥ 50%), “heart failure with mild-range ejection fraction” (HFmrEF) (EF 40% - 49%) and “heart failure with reduced ejection fraction” (HFrEF) (EF < 40%) (Ponikowski et al., 2016). Ejection fraction (EF%) is defined as a ratio of SV to EDV. Through improvements of echocardiographical imaging, EF% has been used for evaluation of HF in a clinical setting and clinical trials (Iwano and Little, 2013; McMurray et al., 2012). Treatment for HFrEF, especially the use of angiotensin-converting enzyme inhibitors and β-blockers reduced mortality and morbidity. However, in patients with HFmrEF and HFpEF, there is no treatment that has yet been shown to reduce mortality or morbidity. HFmrEF has been identified in the recent ESC guidelines in particular to encourage research into its pathophysiology and possible treatment (Ponikowski et al., 2016).

Figure 1.6 Typical symptoms of Heart Failure

(adapted from Haddad, 2016)

1.6.2 Causes of Heart Failure

Large epidemiological studies have shown some unchanging results over the last decades; the most common cause of HF is coronary artery disease (CAD), in particular when leading to myocardial infarction (MI) (He et al., 2001; Levy et al., 1996). CAD and MI cause cardiac dysfunction, leading to reduce ventricular contractility. Reduced contractility causes ventricular dilatation, resulting in a reduction of EF% (Dorn, 2009).

Also, arterial hypertension has been implicated as one of the most important risk factors for the development of HF (Go et al., 2013). Hypertension is defined as systolic blood pressure >140 mmHg and diastolic blood pressure >90 mmHg (Mancia et al., 2014). Cardiomyocytes respond to hypertension by increasing in size, resulting in LVH. The increase in wall thickness reduces wall stress in the beginning. Hence, the left ventricle adapts to the high blood pressure. However, when hypertension is persistent, the heart muscle decompensates and HF occurs (Burchfield et al., 2013). Furthermore, 50% of patients with valvular heart disease (e.g. aortic valve stenosis) develop HF (Maganti et al., 2010). Recently published data indicated that pathological LVH, regardless of the primary cause, increases the incidence of HF as well (Lavie et al., 2014).

Moreover, in several large epidemiological studies, obesity was shown to associate directly with HF. The Framingham Heart Study revealed that 11% of HF cases in men and 14% in women are attributable to obesity (Kenchaiah et al., 2002). Additional individual risk factors for HF are physical inactivity, persistent hypertension after MI, tobacco smoking, diabetes as well as less education and male sex (He et al., 2001).

1.6.3 Pathophysiology of Heart Failure

During the development of HF, several changes are taking place in the heart and cardiometabolic system. Early stages of HF are characterized by compensatory mechanisms. However, in advanced stages, ventricular wall stress and massive LVH may result in decompensated HF. Cellular changes, such as cardiomyocyte lysis and necrosis, pro-inflammatory cytokine release, cardiac fibrosis and autophagy occur. Importantly, the cardiac metabolism changes dramatically. In addition, neurohormonal alterations, such as increased catecholamine and natriuretic peptide levels also affect systemic metabolism.

1.6.3.1 Ventricular remodeling during Heart Failure

In early stages of HF, the Frank-Starling mechanism is an important compensatory process. It describes the increase in cardiac output (CO) in response to an increase in left-ventricular end-diastolic volume (LVEDV) (Kemp and Conte, 2012; Westerhof and O'Rourke, 1995). The increase blood volume into the LV cavity causes wall stretching, which results in increased contractility and hence higher CO of the LV. (Schmidt and Lang, 2011). However, as the LVEDV increases more in later stages of HF the resultant CO does not increase further and eventually decreases as the heart begins to decompensate (Kemp and Conte, 2012).

Chronic volume and pressure overload results in long-term modifications of wall thickness, size and function of the ventricles (Curry et al., 2000). Especially the former described pathological LVH is considered to play a significant role in the progression of HF (Burchfield et al., 2013; Frey et al., 2004). LVH leads to further wall thickness, tension, and fibrosis, which severely reduces contractility and reduced CO of the LV (Kemp and Conte, 2012). In the setting of LVH, not only cardiomyocytes are hypertrophic, but also endothelial vessel cells are enlarged. MI causes increased medial thickening of vessels (Roman et al., 2012). These vascular remodeling processes influence the supply of cardiomyocytes with oxygen and metabolic substrates (Burchfield et al., 2013).

1.6.3.2 Cellular changes during Heart Failure

Ventricular wall stress increases due to ventricular pressure and cavity radius and decreases with increased wall thickness (Grossman et al., 1975). Increased ventricular wall stress results in multiple cellular and molecular processes, such as cardiomyocyte lysis and necrosis, leading to the release of intracellular molecules. Some of those

molecules released during HF can be measured in a clinic (e.g. troponin, creatine kinase, brain natriuretic peptide and atrial natriuretic factor) (Burchfield et al., 2013).
In addition, several pro-inflammatory cytokines are highly expressed and released in patients with HF for example; Transforming Growth Factor-alpha (TNF-α), Interleukin-1 (IL-1), IL-6 and IL-18 (Ueland et al., 2015). Besides, inflammatory cells, such as macrophages and mast cells are elevated in the serum and cardiac tissue of HF patients, which contribute to cardiac inflammation and fibrosis (Kong et al., 2014).
Cardiac fibrosis, mediated by the accumulation of excessive extracellular matrix (ECM), is strongly associated with ventricular dysfunction and the risk of arrhythmia (Spinale, 2007). The ECM causes scarring of the myocardium and increases the risk of cardiac death due to HF (Wu et al., 2008).
Recent studies suggest that autophagy, considered as degradation and recycling process of intracellular organelles such as mitochondria (Lamb et al., 2013), is upregulated in cardiomyocytes in phases of cardiac remodeling and causes the delay of HF, by removing damaged mitochondria and more toxic proteins (Nishida and Otsu, 2015).
An important cellular change in cardiomyocytes during HF, often used in experimental settings, is the reexpression of β-myosin heavy chain (β-MyHC). β-MyHC increases in rodents with HF and cardiac hypertrophy (Tardiff et al., 2000). In hearts of rodents, myosin is a hexamer consisting of two heavy chains (MyHC) and two pairs of light chains. The heart expresses a α- and β-form of MyHC. α-MyHC replaces β-MyHC during fetal development (Cox and Marsh, 2014; Gustafson et al., 1987). The reexpression of β-MyHC in adult hearts has been observed in experimental models of HF and cardiac hypertrophy. It has been suggested that β-MyHC is associated with a poorer cardiac contractility (Tardiff et al., 2000). However, the reexpression of β-MyHC as a marker for cardiac hypertrophy is recently controversially discussed. Though β-MyHC was found to be reexpressed in non-hypertrophic myocytes of hypertrophic hearts (Lopez et al., 2011) and also in particular in fibrotic and perivascular areas of the (Pandya et al., 2006).

1.6.3.3 Neurohormonal changes during Heart Failure

Importantly, chronic HF causes increased central sympathetic nervous system (SNS) activity with elevated plasma catecholamine levels (epinephrine and norepinephrine) (Chaggar et al., 2009; Cohn et al., 1984; Leimbach et al., 1986). During early stages of

HF, increased SNS activity causes an increase in CO and MAP and can be considered to be a compensatory mechanism (Chaggar et al., 2009). This changes in advanced stages of HF. For example, norepinephrine correlates with increasing rates of mortality over time (Anand et al., 2003) and is even closely related to the NYHA classification (Bolger et al., 2002) (further details see below).

In addition, the natriuretic peptides (NPs) atrial natriuretic factor (ANF) and brain natriuretic peptide (BNP) are elevated during ventricular and atrial overload in the setting of HF (Yoshimura et al., 1993). Elevated BNP levels reflect ventricular dysfunction and even correlate with NYHA classification (Yasue et al., 1994; Zaphiriou et al., 2005). ANF and BNP have been identified as antifibrotic and antihypertrophic mediators on the heart (Oliver et al., 1997; Tamura et al., 2000). Interestingly, both hormones also cause systemic metabolic effects (Schlueter et al., 2014) (further details see below).

Also, the renin-angiotensin-aldosterone system (RAAS) is stimulated during the development of HF through increased SNS activity (Chaggar et al., 2009; Levine et al., 1982). Through the activation of β1-adrenergic-receptors on juxtaglomerular cells in the afferent arterioles of the kidney, renin is released. Renin causes angiotensinogen to make angiotensin I. Angiotensin I results in an increase of angiotensin II, which directly causes vasoconstriction and aldosterone release. Finally, the RAAS increases sodium reabsorption in the kidneys, vasoconstriction, norepinephrine release and hypertrophy and fibrosis of the heart (Kemp and Conte, 2012; Lüllmann et al., 2010). The use of angiotensin-converting enzyme inhibitors and β-blockers, which reduces the effects of RAAS and the SNS, are essential elements for the treatment of HFrEF (Ponikowski et al., 2016).

1.6.3.4 Metabolic changes during Heart Failure

The cardiac metabolism changes tremendously during the development of HF. The heart in physiological conditions relies predominantly on FFA (70%) and glucose (30%) metabolism (Neubauer, 2007). In particular in advanced stage HF a reduced FFA uptake and FFA oxidation (FAO) is reported (Doenst et al., 2010).

However, also the systemic metabolism experiences alterations due to the effects of HF. Major mediators are catecholamines, which stimulate lipolysis via β2-adrenergic receptors (Morigny et al., 2016). In patients with HF, lipolysis is stimulated via increased levels of catecholamines (Collins, 2014; Lamba and Abraham, 2000). Furthermore, ANF

and BNP increase circulating levels of FAs via increased lipolysis in patients with HF (Polak et al., 2011; Szabo et al., 2013) (Polak et al., 2011). Catecholamines and NPs link the heart and the lipolysis in adipose tissue (further details see below).

1.7 Cardiac metabolism

In the following part of the work, the cardiac metabolism is described in its physiological state and during HF-pathology.

1.7.1 Energy consumption of the heart and sources of ATP

The heart consumes more energy than any other organ. It requires about 6 kg ATP every day to pump around 10 tons of blood through the body (Neubauer, 2007). ATP binds to myosin and regulates its binding status to actin filaments, known as cross bridge cycle (Schmidt and Lang, 2011). In addition, ATP is also required for the active transport of Ca^{2+} and fuelling the Na^{+}/K^{+}-ATPase (Schmidt and Lang, 2011). However, storage of ATP lasts only for about one minute in cardiomyocytes to maintain all these processes. Therefore, the heart requires constant ATP production (Balaban, 2002; Mootha et al., 1997).

It is widely accepted that the heart is a metabolic omnivore and is capable of gaining energy from the oxidation of different substrates (Taegtmeyer, 2000). It has been reported that the heart relies predominantly on FFA (70%) and glucose (30%) (Neubauer, 2007; Nickel et al., 2013; Wang et al., 2014). In contrast, amino acids, ketone bodies, and lactate contribute to the overall cardiac metabolism only to a minor extent (Nickel et al., 2013).

1.7.2 Physiological Glucose and Fatty Acid Metabolism in the heart

Glucose uptake into the cardiomyocyte is mediated mainly by Glucose transporter GLUT1, GLUT4 and GLUT8 (Abel, 2004; Aerni-Flessner et al., 2012). In glycolysis, glucose is transformed to pyruvate. Pyruvate can enter the mitochondria through oxidation-pathway as acetyl-CoA. The ATP yield of glycolysis in the cytosol (2 ATP per molecule glucose) is relatively small when compared to FAO (130.7 ATP) (Loeffler, 2014; Nickel et al., 2013). However, glycolysis also produces ATP in an anaerobe environment without the requirement of mitochondria, which might be beneficial in the state of ischemia (Korvald et al., 2000).

FAO requires the uptake of FA in the cardiomyocyte. Fatty Acid Translocase (FAT/CD36) is a major translocase allowing FA uptake into cardiomyocytes (Ibrahimi et

al., 1999; Irie et al., 2003). FA is intracellularly esterified by fatty-acyl-CoA-synthase (FACS) to fatty acyl-CoA and finally translocated into the mitochondria for β-oxidation by carnitine palmitoyltransferase I (CPT-1) (Wang et al., 2014). CPT-1 is the rate-limiting enzyme of FAO and malonyl-CoA, which increases in FAO, is an inhibitor of CPT-1 (Beauloye et al., 2011). In addition, FAO is decreased by a higher concentration of its products $FADH_2$, NADH and acetyl-CoA and increased by β-adrenergic stimulation (Zhou et al., 2008).

1.7.3 Changes in Glucose Metabolism in Heart Failure

Studies investigating changes in glucose uptake and glucose utilization in HF are still inconsistent (Neubauer, 2007). In early stages of HF and especially in cardiac hypertrophy, animal studies reveal an increase in glucose uptake and glycolysis (Kolwicz and Tian, 2011; Nascimben et al., 2004; Remondino et al., 2000). The AMP-activated protein kinase (AMPK) is activated in the compensated stage of HF and increases glucose uptake and glycolysis (Abel and Doenst, 2011) (**Figure 1.7**).

However, in late-stages of HF in mice, the myocardium develops an insulin resistance (IR) with an impaired glucose uptake (Nikolaidis et al., 2004; Zhabyeyev et al., 2013). In addition, several studies in rodents report that in HF glucose utilization, including glucose oxidation, is impaired (Bugger et al., 2010; Doenst et al., 2010). Reduced glucose oxidation can be explained by the reduced expression of genes responsible for glycolysis and glucose oxidation in HF (Kato et al., 2010).

Moreover, in studies with rapid pacing-induced HF in dogs, glucose oxidation rather increases (Osorio et al., 2002). In addition to animal experiments, also the studies in humans indicate that cardiac glucose metabolism increases in idiopathic dilated cardiomyopathy (Davila-Roman et al., 2002). Doenst and colleagues suggest that changes in cardiac glucose metabolism might depend on the stage of HF or the model used to induce HF (Doenst et al., 2013). Importantly, while FAO decreases to a greater extent than glucose utilization, glucose oxidation is unable to compensate for the lack of ATP production in cardiomyocytes (Abel and Doenst, 2011).

1.7.4 Changes in Fatty Acid Metabolism in Heart Failure

The heart undergoes dramatic changes in FA metabolism in the development of HF, especially in the late stages (Neubauer, 2007). However, FA uptake and FAO are not negatively affected in mild-to-moderate stages of HF (NYHA II-III) (Wang et al., 2014). Studying induced compensated HF in dogs could not demonstrate a downregulation of

the expression of FAO enzymes (Chandler et al., 2004). Also in a Dahl salt-sensitive rats study, FA uptake and gene expression of FAO remained unchanged (Kato et al., 2010). In clinical studies, FA cardiac uptake of NYHA II-III patients remains unchanged (Funada et al., 2009). Some reports even suggested an increase in FAO in patients with NYHA II-III when compared to control patients (Paolisso et al., 1994).

In late-stage HF, the heart undergoes a reduction in myocardial ATP by about 30% (Ingwall, 2009; Ingwall and Weiss, 2004; Neubauer, 2007). In animal models, a switch in metabolic substrate utilization in advanced HF has been observed. The majority of studies point towards a reduction of FAO in the cardiomyocytes and a decrease of FA uptake (Abel and Doenst, 2011; Lionetti et al., 2011; Neubauer, 2007; Stanley et al., 2005) (**Figure 1.7**). FA uptake was reduced in Dahl salt-sensitive rats (Kato et al., 2010) and in decompensated pacing-induced HF in dogs (Osorio et al., 2002). It is widely accepted that FAO is reduced in advanced stages of HF. Ex-vivo studies on isolated rat hearts undergoing pressure overload (Allard et al., 1994; Christe and Rodgers, 1994) showed a reduced FAO. Also, in-vivo experiments in rats confirm a reduction of FAO in congestive HF (Akki et al., 2008; Doenst et al., 2010). Decompensated pacing-induced HF experiments in dogs confirm a reduction in FAO in advanced stages of heart failure (Lei et al., 2004; Osorio et al., 2002; Recchia et al., 1998). Positron emission tomography studies in patients with idiopathic dilated cardiomyopathy suggest a correlation with reduced FFA uptake and metabolism and the severity of hemodynamic impairment (Davila-Roman et al., 2002; Yazaki et al., 1999).

Changes in cardiac metabolism in heart failure have been investigated in several animal and human studies. In early stages of HF, FA cardiac uptake and FAO remain almost constant (Funada et al., 2009), while glycolysis increases (Kato et al., 2010). In late-stage HF, FAO and glycolysis decrease, but FAO to a much larger extent compared to glycolysis (Abel and Doenst, 2011) (**Figure 1.7**).

The change of FA uptake and FAO in the development of HF raises the question about the influence of FA release from adipose tissue on the development of HF.

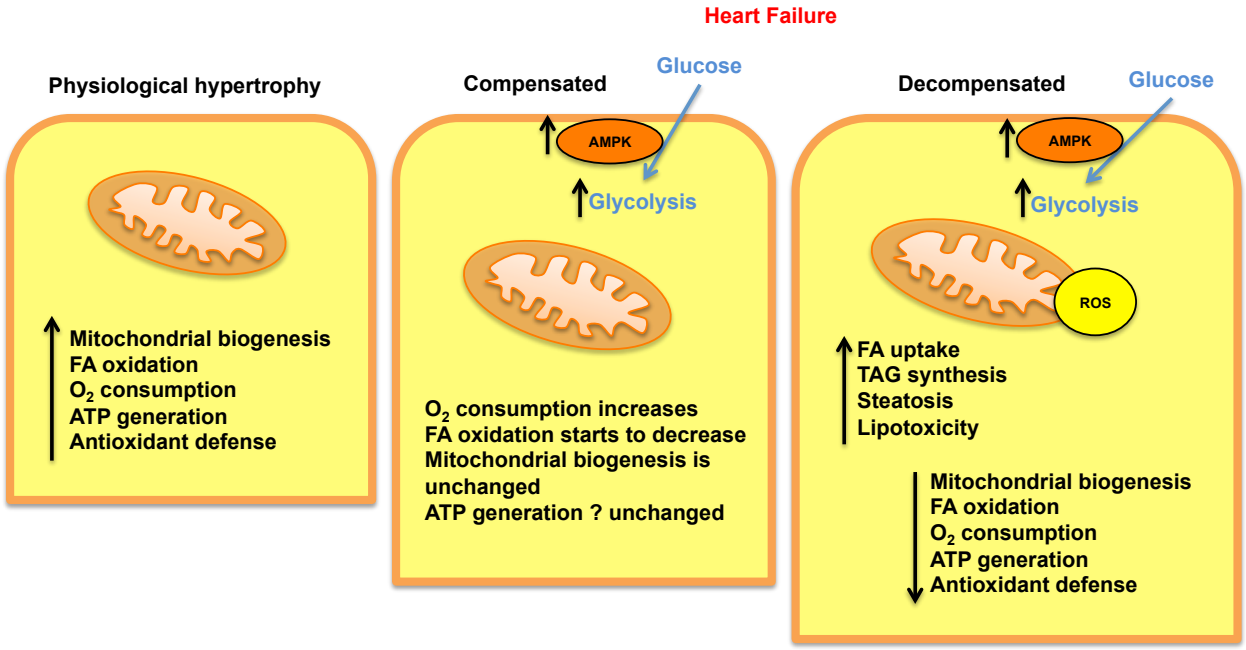

Figure 1.7 Changes in cardiac metabolism in heart failure

In physiological cardiac hypertrophy, there is an increase in mitochondrial biogenesis, FA oxidation, leading to higher O_2 consumption and consequently to more adenosine triphosphate (ATP) generation. In compensated heart failure glucose uptake and glycolysis are elevated due to an increase in AMP kinase (AMPK). Therefore O_2 consumption increases and FA oxidation starts to decrease. In decompensated heart failure FA uptake increases. The resulting lipotoxicity causes reduced mitochondrial function due to reactive oxygen species (ROS). This causes reduced FA oxidation and eventually reduced ATP generation (adapted from Abel and Doenst, 2011).

1.8 Systemic Metabolism and Lipolysis during Heart Failure

1.8.1 Role of Catecholamines during Heart Failure

The maintenance of mean arterial blood pressure (MAP) and heart rate strongly depends on the stimulation of the sympathetic nervous system (SNS) and the release of catecholamines, such as norepinephrine and epinephrine (Chaggar et al., 2009; Kemp and Conte, 2012). Preganglionic neurons of the SNS lie in the thoracolumbar region of the spinal cord. Their axons travel to the paravertebral ganglia and from here synapse with the postganglionic neurons, which transport their signal across the body. Postganglionic neurons release norepinephrine. The SNS also stimulates the adrenal medulla resulting in a release of norepinephrine and epinephrine directly into the blood (Schmidt and Lang, 2011).

Clinical studies showed that patients with HF had significantly higher norepinephrine levels than controls (Bolger et al., 2002; Cohn et al., 1984). The increased norepinephrine levels during HF cause elevated heart rates and contractility via β1-receptors and higher vascular resistance via α1-receptors resulting in an increase of

ventricular preload (LVEDV) (Kemp and Conte, 2012; Leimbach et al., 1986). These effects cause an increase in CO and MAP in patients with HF and are considered to be an initially compensatory mechanism (Chaggar et al., 2009). However, in patients with severe HF increased levels of norepinephrine correlate with increasing rates of mortality over time (Anand et al., 2003) and are closely related to the NYHA classification (Bolger et al., 2002). Norepinephrine was identified to promote adverse cardiac events such as ventricular arrhythmias, atrial fibrillation and hypertrophy (Chaggar et al., 2009; Parati and Esler, 2012).

Clinical trials demonstrated that the antagonism of SNS with β-blockers, such as metoprolol, improve cardiac function and clinical outcome in patients with chronic HF and are therefore recommended for treatment of chronic HF (Hjalmarson et al., 2000; Ponikowski et al., 2016).

1.8.2 Role of Natriuretic Peptides during Heart Failure

In addition to an increased catecholamine release, the levels of natriuretic peptides (NP), such as ANF and BNP are also elevated during ventricular and atrial overload (Yoshimura et al., 1993). Elevated BNP plasma levels reflect the ventricular dysfunction and correlate with NYHA classification (Yasue et al., 1994; Zaphiriou et al., 2005). Hence, measuring BNP or N-terminal pro-BNP in plasma is recommended as a diagnostic marker for HF in clinical practice (Ponikowski et al., 2016).

ANF was first discovered in atria of rats as a regulator of body fluid and salt homeostasis (de Bold, 1985). A few years after the discovery of ANF, BNP was identified in the porcine brain (Sudoh et al., 1988). Later, a third NP was discovered and called C-type natriuretic peptide (CNP) (Sudoh et al., 1990). ANF and BNP are mainly secreted from myocardium while CNP is predominantly produced in vascular endothelial cells (Don-Wauchope and McKelvie, 2015).

The main effect of NPs is the increase of diuresis and natriuresis. ANF and BNP are stored in specific atrial granules and released into the circulation due to ventricular wall stress caused by pressure or volume overload. Challenging mice with the overload-induced TAC model cause a significant increase in ANF and BNP levels in the myocardium in several studies (Gitau et al., 2015; Han et al., 2015; Westphal et al., 2012). ANF and BNP have overlapping effects. ANF induces relaxation of vascular smooth muscle cells and increases microvascular permeability. On the kidney, ANF causes a dilatation of afferent arterioles, a constriction of efferent arterioles and hence a

rise in glomerular filtration rate (GFR) and a reduction of sodium and water retention in the proximal tubules and collecting ducts. ANF also acts on the adrenal gland and reduces the aldosterone production. All these effects cause a reduction in blood pressure (Hayek and Nemer, 2011; Song et al., 2015). In addition, ANF and BNP have been identified as antifibrotic and antihypertrophic mediators on the heart (Oliver et al., 1997; Tamura et al., 2000).

Since ANF and BNP have such beneficial effects in the setting of pressure and volume overload, they are targets for HF treatment. While Nesiritide, a recombinant human BNP, showed no evidence of a decrease in the rate of death and rehospitalization in patients with acute HF (O'Connor et al., 2011), Carperitide, a recombinant human ANF, is in use for patients with HF in Japan (Mitaka et al., 2011).

1.8.3 Lipolytic activity of Catecholamines and Natriuretic Peptides

As catecholamines increase during HF, they have additional systemic metabolic effects. Catecholamines are described as the “master regulators of lipolysis” (Morigny et al., 2016). They stimulate lipolysis via β2-adrenergic and inhibit via α2- adrenergic receptors. The stimulation of G_s-protein coupled β2-adrenergic receptors activates adenylate cyclase (AC), which increases cAMP levels. Higher cAMP levels stimulate PKA, which activates HSL via phosphorylation. As explained above (1.4.4), PKA also phosphorylates Perilipin-1 causing lipid droplet fragmentation. Phosphorylated Perilipin-1 also releases CGI-58, causing it to interact with ATGL and allowing it to increase lipolytic activity (Morigny et al., 2016; Young and Zechner, 2013). In addition, β-adrenergic activation stimulates ATGL via PKA-mediated phosphorylation of ATGL on Ser406 (Pagnon et al., 2012) (**Figure 1.8**). In patients with HF, lipolysis is stimulated via increased levels of catecholamines resulting in elevated FA release (Lamba and Abraham, 2000; Riehle and Abel, 2016).

Interestingly, clinical studies demonstrated that ANF also increases circulating levels of FAs and glycerol in healthy subjects and patients with HF (Birkenfeld et al., 2005; Birkenfeld et al., 2006; Szabo et al., 2013). In addition, BNP was also identified to increase lipolytic activity in patients suffering from advanced HF and elevate FAs release (Polak et al., 2011). Receptors for ANF and BNP were found in human adipose tissue (Sarzani et al., 1996) and later both NPs were identified to stimulate lipolysis in adipose tissue (Sengenes et al., 2000). Importantly, the simultaneous stimulation with ANF and isoproterenol, a β-receptor agonist, results in an additive lipolytic effect. This

indicates that two independent signaling pathways are stimulating adipose tissue lipolysis (Moro et al., 2004).

ANF and BNP bind to natriuretic peptide receptor-A (NPR-A), a guanylyl cyclase-A (GC-A) coupled transmembrane receptor (Song et al., 2015). Binding to NPR-A activates the cytosolic GC-A receptor domain and results in increasing intracellular levels of cyclic guanosine monophosphate (cGMP) (Schlueter et al., 2014; Sengenes et al., 2003). Intracellular cGMP activates cGMP-dependent Protein Kinase G (PKG), which stimulates Perilipin-1 resulting in increased activity of HSL and higher lipolytic activity (Schlueter et al., 2014; Sengenes et al., 2003) (**Figure 1.8**). Natriuretic peptide receptor-C (NPR-C) is responsible for NP degradation and expressed in an opposite manner to NPR-A in adipose tissue (Morigny et al., 2016; Sarzani et al., 1995).

Catecholamines and NPs also induce “browning” of WAT and beige AT (Schlueter et al., 2014). Catecholamines phosphorylate p38 mitogen-activated protein kinase (p38-MAPK) via PKA, resulting in an increase of mitochondrial UCP1 expression (Cao et al., 2004; Cao et al., 2001). NPs mediate this process through cGMP (Bordicchia et al., 2012). In addition, ANF activates AMPK, which induces mitochondrial biogenesis and lipid oxidation (Souza et al., 2011) (**Figure 1.8**).

During the development of HF, catecholamines and NPs increase, which also results in increased lipolytic activity in adipocytes.

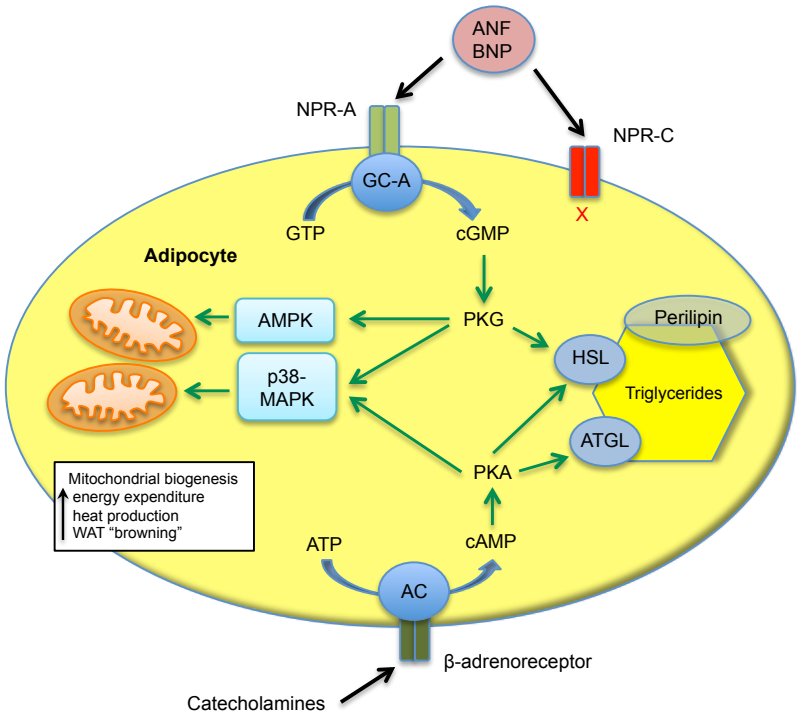

Figure 1.8 Natriuretic peptides and catecholamines effects in adipose tissue

Atrial natriuretic factor (ANF) and brain natriuretic peptide (BNP) bind to atrial natriuretic peptide receptor type A (NPR-A) in adipocytes. NPR-A is linked to guanylyl cyclase-A (GC-A), increasing cyclic guanosine monophosphate (cGMP), which activates Protein Kinase G (PKG). Catecholamines bind to β2-adrenergic receptors, causing an increase of cyclic adenosine monophosphate (cAMP) and Protein Kinase A (PKA). PKG and PKA phosphorylate hormone-sensitive lipase (HSL). PKA stimulates adipocyte triglyceride lipase (ATGL) via Perilipin. NPR-C causes NP degradation. PKG and PKA causing "browning" of WAT via AMP-activated protein kinase (AMPK) and p38 mitogen activated protein kinase (p38-MAPK). AC - adenylate cyclase; ATP - adenosine triphosphate; GTP - guanosine triphosphate (adapted from Schlueter et al., 2014).

1.8.4 Insulin Resistance during Heart Failure

As lipolysis increases during HF, the increased levels of FAs play a critical role in changes of the systemic metabolism, such as in the development of insulin resistance (IR) and increased glucose levels. Other mediators, besides FAs, responsible for IR are tumor necrosis factor α and IL-6 (Hajer et al., 2008). IR is defined as the failure of insulin to mediate glucose uptake in adipose tissue, skeletal muscle, and liver. However, IR is also a feature of HF (Riehle and Abel, 2016).

Acutely, FAs stimulate insulin secretion via increased intracellular calcium concentration in β-cells of the pancreas (Olofsson et al., 2004; Zhao et al., 2006). However, chronically elevated plasma FA levels result in IR and decreased glucose-stimulated insulin release through various mechanisms (Zhao et al., 2006). FAs induce serine phosphorylation of insulin receptor substrate, leading to a reduced capacity to be phosphorylated by insulin causing diminished GLUT4 translocation to the plasma membrane (Boden and Shulman, 2002; Hajer et al., 2008). Another mechanism is the

upregulation of UCP-2 in β-cells through FAs, which reduces ATP production and results in a decrease of glucose-stimulated insulin release (Rousset et al., 2004). Furthermore, FAs were identified to induce β-cell apoptosis through nuclear factor-kappaB (NF-kappaB) (Kharroubi et al., 2004). Increased IR and decreased β-cell insulin release result in higher levels of glucose and type 2 diabetes mellitus (T2DM) (Hajer et al., 2008).

In a clinical setting, a link between HF and T2DM has been recognized. Several large clinical trials demonstrated that a poor controlled glycemic index, IR, and hyperinsulinemia are associated with an increased risk of developing HF in patients with T2DM (Ingelsson et al., 2006; Iribarren et al., 2001; Velez et al., 2014). However, more evidence indicates that chronic HF itself could is causing IR. Patients with T2DM suffering from advanced HF were treated with left ventricular assist device (LVAD) and experienced an improvement in insulin sensitivity (Uriel et al., 2011). Chokshi and colleagues analyzed myocardium of non-diabetic patients with HF. Those patients showed systemic IR with reduced levels of myocardial insulin signaling molecules Akt, phosphorylated forkhead box O (pFoxO) and reduced expression of GLUT4. After implantation of LVAD Akt and pFoxO improved dramatically. These findings point towards increased IR in patients with HF (Chokshi et al., 2012).

As discussed above, the cardiac metabolism relies primarily on FAO and switches in late-stage HF to glycolysis (Abel and Doenst, 2011; Neubauer, 2007). In HF patients with IR however, the metabolic switch from FAO to glycolysis is abnormal (Peterson et al., 2004; Velez et al., 2014). Increased levels of malonyl-CoA inhibit CPT1, responsible for transferring FFA into mitochondria, during IR. This causes a redirection of Acyl-CoA toward lipid storage molecules such as TAG (Rasmussen et al., 2002). The excess lipid uptake results in lipotoxicity (Wende and Abel, 2010). The process of lipotoxicity may lead to reduced cellular signaling, mitochondrial dysfunction, decreased FAO, and increased apoptosis in the heart. These processes lead to further cardiac dysfunction (Riehle and Abel, 2016).

In summary, HF causes increased lipolysis in WAT via activation of SNS. This results in elevated FA levels and severe systemic metabolic changes, which may worsen cardiac metabolism and function.

1.9 Fatty Acids as mediators on the heart

As described above, WAT stores and releases FAs into the blood circulation, used by the heart as the primary source of ATP in a physiological state (Neubauer, 2007; Rosen and Spiegelman, 2006). In addition, FAs have recently been identified as signaling molecules capable of inducing cardiac hypertrophy (Riquelme et al., 2011). Riquelme and colleagues used the model of Burmese python to investigate physiological cardiac hypertrophy after feeding. The group observed a progressive increase in heart size post-prandial and could identify the FA mixture of myristic (C14:0), palmitic (C16:0) and palmitoleic acid (C16:1), causing a significant increase in LVM (Riquelme et al., 2011). Our previous study indicated, that palmitoleic acid (C16:1) could be considered as molecular co-mediator to induce non-proliferative cardiomyocyte growth in exercise-induced cardiac hypertrophy (Foryst-Ludwig et al., 2015). Our study demonstrated for the first time that adipose tissue lipolysis regulates the development of physiological hypertrophy and leads to the question of how important is WAT lipolysis and the release of FA into the blood circulation for the development of pathological LVH and HF.

2 Aim of Study

Myocardial metabolism undergoes dramatic changes in response to pathological LVH and HF, characterized by increased reliance on glucose oxidation, decreased FA uptake and oxidation, leading to a loss of metabolic flexibility (Neubauer, 2007). During the development of pathological LVH and HF, the sympathetic nervous system activity increases, resulting in elevated plasma levels of catecholamines and natriuretic peptides (Kemp and Conte, 2012). These mediators induce lipolysis in WAT and FA release in patients with HF compared to healthy controls (Polak et al., 2011; Riehle and Abel, 2016; Szabo et al., 2013). WAT lipolysis also causes insulin resistance and reduced glucose uptake (Morigny et al., 2016). The severe alterations in the systemic metabolism cause additional perturbations of the cardiac metabolism, which may contribute to further cardiac dysfunction (Riehle and Abel, 2016).

However, it is poorly understood how a stimulated lipolysis in WAT affects cardiac hypertrophy and function during the development of pathological LVH and HF.

Therefore, this study aimed to investigate the influence of WAT-specific lipolysis on the development of pathological LVH and HF in a pressure overload-induced cardiac hypertrophy model in mice. As ATGL is one of the main enzymes responsible for lipolysis in WAT (Young and Zechner, 2013), an adipose tissue-specific ATGL-KO mouse (atATGL-KO) was created. Transverse Aortic Constriction (TAC) was used to induce pathological LVH and HF. This study then tried to answer the following questions:

1. Does atATGL influences the cardiac phenotype and the cardiac function during the development of pathological LVH due to TAC?
2. Does atATGL influences the cardiac phenotype and cardiac function during the development of HF due to TAC?
3. Are there distinct changes in body composition due to atATGL?
4. Which influence does atATGL have on systemic insulin sensitivity and glucose levels?
5. Are any FA-species levels in plasma influenced by atATGL?

3 Methods and Materials

3.1 Materials

3.1.1 Equipment for animal experiments

Table 3.1 Equipment for animal experiments

Equipment	Company
26 – Gauge needle	Beckson Dickinson (Heidelberg, GER)
Animal cages type 2 IVC	Ehret Labor- und Pharmatechnik (Schönwalde, GER)
Baby-Mixter Hemostat - Curved 14 cm	Fine Science Tools (Heidelberg, GER)
BD Microlance 3 cannulas	Beckton Dickinson (Heidelberg, GER)
BD Plastipak 1 ml Sub-Q syringe	Beckton Dickinson (Heidelberg, GER)
Castroviejo Micro Needle Holder – 9 cm	Fine Science Tools (Heidelberg, GER)
Echo MRI-700	EchoMRI (Houston, USA)
ETHIBOND EXCEL™ Polyester Suture – 6.0, green braided	Ethicon (Norderstedt, GER)
Graefe Forceps - 0.8 mm Tips Curved	Fine Science Tools (Heidelberg, GER)
Heating pad	Sanitas (Uttenweiler, GER)
Infrared light	Petra (Burgau, GER)
Iris Scissors - ToughCut Straight (length 9cm)	Fine Science Tools (Heidelberg, GER)
Iris Scissors - ToughCut Tungsten Carbide Straight (length 11.5 cm)	Fine Science Tools (Heidelberg, GER)
Mouse Ventilator minivent Type 845, 230 V	Hugo Sachs Elektronik - Havard Apparatus GmbH (March, GER)
Non-sterile silk suture thread – 6.0	Fine Science Tools (Heidelberg, GER)
PERMA-HAND™ Silk Suture – 6.0, black braided	Ethicon (Norderstedt, GER)
Precision XTRA Blood Glucose Meter	Abbott (Wiesbaden, GER)
Precision XTRA Blood Glucose Test Strips	Abbott (Wiesbaden, GER)
Scale for weighting animals PK2000	Mettler-Toledo (Gießen, GER)
Stereomicroscope MZ12.5	Leica (Biberach, GER)

TSE PhenoMaster / LabMaster	TSE Systems (Bad Homburg, GER)
Vevo 770 High-Resolution In Vivo Micro-Imaging System with RMV 707 transducer	VisualSonics (Toronto, CAN)

3.1.2 Substances for animal experiments

Table 3.2 Substances for animal experiments

Substances	**Company**
Acepromazine	Sigma-Aldrich (Taufkirchen, GER)
Actrapid HM ® 40 I.E. / mL	Novo Nordisk (Küsnacht, CHE)
Braunol	Braun Melsungen (Melsungen, GER)
Ethanol 96 %	Merck (Darmstadt, GER)
Isoflurane Forene®	Abbott (Wiesbaden, GER)
Ketamine hydrochloride	Sigma-Aldrich (Taufkirchen, GER)
Metamizole (Novaminsulfon-Ratiopharm)	Ratiopharm GmbH (Ulm, GER)
NaCl	Merck (Darmstadt, GER)
Rimadyl (carprofen)	Pfizer (Berlin, GER)
Veet hair removal cream with Aloe vera	Reckitt Benckiser (Slough, GBR)
Xylazine hydrochloride	Sigma-Aldrich (Taufkirchen, GER)

3.1.3 Laboratory equipment

Table 3.3 Laboratory equipment

Equipment	**Company**
96-well multiply PCR plates	Sarstedt AG (Nümbrecht, GER)
Agilent 1200 HPLC system	Agilent Technologies® (Böblingen, GER)
Agilent 6460 Triple Quadrupole LC/MS	Agilent Technologies® (Böblingen, GER)
Bioruptor, Tissue ruptor	Diagenode (Liège, BEL)
Centrifuge 5810R	Eppendorf (Hamburg, GER)
Centrifuges	Eppendorf (Hamburg, GER)
Descosept AF	Dr. Schumacher (Malsfeld, GER)
Falcons (different sizes)	Beckton Dickinson (Heidelberg, GER)
Gel Dokumentation System	INTAS (Göttingen, GER)

Incubator	GFL 3033 (Burgwedel, GER)
Lysis Tubes	Analytik Jena (Jena, GER)
Mastercycler® Gradient	Eppendorf (Hamburg, GER)
Microscope	Keyence Deutschland GmbH (Neu-Isenburg, GER)
Microscope Slides (Superfrost)	Menzel-Gläser (Braunschweig, GER)
Microtome Biocut	Leica (Wetzlar, GER)
Multipipette®, Research PLUS® pipettes	Eppendorf (Hamburg, GER)
Nanodrop® ND-1000	PeqLab (Erlangen, GER)
Parafilm® M Barrier Film	SPI supplies (Glasgow, GBR)
Phenomenex Kinetex-C18	Phenomenex (Torrance, USA)
Proline® pipettes	Biophit (Helsinki, FIN)
Real-Time Device Strategene® MX3000P	Agilent Technologies (Waldbronn, GER)
Shandon Citadel 2000 tissue processor	Thermo Fisher Scientific (Waltham, USA)
Speed Mill	Analytik Jena (Jena, GER)
Vortex-Genie® 2T	Scientiis (Baltimore, USA)

3.1.4 Laboratory substances

Table 3.4 Laboratory substances

Substances	**Company**
Agarose Gel (for gel electrophoresis)	Biozym (Hess. Oldendorf, GER)
Aqua dist.	Braun Melsungen (Melsungen, GER)
Eosin-Phloxine	Sigma-Aldrich (Taufkirchen, GER)
Ethanol absolute (<99,9 %)	J.T Baker (Deventer, NED)
Ethidium Bromide solution (1%)	Avantor Performance Materials (Deventer, NED)
Eukitt® mounting medium	Sigma-Aldrich (Taufkirchen, GER)
Formaldehyde solution	Merck (Darmstadt, GER)
Hämatoxylin	Sigma-Aldrich (Taufkirchen, GER)
Hydrogen Peroxide Solution	Sigma-Aldrich (Taufkirchen, GER)
Hydromount®	Biozym Scientific GmbH (Hessisch

	Oldendorf, GER)
Isopropyl Alcohol	Morphisto (Frankfurt am Main, GER)
Methanol	Merck (Darmstadt, GER)
Orange G	Merck (Darmstadt, GER)
Paraffin Typ 6 und 9	Richard-Allan Scientific (Kalamazoo, USA)
PCR 50 - 2,000 bp Marker	Sigma-Aldrich (Taufkirchen, GER)
Phosphate buffered saline (PBS)	Gibco by Life technologies (Karlsruhe, GER)
Proteinase K	Invitek (Berlin, GER)
Real-Time SYBR-Green® Mastermix	Applied Biosystems (Darmstadt, GER)
RNase ZAP	Sigma-Aldrich (Taufkirchen, GER)
Roti®-ImmunoBlot	Carl Roth (Karlsruhe, GER)
Taq and Buffer for PCR (Gen Therm DNA-Polymerase) (GEN-003-1000)	Rapidozym (Berlin, GER)
Ultrapure Water	Biochrom AG (Berlin, GER)
Weigert´s iron hematoxylin	Morphisto (Frankfurt am Main, GER)
Xylol	Merck (Darmstadt, GER)
β-Mercaptoethanol	Sigma-Aldrich (Taufkirchen, GER)
Chloroform	Merck (Darmstadt, GER)

3.1.5 Kits

Table 3.5 Kits

Kits	**Company**
dNTP-Set (GEN-009-250)	Rapidozym (Berlin, GER)
Invisorb® Spin Tissue Mini Kit	STRATEC Molecular GmbH (Berlin, GER)
NEFA Standard	Wako Chemicals (Neuss, GER)
NEFA-HR (2) R1-Set	Wako Chemicals (Neuss, GER)
NEFA-HR (2) R2-Set	Wako Chemicals (Neuss, GER)
RNase-Free DNase Set	Qiagen (Hilden, GER)
RNeasy® Micro Kit	Qiagen (Hilden, GER)

Vectastain Elite ABC Kit	Vector Laboratories (Burlingame, USA)

3.1.6 Antibodies

Table 3.6 Antibodies

Antibody	**Company**
Biotinylated Goat Anti-Mouse IgG Antibody	Vector Laboratories (Burlingame, USA)
Myeloid/Histiocyte Antigen MAC387	Dako (Hamburg, GER)

3.1.7 Primer sequences

Table 3.7 Primer sequences for Genotyping

Gene	**Primer sequence**
ATGL for (ET7)	CggTgAgggTggggAACggAgTC
ATGL rev (ET8)	CAgggggCCAggCggTCAgA
Cre for (G6)	gCATTACCggTCgATgCAACgAgTg
Cre rev (G7)	gAACgCTAgAgCCTgTTTTgCACgTTC

Table 3.8 Primer sequences for qRT-PCR

Gene	**Forward primer sequence**	**Reverse primer sequence**
mm18S	ACCTggTTgATCCTgCCAgTAg	TTAATgAgCCATTCgCAgTTTC
mmANF	AggAgAAgATgCCggTAgAAgA	gCTTCCTCAgTCTgCTCACTCA
mmBNP	CACCgCTgggAggTCACT	gTgAggCCTTggTCCTTCAA
mmβ-MyHC	TTCCTTACTTgCTACCCTC	CTTCTCAgACTTCCgCAg

3.1.8 Nucleic acid and enzymes

Table 3.9 Substances for cDNA synthesis

Substances	**Company**
Deoxynucleotide triphosphates (dNTPs)	Promega (Mannheim, GER)
M-MLV Reverse Transcriptase	Promega (Mannheim, GER)
M-MLV RT 5x Puffer	Promega (Mannheim, GER)

Random Primer	Promega (Mannheim, GER)
RNAsin	Promega (Mannheim, GER)

3.1.9 Animals

B6.129-Pnpla2tm1Eek (ATGL-flox) — Erin E. Kershaw, M.D.
Division of Endocrinology, Diabetes, and Metabolism
University of Pittsburgh
200 Lothrop Street, BST E1140
Pittsburgh, PA 15261, USA

B6.Cg-Tg(Fabp4-cre)1Rev/J (aP2-Cre) mice — Jackson Laboratory (Sulzfeld, GER)

3.1.10 Software

Table 3.10 Software

Software	**Company**	**Used for**
Endnote	Thomson Reuters	Citation Manager
Grammarly	Grammarly, Inc. (San Francisco, USA)	Proofreader
Labmaster Software	TSE Systems (Bad Homburg, GER)	LabMaster and indirect calorimetry analysis
Olympus Stream	Olympus GmbH (Hamburg, GER)	Analysis software for microscopic images
PlagAware	PlagAware Unternehmergesellschaft	Plagiarism Check
Prism 6 for Mac OS X	GraphPad Software, Inc.	Statistical analysis and Figures
PubMed	US National Library of Medicine National Institutes of Health	References
RT2 ProfilerTM PCR Array Data Analysis version 3.5	Qiagen (Hilden, GER)	Data analysis for qrt-PCR
Vevo 770 3.0.0	Visual Sonics	Echocardiographic analysis
Word, Excel and Powerpoint 2011	Microsoft	Data analysis

3.2 Methods

3.2.1 Ethical statement

All animal procedures were performed in agreement with the guidelines of the Charité-Universitätsmedizin Berlin and the German Law on the Protection of Animals. The Regional Office for Health and Social Affairs Berlin (LaGeSo) approved all animal experiments (approval number: 0272/12).

3.2.2 Generating adipose tissue-specific ATGL knockout mice

Adipose tissue-specific ATGL knockout mice (atATGL-KO) were generated by crossing B6.129-Pnpla2tm1Eek (ATGL-flox) mice (Sitnick et al., 2013; Villena et al., 2004) with B6.Cg-Tg(Fabp4-cre)1Rev/J mice (aP2-Cre). In ATGL-flox mouse the region of the target gene (Patatin-Like Phospholipase Domain Containing 2 - PNPLA2 = ATGL) is flanked (floxed) by two lowP sites, inserted into introns 1 and 7 of the ATGL gene by using bacterial cloning vectors (Obrowsky et al., 2013). The aP2-Cre mouse expresses Cre protein (cre – “causes recombination”) in adipocytes in white and brown adipose tissue (Abel et al., 2001). By crossing ATGL-flox with aP2-Cre mouse, recombination occurs when the two loxP-sites on the DNA string interact with the Cre recombinase. The result is an excision of DNA-fragment flanked by both loxP sites (Barlow et al., 1997). Hence, the ATGL gene is excised in adipose tissue. PCR was used for genotyping the male transgenic mice at the age of three weeks. Only male mice were used for the experiments.

3.2.3 PCR for Genotyping

For genotyping the Polymerase Chain Reaction (PCR) - Amplification was used to differentiate between atATGL-KO and wild-type (WT) mice. Genomic DNA (gDNA) was isolated from mouse tail cuts. Isolation of DNA was performed using Invisorb® Spin Tissue Mini Kit and manufacture’s protocol was followed. After successful isolation, gDNA was analyzed using PCR-based method (**Table 3.11**). To identify the mice throughout the entire experiment ear-punching system was used.

Table 3.11 PCR Protocol

A

PCR Mix	Volumes
DNA	2.0 µl
dNTPs	1.0 µl
Buffer + MgCl	5.0 µl
Cre for	0.5 µl
Cre rev	0.5 µl
Taq	0.25 µl
H_2O	38.75 µl
Total volume	50.00 µl

B

Thermal profile	Time
95°	3 min
95°	30 sec
55°	30 sec
72°	45 sec
72°	10 min
4°	forever
35 cycles	

A PCR Mix used for Genotyping. **B** Thermal profile used for PCR.

Primer-specific PCR amplification products were subjected to gel electrophoresis (110 Volts for 25 min) using 1% to 1,5% agarose gel (1xTAE-Buffer) together with size markers, a positive (DNA from Cre+/Cre+/flox+/flox- mouse) and negative (without DNA) PCR-control products. Results were documented by photography (**Figure 3.1**).

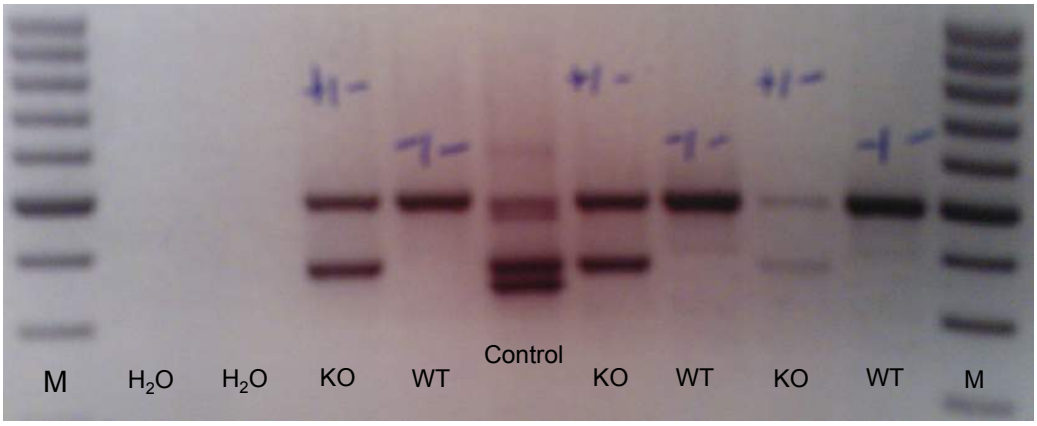

Figure 3.1 Representative photos of genotyping atATGL-KO and WT mice

M = Marker; H_2O = Water negative control; KO = atATGL-KO mice (1st DNA band = 380bp, 2nd DNA band = 497bp); WT = WT mice (1st DNA band = 380bp)

3.2.4 Experimental procedure with animals in TAC model

Male WT and atATGL-KO mice were housed, in a temperature controlled facility with a 12-h light-dark cycle and fed ad libitum with standard diet, as previously described (Foryst-Ludwig et al., 2015). As sex-specific differences in the development of cardiac hypertrophy and heart failure between male and female mice are well described (Kararigas et al., 2014; Skavdahl et al., 2005), only male mice were included in this

study. 8 to 9 weeks old male atATGL-KO and WT mice underwent transverse aortic constriction (TAC) or Sham-surgery. Animals were divided into four groups:

A.) Sham-operated WT mice

B.) TAC-operated WT mice

C.) Sham-operated atATGL-KO mice

D.) TAC-operated atATGL-KO mice

Echocardiographical evaluation of cardiac hypertrophy and cardiac function were performed 5 and 11 weeks after surgery. Ten weeks post-OP Nuclear Magnetic Resonance (NMR) and intraperitoneal Glucose Tolerance Test (ipGTT) were completed, following by the Intraperitoneal Insulin Tolerance Test (ipITT). After the recovery period (week 11 post-OP) the animals were sacrificed and the organs were harvested and used for gene expression, histological and metabolic analyses (**Figure 3.2**).

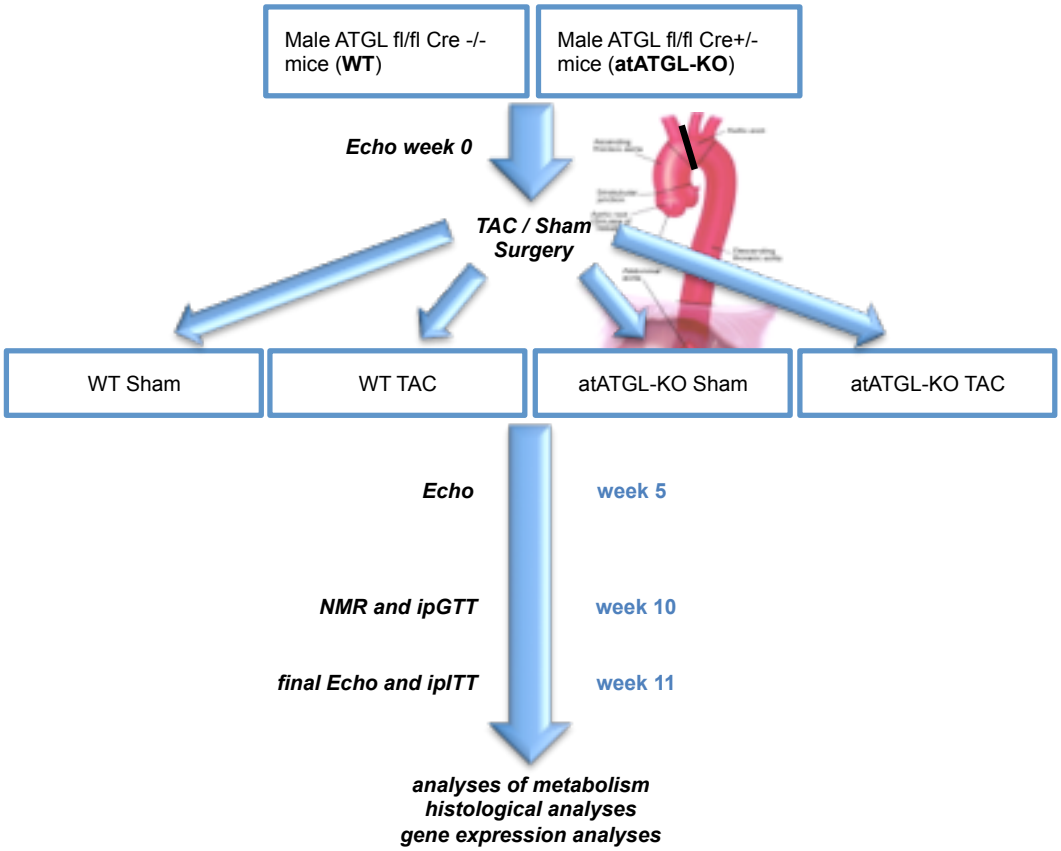

Figure 3.2 Overview of experimental procedure with TAC model

3.2.5 Transverse aortic constriction

Standard transverse aortic constriction (TAC) was used to induce cardiac hypertrophy and chronic heart failure (Fliegner et al., 2010; Kararigas et al., 2014). Briefly: mice were anesthetized by injecting an intraperitoneal (i.p.) ketamine hydrochloride/xylazine hydrochloride/acepromazine (80 mg/ml; 12 mg/ml; 10mg/ml) solution with a dose of 1 mg/kg (Fliegner et al., 2010; Grune et al., 2016). Then, mice were placed in a supine position on top of a heating pad. After anesthesia mice were intubated using the plastic tube of an intravenous catheter and ventilated using a Mouse Minivent Type 845 (Hugo Sachs Elektronik). All mice were ventilated with a breathing volume of 200 µL and 200 breaths per minute. Fur was removed by using Veet hair removal cream and Rimadyl (5.0 mg/kg per kg BW) was injected i.p. as analgesia during surgery. Partial thoracotomy was performed until the second rip, before thymus was gently separated. Aorta and carotid arteries were then exposed. The transverse aorta was ligated between innominate artery and common carotid artery. Hereby a 6.0 non-sterile silk suture (FST) was ligated against a 26.0 Gauge needle. The needle was quickly removed, leaving a narrowing of the aorta of 0.46 mm in diameter (Tarnavski et al., 2004). Rip cage was closed using 6.0 sterile PERMA-HAND Silk Suture (Ethicon). The skin was sutured using a 6.0 sterile Polyester Suture (Ethicon). The surgery lasted for approximately 30 minutes. Mice recovered from anesthesia under normal conditions and normal ventilation using an infrared light lamp. For analgesia after TAC mice were given Metamizole by drinking water for seven days. To evaluate the narrowing of the transverse aorta, animals underwent echocardiography one week after TAC.

3.2.6 Sham surgery

For the placebo surgical intervention (Sham), mice were anaesthetised and the rip cage was opened in the same way as in TAC-operated mice. However, no constriction of the transverse aorta was performed. Rip cage and skin were closed in the same manner as described in 3.2.5. SHAM operated animals also underwent echocardiography one week after surgery to evaluate transverse aorta.

3.2.7 Echocardiography

Two-dimensional echocardiography was used to evaluate cardiac hypertrophy, cardiac function and ligation of the aortic arch after TAC. It was performed one week before, as well as one-, five- and eleven- weeks after surgery (TAC or Sham) using Vevo 770 High-Resolution In Vivo Micro-Imaging System with RMV 707 transducer

(VisualSonics). To perform echocardiography, mice were anesthetized with 3% Isoflurane inhalation, which was reduced to 1.5% as soon as mice were seduced. Afterward, the mice were fixed on a heating pad at 37°C to reduce body heat loss and continuously monitored with an electrocardiogram. Fur was removed using Veet hair removal cream. In parasternal short axis view, B-Mode was used to film left ventricle. M-Mode was used for measurements of the wall thickness of left ventricle in diastole and systole. To evaluate ligation, the transducer was held just above transverse aorta and Doppler images of velocity were taken (**Figure 3.3**). The entire procedure lasted for 10-15 minutes.

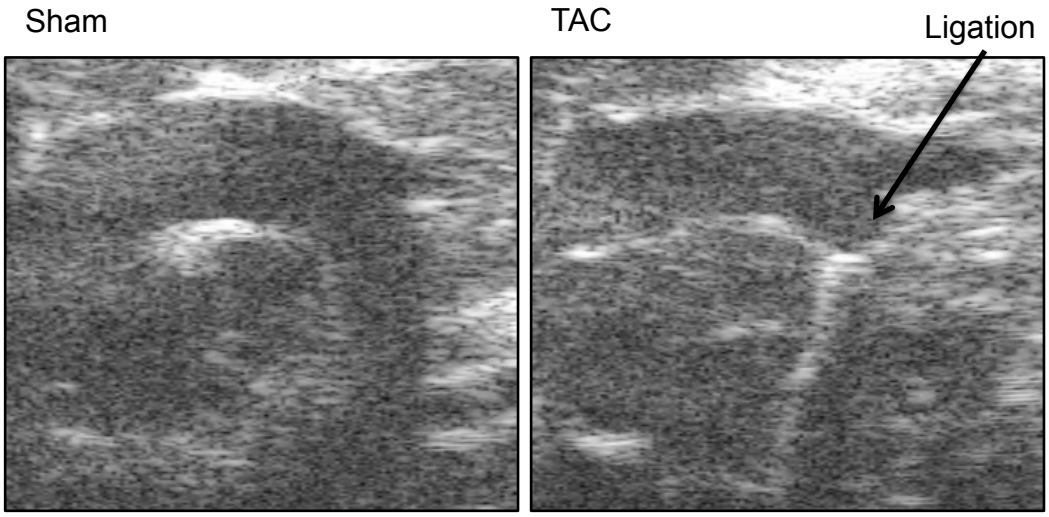

Figure 3.3 Representative B-mode pictures of Sham and TAC ligation at aorta

Doppler echocardiography over the aorta was used to verify the success of ligation.

3.2.8 Echocardiographical calculation

M-Mode images were used to measure interventricular septum thickness (ISV), left ventricular internal diameter (LVID) and left ventricular posterior wall (LVPW). Doppler images were used to measure velocity on ligation of the transverse aorta. Left ventricular mass (LVM) was calculated using IVS, LVID and LVPW, according to manufacturer's instructions (Vevo 770, VisualSonics). For calculation, the LVM Penn Cube formula was used (Armstrong et al., 2012; Collins et al., 2003; Perdrix et al., 2011):

$$LVM = 1.05\ x\ ((IVS + LVID + LVPW)^3 - LVID^3)$$

In the Penn Cube formula, LVM estimation is based on subtraction of the LVID from the "volume enclosed by the surrounding epicardium to obtain the myocardial volume, then multiplying by the myocardial density (1.05 g/ml)" (Armstrong et al., 2012).

For evaluating of cardiac function, ejection fraction (EF%) and fractional shortening (FS%) were used. EF% is the volume of blood pumped out by each single heartbeat in comparison to the end-diastolic volume in the left ventricle. FS% represents the reduction in size of the left ventricle from diastole to systole and was also presented in percentage:

$$EF\% = \frac{LVvol, diastole - LVvol, systole}{LVvol, diastole} x100$$

LVvol, diastole – end-diastolic left ventricular volume
LVvol, systole – end-systolic left ventricular volume

$$FS\% = \frac{LVID, diastole - LVID, systole}{LVID, diastole} x100$$

LVID, diastole – end-diastolic left ventricular internal diameter
LVID, systole – end-systolic left ventricular internal diameter

To evaluate the success of the ligation at the transverse aorta, Doppler echocardiography was performed. Blood flow velocities in the site of the transverse aorta constriction and proximal to the ligation were measured. By using Bernoulli´s equation pressure differences (Δp) were calculated. Bernoulli´s equation states that an increase in the velocity of fluid causes a decrease of internal pressure (Fritsche, 2013). It describes a conservation of energy in an ideal fluid that flows through different large tubes. However, the equation only applies to a laminar flow without any energy loss.

$$p_1 + \frac{1}{2}\rho v_1^2 = p_2 + \frac{1}{2}\rho v_2^2 = constant$$

Bernoulli´s equation
p – Pressure [Pa = kg*m^{-1}*s^{-2}]; ρ – density [kg*m^{-3}]; v – velocity [m*s^{-1}]

Bernoulli´s formula it can be used to calculate a pressure difference (Δp) between the pressure on the ligation site and proximal to it. The density of blood was taken to be 1060 kg* m^{-3} (Shmukler, 2004) and the pressure was expressed in mmHg.

$$p_1 + \frac{1}{2}\rho v_1^2 = p_2 + \frac{1}{2}\rho v_2^2 = constant$$

$$p_1 - p_2 = \frac{1}{2}\rho(v_2 - v_1)^2$$

$$\Delta p = 3.97(v_2 - v_1)^2 \approx 4(v_2 - v_1)^2$$

Bernoulli´s equation rearranged for calculating pressure difference.

Animals with pressure differences of less than 30mmHg after TAC were excluded from the experiments.

3.2.9 Measurement of body composition

To determine fat mass, lean mass, free water and total water body content Nuclear Magnetic Resonance (NMR) was used. Mice were weighed and then placed in a plastic tube and transferred in the Echo MRI-700. The whole procedure took 30 seconds. All measurements were divided by the individual body weight of each animal measured on the day of NMR measurement.

3.2.10 Glucose Tolerance Test (ipGTT)

Glucose tolerance was measured ten weeks after surgery. Before measurement, mice fasted overnight. Mice were weighed and blood samples of the tail vein were taken to measure basal fasting glucose levels (time = 0 min). Then glucose was injected intraperitoneally (1 g/kg BW). Glucose levels were measured 15, 30, 60, 90, 120 and 150 min after glucose injection.

The Area under the Curve (AUC) was used to calculate the ipGTT results (Haffner et al., 1986; Psyrogiannis et al., 2003). The sum of two following points in time of blood glucose levels was divided by two and then multiplied by the time between the points.

Example:

Time (min):	0	15	30	60	90	120
Blood glucose levels:	A	B	C	D	E	F

$$AUC = \left(\frac{A+B}{2x15}\right) + \left(\frac{B+C}{2x15}\right) + \left(\frac{C+D}{2x30}\right) + \left(\frac{D+E}{2x30}\right) + \left(\frac{E+F}{2x30}\right)$$

3.2.11 Insulin Tolerance Test (iplTT)

Insulin tolerance test was carried out 11 weeks after surgery. Again, mice fasted overnight and were weighted before the experiment. First, blood samples were taken from the tail vein to measure glucose levels before injecting insulin. Insulin (Actrapid HM, Novo Nordisk) 0.25 I.E./kg BW was injected intraperitoneally (time = 0 min). Then glucose levels were measured 15, 30, 60, 90, 120, 150 and 180 min after insulin injection. AUC was calculated according to the formula shown in 3.2.10.

3.2.12 Metabolic investigations using LabMaster

11 weeks after surgery, metabolic phenotype of the animals was investigated using the TSE-LabMaster (TSE Systems). The mice were set in individual metabolic cages for 24 h. Mice were fed ad libitum with a standard diet. Food and water intake was measured using an electronic scale. Locomotor activity of the animals was measured using an infrared light beam in the X and Y plane. Integrated indirect gas calorimetry allowed

measurements of O_2 consumption, CO_2 production, respiratory exchange rate, substrate utilization and energy expenditure (Gribok et al., 2013).

3.2.13 Indirect Gas Calorimetry

Indirect Gas Calorimetry uses the measurements of carbon dioxide (CO_2) production and the oxygen (O_2) consumption to calculate which substrate (FFA or glucose) was primarily metabolized by the animals. The amount of O_2 consumption can be used to determine energy expenditure. Proteins play a minor role in energy expenditure (Gekle, 2014). For the oxidation of glucose, the same amount of O_2 is consumed as CO_2 is produced:

$$Glucose + \mathbf{6O_2} + 31ADP + 31P_i \longrightarrow Heat + \mathbf{6CO_2} + 31ATP + 6H_2O$$

For 1 mole of glucose, 6 moles of O_2 need to be consumed. If the energy expenditure were based on FFA, more oxygen would be consumed than CO_2 is produced (example: 1 mole of palmitic acids needs 23 moles of O_2 and produces 16 moles of CO_2). A parameter of CO_2-production/O_2-consumption (VCO_2/VO_2) is called respiratory quotient (RQ). It is a dimensionless number, which represents the main substrate being consumed by the body. RQ is 1.0 if the body would consume glucose only. Under high-fat diet feeding, RQ value would be about 0.7 (Hall, 2011).

VCO_2 and VO_2 were measured every 15 min over a period of 24 h. Mice were put into cages one day before taking measurements so that they could adapt to environmental change. By using VCO_2 and VO_2, energy expenditure could be determined using the Frenz formula (Frenz, 1999):

$$EE = 16.17VO_2 + 5.03VCO_2 + 5.98N$$

EE-energy expenditure (kJ/d); VO_2 - rate of oxygen consumption (l / d); rate of carbon dioxide production (l /d); N - excreted nitrogen in the urine (g/d) was estimated as being 0.1.

3.2.14 Organ extraction, tissue fixation and embedding

Animals were anesthetized using isoflurane and sacrificed 11 weeks after surgery. Final blood samples were taken retrobulbar after mice were anesthetized using isoflurane. Then animals were sacrificed and organs were harvested. Organs were weighed and then immediately placed in 10% formalin solution. Parts of the organs which were used for determination of RNA and protein expression were shock-frozen in liquid nitrogen and stored at -80°C. For histological analysis, tissues were formalin-fixed for up to 24 h. After washing in PBS-Puffer, tissues were embedded in paraffin using Shandon Citadel 2000 tissue processor. For embedding tissue manufacturer´s protocol was followed. To remove alcohol from tissue, tissue samples were placed in xylol for one hour. Afterward,

tissues were put in paraffin 6 for 1.5h and then in paraffin 9 for 1.5h. Paraffin blocks were prepared, microtome sections of 2-5µm thickness were cut and put onto slides. Slides were allowed to dry in an incubator overnight.

3.2.15 Hematoxylin-Eosin staining

Histological methods and analyses were performed in collaboration with Prof. R. Klopfleisch´s Lab in the Department of Veterinary Pathology, Freie Universität (FU) Berlin (Klopfleisch et al., 2013). Hematoxylin-Eosin (HE) staining (**Table 3.12**) was used to analyze heart diameter and left-ventricular diameter for each sample.

Table 3.12 Hematoxylin-Eosin staining protocol

Step		**Time**
1	Deparaffinized sections in xylol	2 x 5 min
2	Rehydrate in descending ethanol series (96%, 80%, 70%, 50%)	3 min each
3	Wash in Aqua dest.	3 min
4	Stain in Hematoxylin solution	13 min
5	Wash in warm tap water	10 min
6	Stain in Eosin-Phloxine solution and brief wash in Aqua dest.	2 min
7	Dehydrate in ascending ethanol series (70%, 80%, 90%, 2x100%)	10-20 sec
8	Clear in Xylol solution	2 x 5min
9	Mount with Eukitt®	

3.2.16 Picrosirius Red staining

Picrosirius Red staining (**Table 3.13**) was used to evaluate fibrosis in heart tissue.

Table 3.13 Picrosirius Red staining protocol

Step		**Time**
1	Deparaffinized sections in xylol	2 x 10 min
2	Rehydrate in descending ethanol series (96%, 80%, 70%, 60%)	4 min each
3	Wash in Tap water	8 min
4	Stain with Weigert´s iron hematoxylin	13 min
5	Wash in Aqua dest.	5 sec.

6	Wash under warm tap water	10 min
7	Aqua dest.	1 min
8	Stain in Picrosirius Red Solution	1 h
9	Acetic Acid 30%	2 x 1 min
10	96% Ethanol	2 x 4 min
11	Isopropyl Alcohol	4 min
12	Clear in Xylol solution	2 x 10 min
13	Mount with Eukitt®	

In collaboration with Prof. Klopfleisch´s Lab, slices were evaluated while the investigator was blinded. The degree of fibrosis was assigned with score of 0 (none/slight), 1 (mild), 2 (moderate) and 3 (severe) (semiquantitative analysis). HE and Picrosirius Red-stained heart tissue sections of mice were analyzed using Analysis Software (Olympus). For this purpose, the heart-size was measured using following procedure: three axes were drawn through both ventricles and the midpoint (interventricular septum). Using these axes, ventricular volumes were measured. The mean of all three values was taken for further calculations.

3.2.17 Immunohistochemical analysis

Immunohistochemical staining (**Table 3.14**) was used to identify macrophages in heart using macrophage-specific marker MAC3 (MAC387 – mouse monoclonal antibody to macrophages). For the staining, 4 to 5 µm sections of Formalin-fixed and paraffin-embedded heart tissues were prepared as previously described (Klose et al., 2011).

Table 3.14 Immunohistochemical staining protocol with MAC387-antibody

Step		**Time**
1	Deparaffinized in Xylol	2 x 10 min
2	Rehydrate in descending ethanol series (96%, 80%, 70%, 60%)	4 min each
3	Incubate in methanol/3% hydrogen peroxide	20 min
4	Put Slides in heated citric buffer	12 min
5	Let Slides cool down	15 min
6	Wash in PBS	10 sec.
7	Blocking with 10% Roti-Immunoblot	30 min

8	Put 150µl of 1:100 mouse-antihuman MAC387 antibody for macrophages on slides	
9	Incubate overnight at 4°C	24 h
10	Wash in PBS	3 x 5 min
11	Put 150µl of 1:200 biotinylated secondary goat-anti-mouse antibody on slides	
12	Incubate at room temperature	1 h
13	Immunolabeling with Vectastain Elite ABC Kit	30 min
14	Wash in PBS	3 x 5 min
15	Mount with Hydromount®	

3.2.18 RNA isolation and quantification of heart tissue

To isolate total RNA from animal tissue, RNeasy Micro Kit (Qiagen) was used. All steps were performed according to manufacturer's protocol. Before mRNA isolation, all equipment and the working area were disinfected and afterward cleaned using RNase-ZAP (Sigma) to deactivate RNAses. Heart tissue was lysed with Lysis-β-Mercaptoethanol solution. Disruption and homogenization of tissue were performed using Speed Mill (Analytik Jena). Tissue samples were homogenized in Lysis Tubes (13.000 rpm). Afterward, the samples were incubated with 200µl Chloroform, mixed and centrifuged (15 min; 4 °C; 15.000 rpm). The water-fraction was isolated from the samples, mixed (vol/vol) with 70% Ethanol and applied on the silica-gel-based membrane columns, specific for RNA (RNeasy-MinElute-Spin-Filter membrane (QIAGEN®, 2007)). After binding of the RNA to the filter membrane and washing steps (using 350µl RW1-Buffer and centrifugation (15 sec; RT; 10.000 rpm)). DNase was used to remove gDNA from the RNA-sample. DNase was applied directly on the filter membrane, applied as 80µl DNase-RDD-Mastermixs (RNase-Free DNase Set Qiagen). After 15 min of incubation, DNase and other contaminants were washed away using 350µl RW1-Puffer / 2 x 500µl RPE-Puffer, each step, followed by centrifugation (15 sec; RT; 10.000 rpm). After additional centrifugation step (1 min; RT; 10.000 rpm) total purified RNA was eluted twice using RNase-free water for a higher yield. The kit provides a method to isolate up to 15µg total RNA from heart tissue. RNA was then stored at -80°C. Quality and concentration of isolated mRNA were measured using Nano-Drop (PeqLab), a method of photometric determination of nucleic acid concentration.

3.2.19 Reverse transcription for cDNA synthesis

Before quantitative real-time PCR (qRT-PCR) could be performed, the isolated mRNA needed to be transcribed into cDNA. 1µl of mRNA was diluted in 37.0µl H_2O and 1µl of Random Primers was added to the mixture. The mixture was then heated to 70°C for annealing for 5 min before being put on ice. A master mix (**Table 3.15**) was prepared and then added to each sample. Finally, samples were incubated at 37°C for 1 h.

Table 3.15 Protocol for reverse transcriptase

	cDNA-MIX
RNA diluted in water	37.0 µl
Random Primers	1 µl
H_2O	-
M-MLV Puffer	10 µl
dNTPs (10mM)	1 µl
RNAsin	0.50 µl
M-MLV Reverse Transcriptase	0.50 µl
Total volume	50.00 µl

3.2.20 Quantitative real-time PCR (qRT-PCR)

Gene expression levels were measured using qRT-PCR-technique. The principle of that method is based on the measurements of a fluorescent dye, which intercalates with double-stranded DNA during PCR-amplification using specific primer pair. The amount of DNA is then increased in each PCR-cycle, which leads to an increase of the fluorescence signal intensity. SYBR® Green I was used as the fluorescent dye to intercalate with DNA. Specific primers were used to analyze specific gene expressions (**Table 3.8** - Primer Sequences for qRT-PCR). Real-Time PCR was carried out in a thermal cycler (Real-Time Device Strategene® MX3000P). The protocol for qRT-PCR can be found below **Table 3.16**.

Polymerase chain reaction requires the following three steps:

1. Denaturation step: Hydrogen bonds between complementary bases in double-stranded DNA are disrupted.
2. Annealing step: Hybridization of single-stranded primers to single-stranded primers to single-stranded DNA.
3. Elongation step: DNA Polymerase synthesizes new DNA strand complementary to the single-stranded DNA template.

Table 3.16 Protocol for qRT-PCR using SYBR® Green I

	qRT-PCR Mix
cDNA	4.0 µl
Mastermix SYBR® Green I	12.5 µl
Forward Primer	0.25 µl
Reverse Primer	0.25 µl
	ad 25.00 µl H_2O

Primer sequences can be found in **Table 3.8** (Primer Sequences for qRT-PCR).

3.2.21 Measurement of Free Fatty Acids (FFA) in blood

The concentration of FFA was measured in retrobulbar blood samples, which were collected briefly before sacrificing animals. NEFA-Standard (Wako Chemicals) was used to measure FFA. Hereby manufacture's protocol was followed precisely. 5µl of the sample were placed in 96 well plates with 200µl of R1-reagent. After incubation at 37°C for 10 min, 100µl of R2-reagent was added and extinction was measured at 550 nm.

3.2.22 Fatty Acid Profiling

In order to identify individual FAs in the blood serum of animals, FA profiling was performed in collaboration Dr. Michael Rothe of Lipidomix. To perform FA profiling, high-performance liquid chromatography (HPLC) was combined with a triple quad mass spectrometer (MS). Combining HPLC with MS causes physical separation of components from the blood sample and letting them enter the MS at different times (Last et al., 2007). The method was previously described (Foryst-Ludwig et al., 2015). First of all 100µl of the blood plasma sample from mice were hydrolysed with 100µl NaOH (10mol/l) at 80°C for 60 min. Acetic acid (100µl) was used to neutralize the samples. An aliquot of 50µl was diluted with methanol (1:10) containing internal standards (C15:0, C21:0 50µg, C20:4-d8, C18:2-d4 5µg, C20:5-d5, C22:6-d5 1µg). To

perform HPLC, an Agilent 1200 HPLC system (Agilent Technologies®) was used. In HPLC, a small portion of the liquid sample is injected into a tube (column) packed with tiny particles (called the stationary phase). The components of the sample are forced down the column with a liquid or HPLC solvent (mobile phase) by using high pressure, which is delivered by an HPLC pump (**Figure 3.4**) consisted of a binary pump, autosampler and column thermostat. The column thermostat was equipped with a Phenomenex Kinetex-C18 column 2.6µm, 2.1x15mm column using a solvent system of aqueous formic acid (0.1%) and acetonitrile (description adapted from Phenomenex® and Agilent Technologies, Inc (Agilent Technologies)).

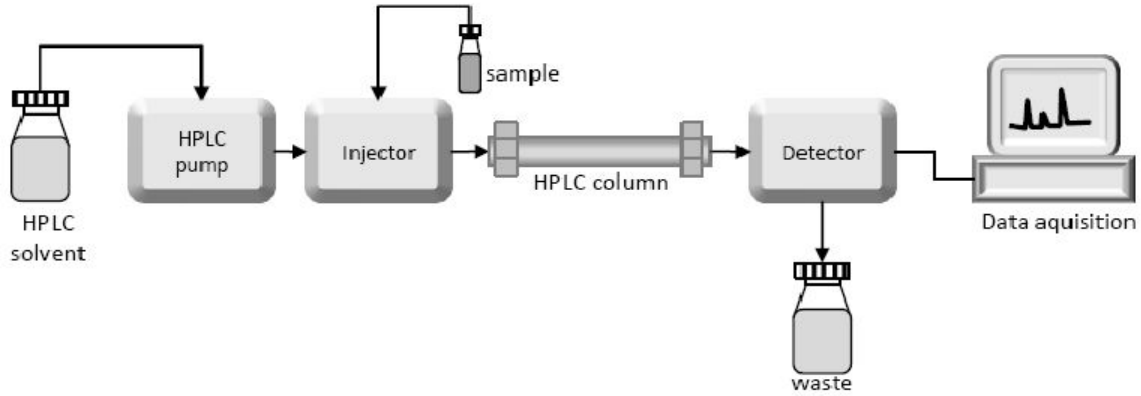

Figure 3.4 High-Performance Liquid Chromatography (HPLC)

(adapted from LaboratoryInfo.com, Giri, 2015)

The HPLC solvent gradient started at 70% acetonitrile and was increased to 98% within 10 min and hold for 14 min at a flow rate of 0.4 ml/min and 5µl injection volume (Foryst-Ludwig et al., 2015). Due to different chemical and physical interactions between the molecules of the components and the particles in the column, components were separated. At the end of the column, a detector identified the components and measured their quantity. HPLC was coupled with a triple quad mass spectrometer (Agilent 6460, Agilent Technologies®), with electrospray ionization source operated in negatively selected ion mode (**Figure 3.5**) (Agilent Technologies).

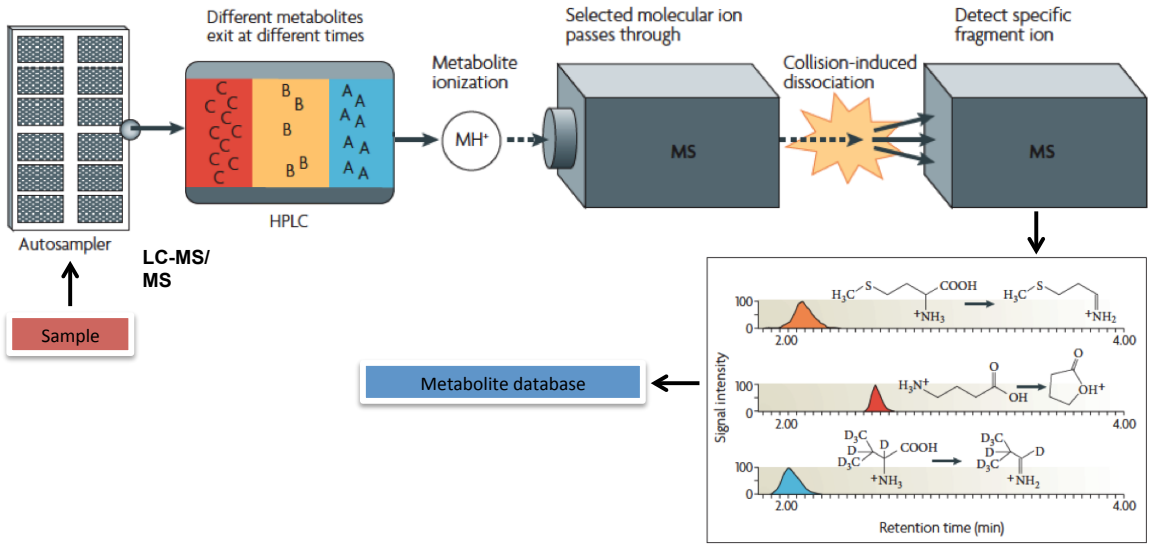

Figure 3.5 Liquid Chromatography (LC) separations with mass spectrometer (MS) (adapted from Last et al., 2007)

3.2.23 Statistical analysis

The statistical analysis was performed using Prism GraphPad 6.0. For parametric testing, 2-way analysis of variance (ANOVA) followed by Bonferroni posttest was carried out. Where appropriate, unpaired T-Test was used. P-values of *p<0.05, **p<0.01, ***p<0.001 and ****p<0.0001 were assumed to be statistically significant. All results are shown as mean ± SEM. Test performed, numbers of individuals in each group (n) and p-values are indicated below each figure.

4 Results

4.1 Cardiac phenotyping

4.1.1 5 weeks after TAC/Sham-surgery

To investigate the impact of adipose tissue ATGL on the development of pathological cardiac hypertrophy in vivo we used the transverse aortic constriction (TAC) model in mice. TAC or Sham surgery was performed in adipose tissue-specific ATGL-deficient mice (atATGL-KO) and WT control mice. Sham-operated atATGL-KO and WT animals were used as controls. Afterward, the animals underwent cardiac phenotyping.

4.1.1.1 Aortic Velocity and Pressure difference due to ligation

To evaluate the success of the TAC-surgery in our model, we first measured the velocity at the site of ligation and pressure differences (∆p - between flow proximal to ligation and in the site of the TAC) using Doppler echocardiography 5 weeks after TAC/Sham-surgery (**Table 4.1**). The rearranged Bernoulli´s equation was used to calculate the pressure difference (∆p) between the pressure on the ligation site and proximal to it as described in 3.2.8. The results clearly show that TAC induced a significantly higher ($p<0.0001$) flow velocity in the site of the ligation. This caused a significantly larger ($p<0.0001$) pressure difference between the point in the site of the ligation and proximal to the ligation. Importantly, there were no differences in between the WT and atATGL-KO mice. The slightly negative ∆p values in both Sham-operated groups indicate just some higher pressures proximal to ligation than at the site of ligation.

Table 4.1 Velocity and Pressure difference on transverse aorta 5 weeks after surgery

	WT Sham	WT TAC	atATGL-KO Sham	atATGL-KO TAC
velocity [$m*s^{-1}$]	891.9 ± 44.8	3432.6 ± 79.4****	961.5 ± 83.4	3552.8 ± 84.4####
∆p [mmHg]	-3.84 ± 2.61	43.28 ± 2.29****	-4.92 ± 2.20	46.02 ± 2.11####

Velocity in the site of the ligation (velocity) and pressure difference (Δp). Mean ± SEM; n(Sham) = 9, n(TAC) = 12, ****p<0.0001 vs. WT Sham, ####p<0.0001 vs. atATGL-KO Sham; 2-way ANOVA (Bonferroni posttest).

4.1.1.2 Left ventricular hypertrophy evaluated by echocardiography

Using echocardiographic measurements of wall thickness and internal diameter, left ventricular mass (LVM), LVM to tibia length (TL) ratio and LVM to body weight (BW) ratio were calculated. LVM of WT and atATGL-KO mice after TAC-surgery were significantly larger compared to Sham-operated mice respectively (**Table 4.2**). Also, LVM/TL and LVM/BW ratio analysis revealed that TAC intervention induces significant development of LVH when compared to Sham-operated control mice (**Table 4.2**). There were no significant differences between the two genotypes concerning LVM, LVM/TL and LVM/BW 5 weeks after TAC (**Table 4.2**). Additionally, LVM values, as well as LVM/TL and LVM/BW ratios, confirmed that WT had a slightly larger LVM compared to atATGL-KO which was however not significant.

Table 4.2 Left ventricular mass 5 weeks after TAC/Sham-surgery

	WT Sham	WT TAC	atATGL-KO Sham	atATGL-KO TAC
LVM [mg]	109.8 ± 3.7	159.2 ± 10.6***	99.6 ± 5.3	147.1 ± 6.8$^{###}$
LVM / BW [mg/g]	3.82 ± 0.12	5.77 ± 0.33****	3.67 ± 0.16	5.19 ± 0.22$^{###}$
LVM / TL [mg/mm]	9.02 ± 0.24	13.13 ± 0.86****	8.44 ± 0.43	12.31 ± 0.52$^{###}$

Left ventricular mass measured (LVM), left ventricular mass to body weight ratio (LVM / BW) and left ventricular mass to tibia length ratio (LVM/TL). Mean and SEM; n(Sham) = 9, n(TAC) = 12, ***p<0.001 / ****p<0.0001 vs. WT Sham, $^{###}$p<0.001 vs. atATGL-KO Sham; 2-way ANOVA (Bonferroni posttest).

4.1.1.3 Wall thickness and internal diameter of hearts

Echocardiographic measurements 5 weeks after surgery revealed that interventricular septum thickness (IVS-d) and left ventricular posterior wall thickness (LVPW-d) in diastole were significantly higher after TAC compared to Sham surgery in WT and atATGL-KO (**Table 4.3**). Left ventricular internal diameter in diastole (LVID-d) remained constant in both genotypes. LVID-d was slightly smaller in atATGL-KO animals compared to WT animals. There were, however, no significant differences in IVS-d, LVPW-d or LVID-d between the two genotypes (**Table 4.3**).

Table 4.3 Wall thickness and internal diameter 5 weeks after TAC/Sham-surgery

	WT Sham	WT TAC	atATGL-KO Sham	atATGL-KO TAC
IVS-d [mm]	0.61 ± 0.02	0.86 ± 0.03****	0.63 ± 0.02	0.85 ± 0.03####
LVID-d [mm]	4.51 ± 0.09	4.50 ± 0.14	4.36 ± 0.09	4.34 ± 0.07
LVPW-d [mm]	0.61 ± 0.02	0.86 ± 0.03****	0.63 ± 0.02	0.85 ± 0.03####

Interventricular septum thickness in diastole (IVS-d), left ventricular posterior wall thickness in diastole (LVPW-d) and left ventricular internal diameter in diastole (LVID-d). Mean and SEM; n(Sham) = 9, n(TAC) = 12, ****p<0.0001 vs. WT Sham, ####p<0.0001 vs. atATGL-KO Sham; 2-way ANOVA (Bonferroni posttest).

4.1.1.4 Ejection fraction and fractional shortening

Ejection fraction (EF%) and fractional shortening (FS%) decreased due to TAC-surgery in both genotypes (**Table 4.4**). However, there were no significant differences between the interventional groups. This indicates, despite TAC-intervention induced development of cardiac hypertrophy in our model, there were no TAC-or genotype-specific differences in the cardiac function 5 weeks after TAC-surgery.

Table 4.4 Ejection Fraction (EF%) and Fractional Shortening (FS%) 5 weeks after TAC/Sham-surgery

	WT Sham	WT TAC	atATGL-KO Sham	atATGL-KO TAC
EF [%]	44.8 ± 3.1	39.1 ± 2.3	45.4 ± 1.9	40.2 ± 3.2
FS [%]	22.4 ± 1.9	18.4 ± 1.0	22.5 ± 1.1	19.8 ± 1.9

Ejection Fraction (EF%) and Fractional Shortening (FS%). Mean and SEM; n(Sham) = 9, n(TAC) = 12; 2-way ANOVA (Bonferroni posttest).

4.1.2 11 weeks after TAC/Sham-surgery

Next, we performed cardiac phenotyping of mice 11 weeks after TAC/Sham-surgery. This was done to investigate the impact of adipose tissue-specific ATGL on the development of heart failure, since long-term pressure overload in this model has been shown to induce LV-dysfunction.

4.1.2.1 Increase of heart weight due to transverse aortic constriction

11 weeks after TAC/Sham-surgery BW of atATGL-KO mice post-TAC was significantly lower compared to WT mice post-TAC (**Figure 4.1** A). Heart weight to BW ratio (HW/BW) and heart weight to tibia length (HW/TL) ratio increased significantly in both genotypes due to TAC-surgery compared to Sham-surgery controls (**Figure 4.1** B and C). atATGL-KO mice showed significantly smaller HW/BW and HW/TL ratios in comparison to WT after TAC-surgery (HW/BW: mean±SEM; WT-TAC 6.48±0.32 g/kg; atATGL-KO-TAC 5.27±0.36 g/kg, $p<0.05$; HW/TL: WT-TAC 164.1±8.2 mg/cm; atATGL-KO-TAC 129.3±9.5 mg/cm, $p<0.01$).

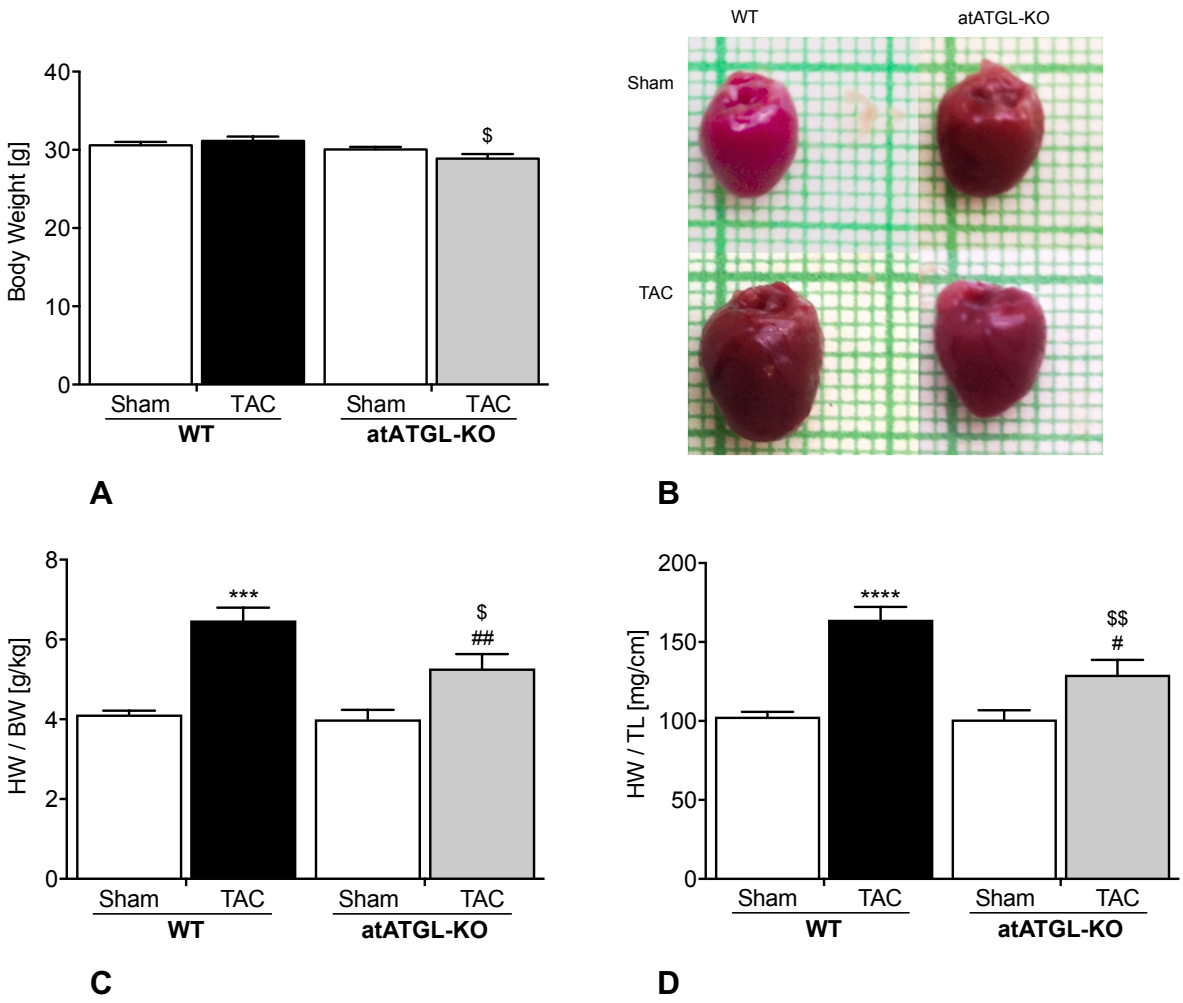

Figure 4.1 Body weight and heart weight to body weight / tibia length ratio 11 weeks after TAC/Sham-surgery

A Body-weight 11 weeks after TAC/Sham-surgery on the day of organ harvesting. **B** Representative images of the hearts 11 weeks after TAC/Sham-surgery. **C** Hearts of all mice were weighted post-mortem. Heart weight / body weight ratio (HW/BW). **D** Heart weight / tibia length (HW/TL). Mean ± SEM; n = 5-6, ***p<0.001 / ****p<0.0001 vs. WT Sham, $p<0.05 / $$p<0.01 vs. WT TAC, #p<0.05 / ##p<0.01 vs. atATGL-KO Sham; 2-way ANOVA (Bonferroni posttest).

4.1.2.2 Aortic Velocity and Pressure difference due to ligation

Similar to experiments performed 5 weeks after TAC-surgery (4.1.1.1) we compared TAC-induced changes in blood velocity proximal to ligation and at the site of ligation using Doppler echocardiography on the aortic arch. Pressure differences (Δp) were calculated according to the formula in 3.2.8. Velocities on the ligation after TAC were significantly higher compared to Sham-operated animals (**Table 4.5**). Importantly, velocities and pressure differences did not vary between WT and atATGL-KO groups after TAC-surgery. This indicates that the degree of ligation was very similar in both TAC-operated groups.

Table 4.5 Velocity and Pressure differences on transverse aorta 11 weeks after surgery

	WT Sham	WT TAC	atATGL-KO Sham	atATGL-KO TAC
velocity [m*s^{-1}]	881.2 ± 83.4	3783.7 ± 91.6****	884.1 ± 112.4	3679.7 ± 161.2$^{\#\#\#\#}$
∆p [mmHg]	-1.97 ± 0.82	54.15 ± 2.48****	-0.74 ± 1.31	48.10 ± 3.36$^{\#\#\#\#}$

Velocity in the site of the ligation (velocity) and pressure difference (Δp). Mean ± SEM; n = 5-6, ****p<0.0001 vs. WT Sham, $^{\#\#\#\#}$p<0.0001 vs. atATGL-KO Sham, 2-way ANOVA (Bonferroni posttest).

4.1.2.3 Left ventricular hypertrophy evaluated by echocardiography

11 weeks after TAC/Sham-surgery, mice underwent final echocardiography. LVM was calculated from myocardial and internal ventricular measurements in M-Mode. In both genotypes, LVM increased after TAC when compared to Sham-operated groups (**Figure 4.2** A, B and C). However, TAC-operated at-ATGL-KO developed an attenuated cardiac hypertrophy, characterized by significant lower LVM compared to WT after TAC (LVM: mean±SEM; WT TAC 211.16±19.73mg; atATGL-KO TAC 124.32±9.06mg). Also LVM/BW ratio (**Figure 4.2** B) and LVM/TL (**Figure 4.2** C) significantly decreased in atATGL-KO mice when compared to WT mice after TAC (LVM/BW: mean±SEM, WT TAC 7.17±0.79mg/g vs. atATGL-KO TAC 4.17±0.23mg/g, p<0.001; LVM/TL: mean±SEM, WT TAC 17.06±1.50 mg/mm vs. atATGL-KO TAC 10.53±0.70 mg/mm, p<0.001).

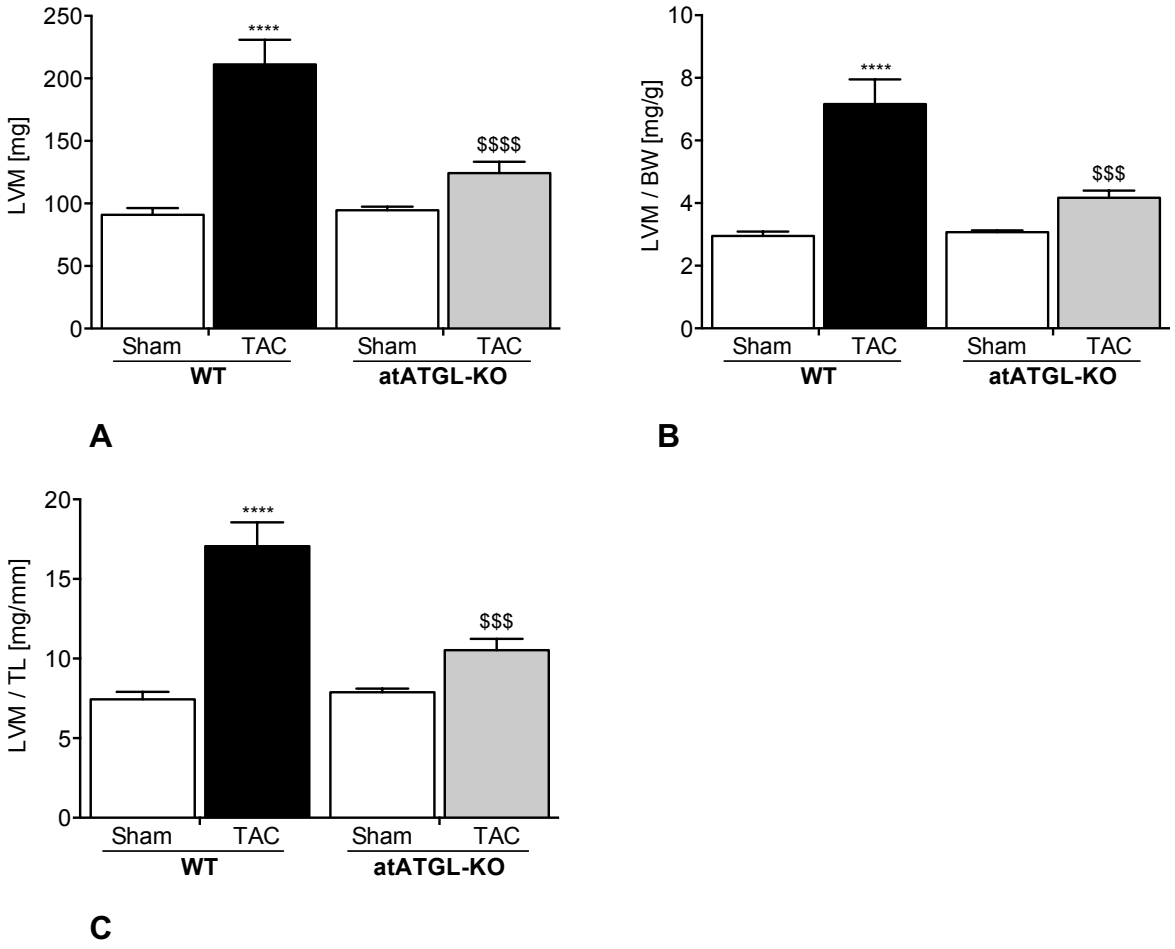

Figure 4.2 TAC-induced cardiac hypertrophy in mice evaluated with echocardiography

A Left ventricular mass measured (LVM). **B** Left ventricular mass to body weight ratio (LVM/BW). **C** Left ventricular mass to tibia length ratio (LVM/TL). Mean ± SEM; n = 7, ****p<0.0001 vs. WT Sham, $^{\$\$\$}$p<0.001 / $^{\$\$\$\$}$p<0.0001 vs. WT TAC; 2-way ANOVA (Bonferroni posttest).

4.1.2.4 Wall thickness and internal diameter of hearts

Next, myocardial wall thickness and left ventricular internal diameters were investigated using echocardiography (**Figure 4.3**). Hereby, IVS-d, LVID-d and LVPW-d during diastole were measured in M-Mode. In atATGL-KO and WT, myocardial walls were significantly thicker 11 weeks after TAC compared to Sham-operated groups (**Figure 4.3** A and B). The increase of IVS-d and LVPW-d in both genotypes indicates the development of cardiac hypertrophy due to TAC 11 weeks after surgery (**Table 4.6**). However, LVID-d significantly increased only in WT mice after TAC compared to Sham-operated mice. There was no significant difference in LVID-d-values measured in Sham- and TAC-operated atATGL-KO mice (**Figure 4.3** C). Representative M-Mode images revealed, that WT mice after TAC had an enlarged LVID-d compared to

atATGL-KO mice after TAC (**Figure 4.4**). Those results indicated, that TAC-induced cardiac dilatation occurred only in WT mice, but did not in atATGL-KO mice.

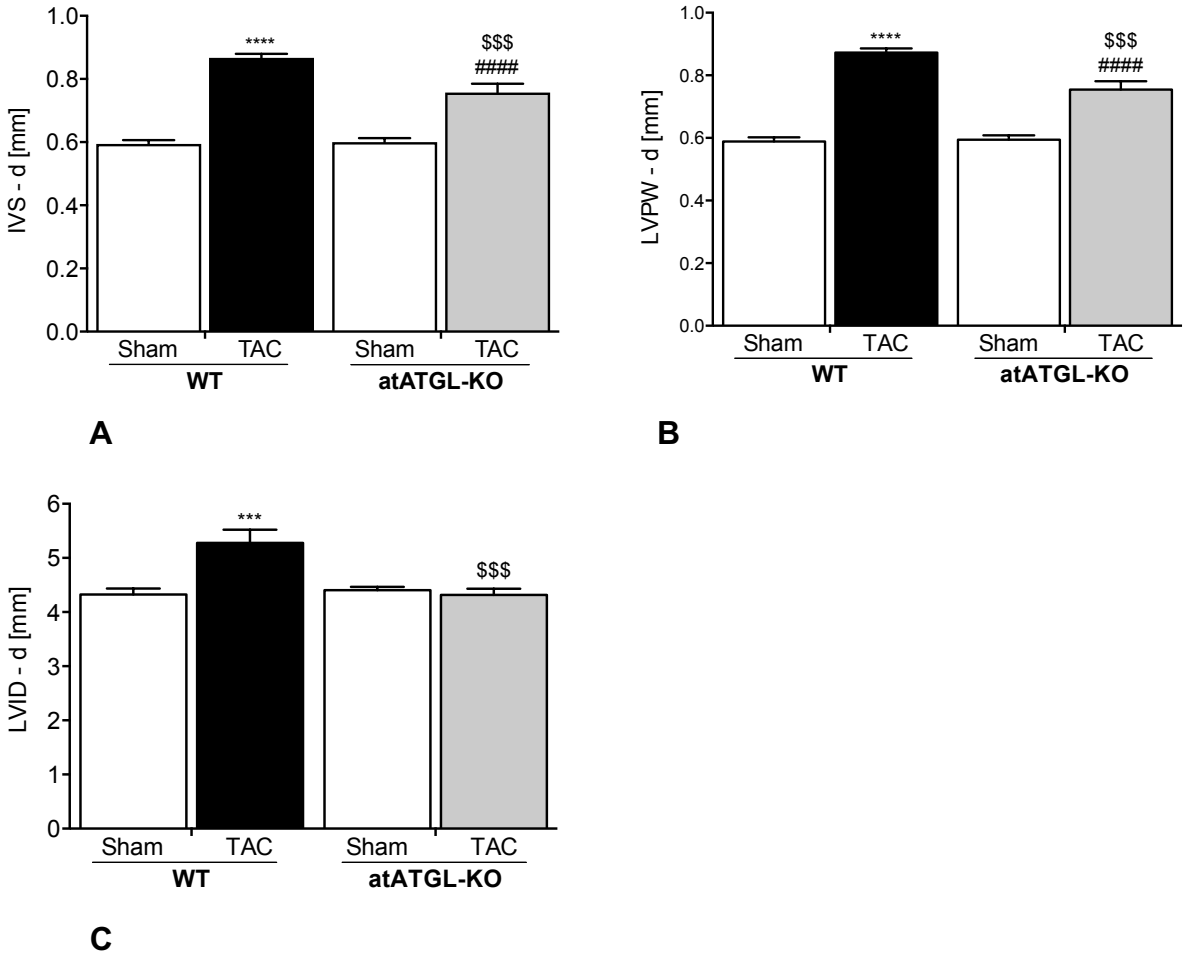

Figure 4.3 Left ventricular wall thickness and left ventricular internal diameter

A Interventricular septum thickness in diastole (IVS-d). **B** Left ventricular posterior wall thickness in diastole (LVPW-d). **C** Left ventricular internal diameter in diastole (LVID-d). Mean ± SEM. n = 7, ***p<0.001 / ****p<0.0001 vs. WT Sham, $^{\$\$}$p<0.01 / $^{\$\$\$}$p<0.001 vs. WT TAC, $^{\#\#\#\#}$p<0.0001 vs. atATGL-KO Sham, 2-way ANOVA (Bonferroni posttest).

Table 4.6 Echocardiographical measurements of IVS-d, LVPW-d, and LVID-d 11 weeks after TAC/Sham-surgery

	WT Sham	WT TAC	atATGL-KO Sham	atATGL-KO TAC
IVS-d [mm]	0.59 ± 0.01	0.87 ± 0.01****	0.60 ± 0.01	0.76 ± 0.03$^{\#\#\#\# \$\$\$}$
LVPW-d [mm]	0.59 ± 0.01	0.87 ± 0.01****	0.59 ± 0.01	0.75 ± 0.03$^{\#\#\#\# \$\$\$}$
LVID-d [mm]	4.32 ± 0.11	5.28 ± 0.24***	4.40 ± 0.06	4.31 ± 0.11$^{\$\$\$}$

Interventricular septum thickness in diastole (IVS-d), left ventricular posterior wall thickness in diastole (LVPW-d) and left ventricular internal diameter in diastole (LVID-d). Mean ± SEM; n = 7, ***p<0.001 / ****p<0.0001 vs. WT Sham, $^{\$\$}$p<0.01 / $^{\$\$\$}$p<0.001 vs. WT TAC, $^{\#\#\#\#}$p<0.0001 vs. atATGL-KO Sham; 2-way ANOVA (Bonferroni posttest).

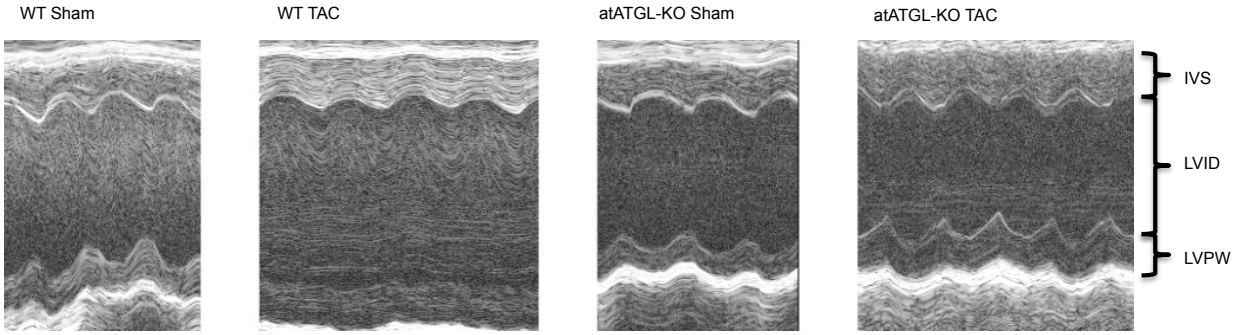

Figure 4.4 Representative echocardiography M-Mode images of WT and atATGL-KO mice after Sham and TAC

Abbreviations: IVS: Interventricular septum thickness; LVID: Left ventricular internal diameter; LVPW: Left ventricular posterior wall thickness.

4.1.2.5 Ejection fraction and fractional shortening

Using echocardiography, the systolic cardiac function was evaluated. As measurements of cardiac function, EF%, and FS% were used. In WT mice, EF% was significantly reduced in TAC group when compared to WT-Sham-operated mice (mean±SEM; WT Sham 47.71±2.06 % vs. WT TAC 23.84±1.78 %, p<0.0001). However, atATGL-KO mice had a preserved EF% after TAC-surgery, which was similar to EF% of Sham-operated mice (mean±SEM; atATGL-KO Sham 43.89±0.88 %; atATGL-KO TAC 40.72±1.34 %). These results indicate, that 11 weeks after TAC-surgery, EF% of atATGL-KO mice was preserved compared to WT mice (p<0.0001) (**Figure 4.5** A).

Eleven weeks after TAC-surgery, WT mice showed a significantly reduced FS% compared to WT-Sham-operated mice (mean±SEM; WT Sham 23.85±1.19 % vs. WT TAC 9.64±1.16 %, p<0.0001). However, FS% of atATGL-KO remained unchanged regardless of intervention (mean±SEM; atATGL-KO-Sham 21.57±0.50 %; atATGL-KO-TAC 19.73±0.75 %) (**Figure 4.5** B). As both, EF% and FS%, characterize the cardiac function, those results indicate a left ventricular cardiac dysfunction in WT mice and a

preserved left ventricular cardiac function in atATGL-KO mice 11 weeks after TAC-surgery.

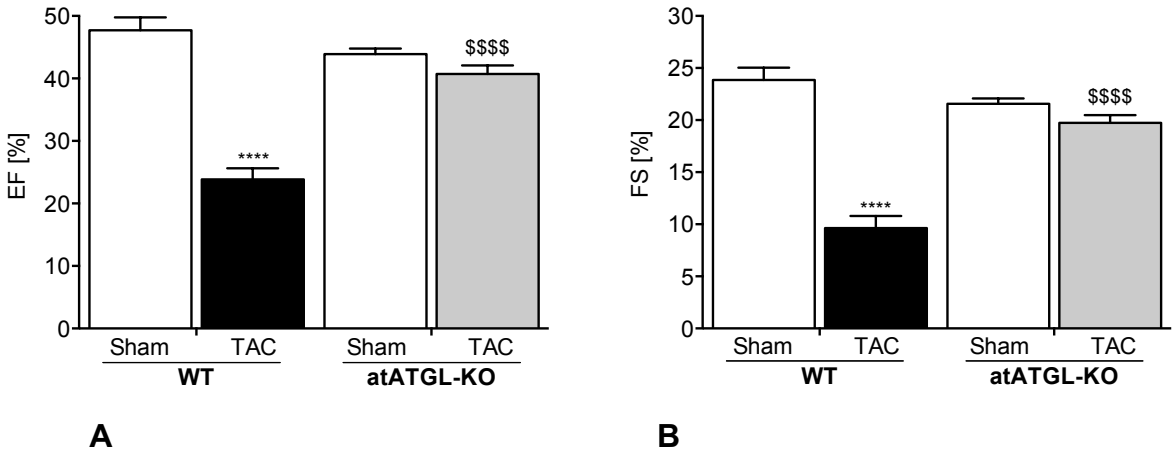

Figure 4.5 Left ventricular cardiac functions 11 weeks after TAC/Sham-surgery

A Ejection fraction (EF%). **B** Fractional Shortening (FS%). Mean ± SEM; n = 7, ****p<0.0001 vs. WT Sham, $^{\$\$\$\$}$p<0.0001 vs. WT TAC; 2-way ANOVA (Bonferroni posttest).

4.1.2.6 Hematoxylin-Eosin staining of heart tissue

HE staining was performed on heart tissues from mice 11 weeks after TAC/Sham-surgery. In line with the results obtained from the echocardiographic analysis also HE-based analysis of the cardiac tissue demonstrates that WT-TAC had the largest cardiac diameter of all four groups (**Figure 4.6** A). The quantification of the myocardial area revealed that WT mice had a significant larger cardiac diameter compared to atATGL-KO after TAC ($p<0.05$) (**Figure 4.6** B). There was no significant difference in the quantification of myocardial between atATGL-KO mice after TAC-and after Sham-surgery (**Figure 4.6** B).

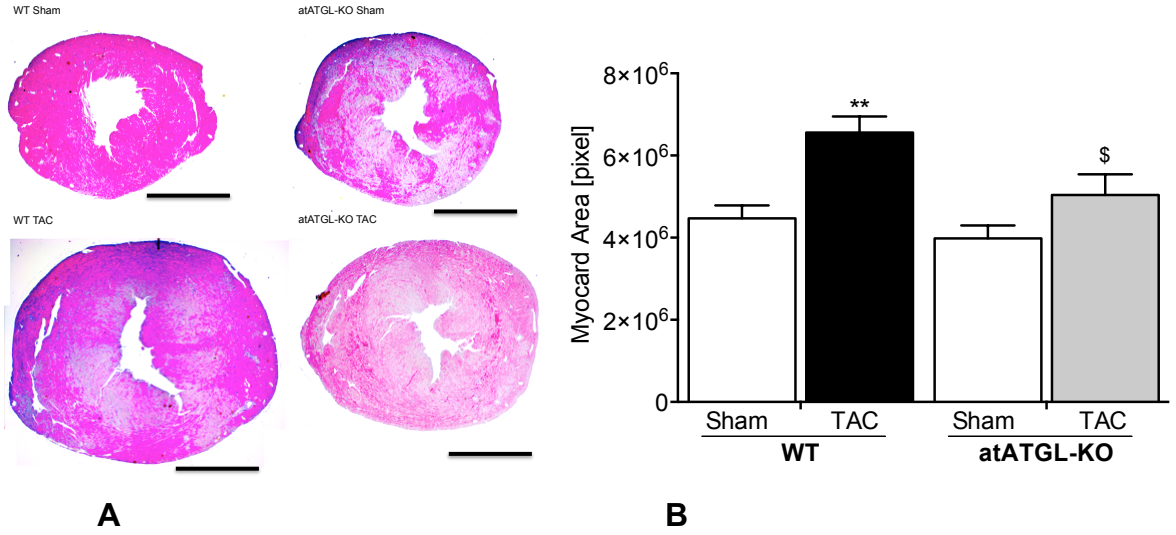

Figure 4.6 Cardiac cross-sections stained with HE 11 weeks after TAC/Sham-surgery

A Representative images of cardiac cross-sections stained with hematoxylin-eosin (HE). Black bar = 2mm. **B** Quantification of myocardial area in all four groups eleven weeks after surgery [pixel]; Mean ± SEM; n = 5-6, **p<0.01 vs. WT Sham, $^{\$}$p<0.05 vs. WT TAC; 2-way ANOVA (Bonferroni posttest).

4.1.2.7 Picrosirius Red staining of heart tissue

Picrosirius Red staining was used to evaluate fibrosis in heart tissue developing 11 weeks after TAC-mediated heart failure. A blinded researcher investigated the slices. The staining revealed that WT and atATGL-KO developed more cardiac fibrosis after TAC compared to Sham surgery (**Figure 4.7** A and B). Fibrosis in WT-TAC was significantly more prominent than in WT-Sham ($p<0.05$) (**Figure 4.7** B). There was no significant difference in the degree of fibrosis between WT and atATGL-KO after TAC-surgery. However, there was also no significant increase in the degree of fibrosis between atATGL-Sham and atATGL-TAC mice, indicating that atATGL-KO mice might have developed slightly less fibrosis in comparison to WT mice. The results showed cardiac fibrosis primarily in perivascular regions in WT mice after TAC-surgery.

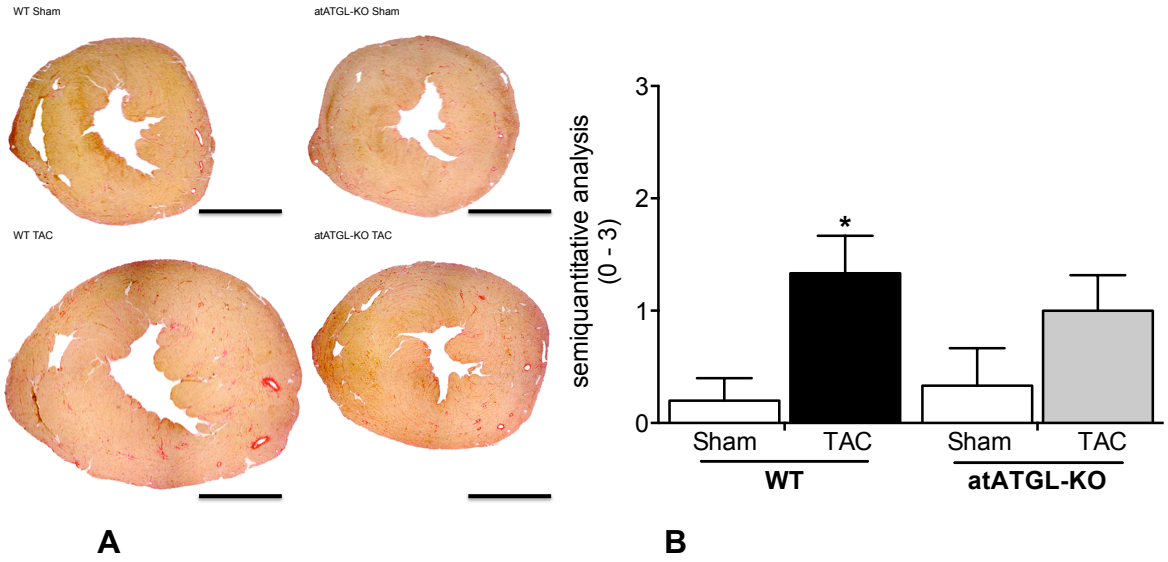

Figure 4.7 Cardiac cross-sections stained with Picrosirius Red 11 weeks after TAC/Sham-surgery

A Representative images of cardiac cross-sections stained with Picrosirius Red. Black bar = 2mm. **B** Semiquantitative analysis of heart tissue after Picrosirius Red Staining (0-3); Mean ± SEM; n = 5-6. *$p<0.05$ vs. WT Sham; 2-way ANOVA (Bonferroni posttest).

4.1.2.8 Immunohistochemical staining of heart tissue

Analysis of pro-inflammatory processes of the heart tissue sections isolated from TAC- and Sham-operated mice was performed using monocyte-macrophage-specific monoclonal anti-macrophage MAC387 antibody. Semiquantitative analysis of the results revealed that slightly more macrophages infiltrated cardiac tissue of TAC-operated mice, in comparison to Sham-operated control mice (**Figure 4.8** A and B). However, there were no significant differences between genotypes.

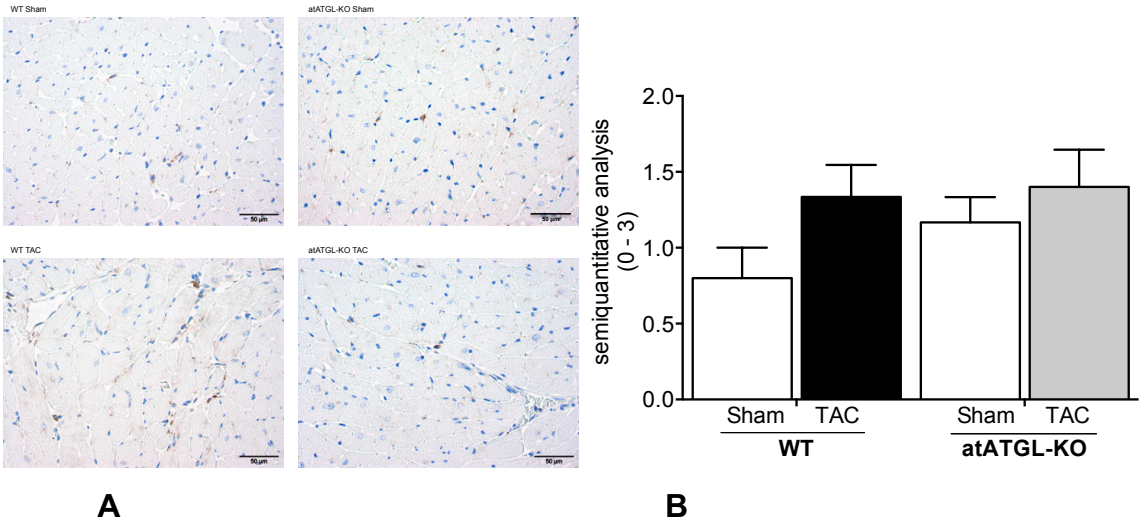

Figure 4.8 MAC387 immunohistochemical staining of heart tissue

A Representative images of macrophages staining with MAC387 antibodies. **B** Semiquantitative analysis of heart tissue (0-3) after MAC387 staining; Mean ± SEM; n = 5-6.

4.1.2.9 Gene Expression Analysis of markers specific for pathological cardiac hypertrophy

Gene expression analysis in heart tissue was performed to identify underlying signaling mechanism responsible for the different development of heart failure in WT vs. atATGL-KO mice. Atrial Natriuretic Factor (ANF) and Brain Natriuretic Peptide (BNP) were highly up-regulated in both genotypes after TAC-surgery (**Figure 4.9** A and B). In comparison to Sham-operated mice, ANF-expression was significantly higher in WT (mean±SEM; WT Sham: 0.73±0.11 vs. WT TAC: 7.73±2.12; $p<0.05$) (**Figure 4.9** A). The results of BNP measurement were even more prominent. Hearts of WT-TAC mice showed significantly higher relative mRNA expression of BNP when compared to Sham-operated control mice (mean±SEM; WT Sham: 1.42±0.14 vs. WT TAC: 5.65±0.26; $p<0.0001$) (**Figure 4.9** B). BNP was also significantly higher expressed in hearts of atATGL-KO after TAC when compared to Sham-operated mice (mean±SEM; atATGL-KO Sham: 1.41±0.27 vs. atATGL-KO TAC: 4.98±1.13; $p<0.001$). Also, β-

Myosin Heavy Chain (β-MyHC) was measured. Relative β-MyHC mRNA expression levels were only highly elevated in WT mice after TAC, but not in atATGL-KO mice after TAC (**Figure 4.9** C). β-MyHC mRNA expression, measured in LV of WT-TAC mice showed 14 times higher expression levels when compared to WT-Sham (mean±SEM; WT Sham: 0.76±0.24 vs. WT TAC: 11.34±3.58; p<0.01). There was also a significant difference between both TAC-groups (mean±SEM; WT TAC: 11.34±3.58 vs. atATGL-KO TAC: 1.85±0.56; p<0.01).

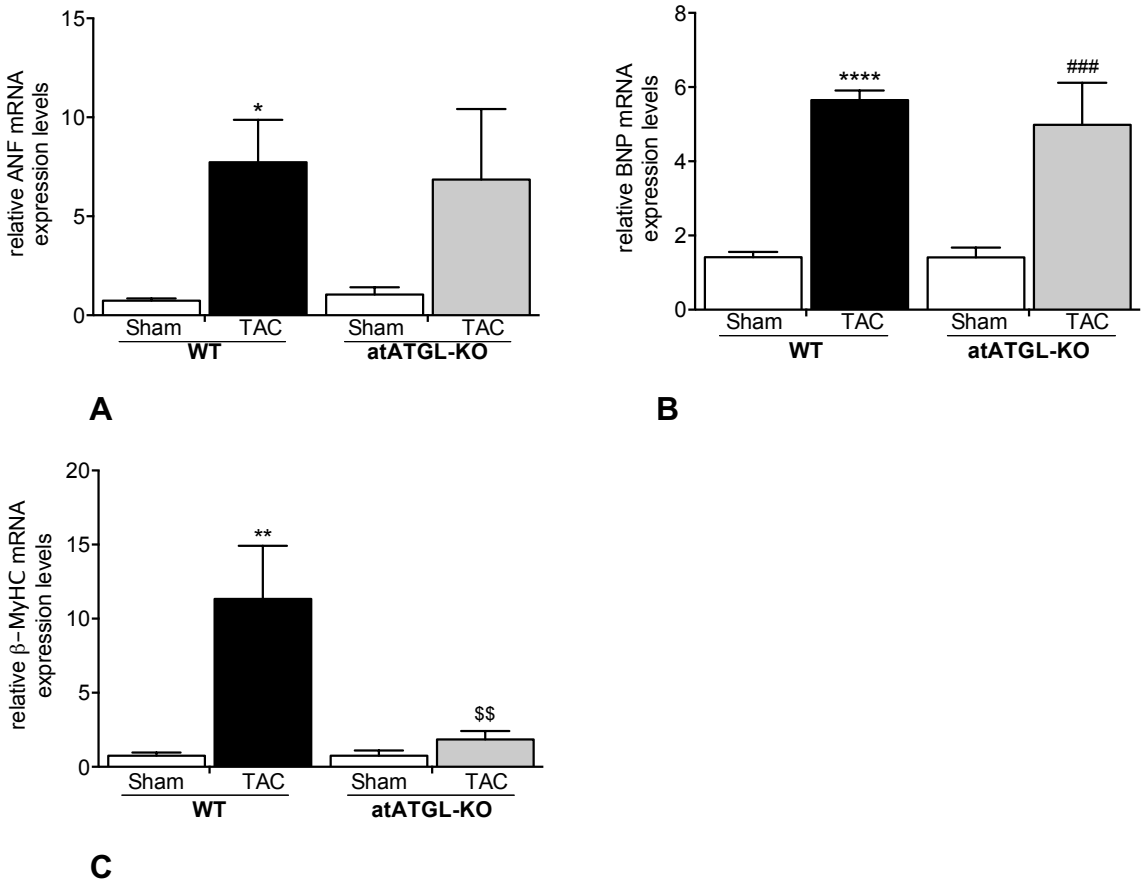

Figure 4.9 Gene Expression of markers of pathological cardiac hypertrophy

A Relative mRNA Expression of Atrial Natriuretic Factor (ANF), **B** Brain Natriuretic Peptide (BNP) and **C** β-Myosin Heavy Chain (β-MyHC). Mean ± SEM; n = 5-6, *p<0.05 / **p<0.01 / ****p<0.0001 vs. WT Sham, $^{\$\$}$p<0.01 vs. WT TAC, $^{\#\#\#}$p<0.001 vs. atATGL-KO Sham; 2-way ANOVA (Bonferroni posttest).

4.2 Metabolic characterization

4.2.1 5 weeks after TAC/Sham-surgery

4.2.1.1 Body composition measured by Nuclear Magnetic Resonance 5 weeks after TAC/Sham-surgery

Body composition was measured in male mice 5 weeks after TAC/Sham-surgery using nuclear magnetic resonance measurements (NMR). There were no significant differences in BW between the four groups (**Table 4.7**). However, total Fat Mass to BW ratio (Fat Mass/BW) was significantly higher in both atATGL-KO groups 5 weeks after TAC/Sham-surgery in comparison to WT mice (**Figure 4.10** A). In addition, Lean Mass to BW ratio (Lean Mass/BW) was significantly lower in atATGL-KO compared to WT mice after TAC (**Figure 4.10** B). Free water to BW ratio (Free water/BW) did not differ between the four group (**Table 4.7**). However, Total Water to BW ratio (Total Water/BW) in atATGL-KO Sham-operated mice was significantly lower compared to WT Sham-operated mice ($p<0.05$). Also, total water/BW ratio in atATGL-KO mice after TAC was significantly lower compared to WT-TAC mice ($p<0.01$) (**Table 4.7**).

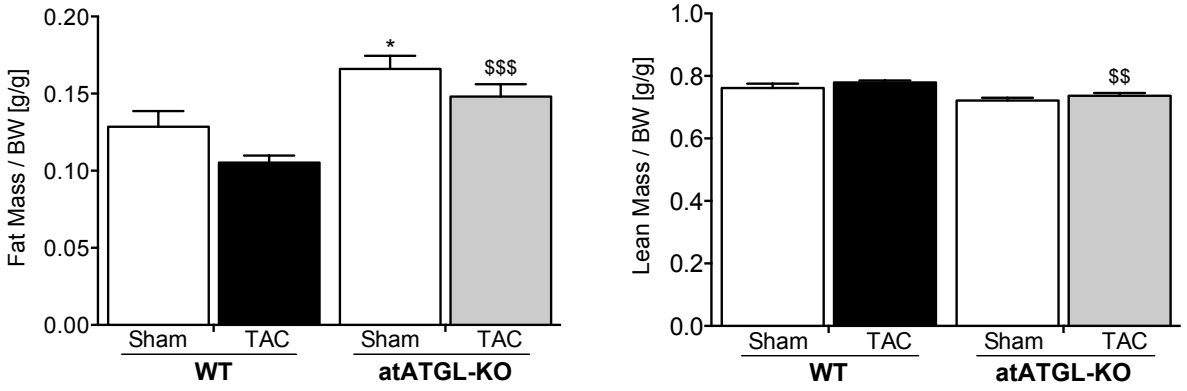

Figure 4.10 Fat Mass/BW ratio and Lean Mass/BW ratio 5 weeks after TAC/Sham-surgery measured with NMR

A Total Fat Mass to Body weight ratio (Fat Mass/BW) 5 weeks after TAC/Sham-surgery. **B** Lean Mass to Body weight ratio (Lean Mass/BW) 5 weeks after TAC/Sham-surgery. Mean ± SEM; n (WT Sham) = 9; n (WT TAC) = 14, n (atATGL-KO Sham) = 9, n (atATGL-KO TAC) = 14, *$p<0.05$ vs. WT Sham, $^{\$\$}p<0.01$ / $^{\$\$\$}p<0.001$ vs. WT TAC; 2-way ANOVA (Bonferroni posttest).

Table 4.7 Nuclear Magnetic Resonance results 5 weeks after TAC/Sham-surgery

	WT Sham	WT TAC	atATGL-KO Sham	atATGL-KO TAC
BW [g]	29.23 ± 0.58	28.07 ± 0.46	27.91 ± 0.89	28.66 ± 0.48
Fat/BW [g/g]	0.129 ± 0.010	0.105 ± 0.005	0.166 ± 0.008*	0.148 ± 0.008$^{\$\$\$}$
Lean Mass/ BW [g/g]	0.761 ± 0.014	0.779 ± 0.006	0.722 ± 0.008	0.736 ± 0.009$^{\$\$}$
Free Water/ BW [g/g]	0.0043 ± 0.00070	0.0037 ± 0.00038	0.0040 ± 0.00067	0.0041 ± 0.00046
Total Water/ BW [g/g]	0.626 ± 0.013	0.635 ± 0.004	0.590 ± 0.008*	0.600 ± 0.007$^{\$\$}$

Body weight (BW), Total Fat Mass to Body weight ratio (Fat/BW), Lean Mass to Body weight ratio (Lean Mass/BW), Free water to Body weight ratio (Free water/BW) and Total Water to Body weight ratio (Total Water/BW). Mean ± SEM; n (WT Sham) = 9; n (WT TAC) = 14, n (atATGL-KO Sham) = 9, n (atATGL-KO TAC) = 14, *p<0.05 vs. WT Sham, $^{\$\$}$p<0.01 / $^{\$\$\$}$p<0.001 vs. WT TAC; 2-way ANOVA (Bonferroni posttest).

4.2.1.2 Organ weights and organ/body weight ratio 5 weeks after TAC/Sham-surgery

Male mice were sacrificed 5 weeks after TAC/Sham-surgery and organs were harvested and weighted. There were no differences in BW at the end of week 5 (**Table 4.8**). Heart weight/BW ratio was significantly higher in WT and atATGL-KO mice after TAC compared to Sham-control mice (**Figure 4.11** A). In addition, heart weight/BW ratio in WT mice after TAC was significantly higher compared to atATGL-KO after TAC (mean±SEM; WT TAC 5.85 ± 0.35 g/kg vs. atATGL-KO TAC 5.03 ± 0.20 g/kg, p<0.05) (**Table 4.8**). Perirenal adipose tissue/BW ratio (PAT/BW) was larger in atATGL-KO mice compared to WT mice (**Figure 4.11** B). AtATGL-KO Sham-operated mice had the largest PAT/BW ratio of all four groups. However, there were no differences between epididymal adipose tissue/BW ratios (EAT/BW) between the four groups (**Table 4.8**). Liver weight/BW ratio of atATGL-KO after Sham-surgery was significantly lower compared to WT Sham-surgery (p<0.01). Also, liver weight/BW ratios of atATGL-KO after TAC-surgery were significantly lower compared to WT TAC-surgery (p<0.01) (**Figure 4.11** C).

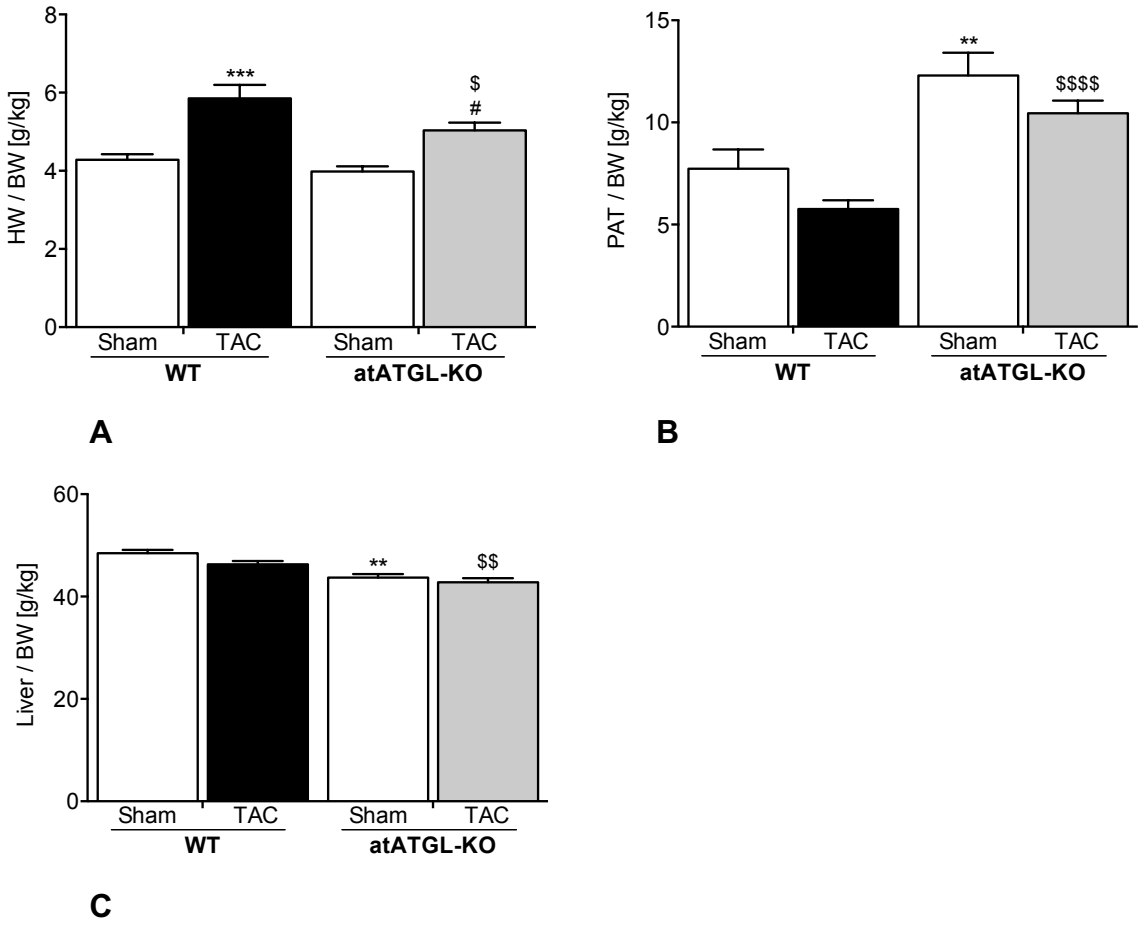

Figure 4.11 Heart, Perirenal Adipose Tissue and Liver to Body weight ratios 5 weeks after TAC/Sham-surgery

A Heart weight to Body weight ratio (HW/BW). **B** Perirenal Adipose Tissue weight to Body weight ratio (PAT/BW). **C** Liver weight to Body weight ratio (Liver/BW). Mean ± SEM; n (WT Sham) = 9, n (WT Sham Liver/BW) = 8, n (WT TAC) = 14, n (atATGL-KO Sham) = 9, n (atATGL-KO TAC) = 14, **p<0.01 / ***p<0.001 vs. WT Sham, $^{\#}$p<0.05 vs. atATGL-KO Sham, $^{\$}$p<0.05 / $^{\$\$}$p<0.01 / $^{\$\$\$\$}$p<0.0001 vs. WT TAC; 2-way ANOVA (Bonferroni posttest).

Table 4.8 Body weight and organ/body weight ratios 5 weeks after TAC/Sham-surgery

	WT Sham	WT TAC	atATGL-KO Sham	atATGL-KO TAC
BW [g]	29.93 ± 0.63	28.79 ± 0.53	28.96 ± 1.03	29.98 ± 0,47
HW/BW [g/kg]	4.28 ± 0.14	5.85 ± 0.35***	3.98 ± 0.13	5.03 ± 0.20$^{\#\ \$}$
PAT/BW [g/kg]	7.73 ± 0.95	5.76 ± 0.42	12.30 ± 1.11**	10.45 ± 0.62$^{\$\$\$\$}$
EAT/BW [g/kg]	16.73 ± 1.31	14.68 ± 0.82	19.09 ± 1.35	16.79 ± 0.91
Liver/BW [g/kg]	48.46 ± 0.67	46.30 ± 0.65	43.71 ± 0.67**	42.80 ± 0.80$^{\$\$}$

Body weight (BW), Heart weight to Body weight ratio (HW/BW), Perirenal Adipose Tissue weight to Body weight ratio (PAT/BW), Epididymal Adipose Tissue weight to Body weight ratio (EAT/BW), Liver weight to Body weight ratio (Liver/BW) and Lung weight to Body weight ratio (Lung/BW). Mean ± SEM; n (WT Sham) = 9, n (WT Sham Liver/BW) = 8, n (WT TAC) = 14, n (atATGL-KO Sham) = 9, n (atATGL-KO TAC) = 14, **p<0.01 / ***p<0.001 vs. WT Sham, $^{\$}$p<0.05 / $^{\$\$}$p<0.01 / $^{\$\$\$\$}$p<0.0001 vs. WT TAC, $^{\#}$p<0.05 vs. atATGL-KO Sham; 2-way ANOVA (Bonferroni posttest).

4.2.2 11 weeks after TAC/Sham-surgery

4.2.2.1 Body composition measured by Nuclear Magnetic Resonance 11 weeks after TAC/Sham-surgery

Body composition was also measured in mice 11 weeks after TAC/Sham-surgery using NMR. BW was measured before NMR. BW was significantly lower in atATGL-KO TAC-operated mice compared to WT TAC-operated mice on the day of NMR (**Table 4.9**). However, there were no significant differences in the fat mass/BW (Fat/BW), lean mass/BW, free water/BW and total water/BW (**Table 4.9**) between genotypes (WT vs. atATGL-KO) or interventions (Sham vs. TAC).

Table 4.9 Nuclear Magnetic Resonance (NMR) results of 11 weeks after TAC/Sham-surgery

	WT Sham	WT TAC	atATGL-KO Sham	atATGL-KO TAC
BW [g]	30.30 ± 0.98	31.85 ± 0.72	28.90 ± 0.45	28.08 ± 0.29$^{\$\$}$
Fat/BW [g/g]	0.141 ± 0.026	0.163 ± 0.010	0.162 ± 0.013	0.145 ± 0.009
Lean Mass/ BW [g/g]	0.740 ± 0.026	0.710 ± 0.009	0.702 ± 0.012	0.727 ± 0.012
Free Water/ BW [g/g]	0.0055 ± 0.00088	0.0058 ± 0.0014	0.0038 ± 0.0013	0.0053 ± 0.0012
Total Water/ BW [g/g]	0.610 ± 0.022	0.585 ± 0.007	0.578 ± 0.011	0.596 ± 0.012

Body weight (BW), Total Fat Mass to Body weight ratio (Fat/BW), Lean Mass to Body weight ratio (Lean Mass/BW), Free water to Body weight ratio (Free water/BW) and Total Water to Body weight ratio (Total Water/BW).Mean ± SEM; n = 5-6, $^{\$\$}$p<0.01 vs. WT TAC; 2-way ANOVA (Bonferroni posttest).

4.2.2.2 Respiratory Quotient and Energy Expenditure

To characterize the metabolic phenotype of the animals concerning the respiratory quotient, energy expenditure and locomotor activity TSE-LabMaster system was used. VCO_2 and VO_2 were used to calculate respiratory quotient (RQ) and energy expenditure (EE). There were no differences in RQ or EE either during the day (6.00am to 6.00pm) or night (6.00pm until 6.00am) among the groups. Also, locomotor activity was similar in all four groups (**Table 4.10**).

Table 4.10 LabMaster and indirect gas calorimetry 11 weeks after TAC/Sham-surgery

	WT Sham	WT TAC	atATGL-KO Sham	atATGL-KO TAC
RQ [VCO_2/VO_2] 6am-6pm	0.833 ± 0.012	0.842 ± 0.022	0.862 ± 0.016	0.883 ± 0.013
RQ [VCO_2/VO_2] 6pm-6am	0.920 ± 0.024	0.935 ± 0.010	0.930 ± 0.019	0.926 ± 0.006
EE 6am-6pm [kcal/kg/h]	14.51 ± 0.39	14.78 ± 0.52	14.98 ± 0.25	15.41 ± 0.19
EE 6pm-6am [kcal/kg/h]	16.63 ± 0,52	16.79 ± 0,65	17.40 ± 0.45	16.78 ± 0.42
Locomotor activity [counts/hour]	3007 ± 315	3397 ± 232	3686 ± 522	3404 ± 543

Respiratory Quotient (RQ) and Energy Expenditure (EE) during day (6am-6pm) and night (6pm-6am) Mean and SEM; n = 5-6; 2-way ANOVA (Bonferroni posttest).

4.2.2.3 Intraperitoneal Glucose Tolerance Test

10 weeks after TAC/Sham-surgery, mice underwent intraperitoneal glucose tolerance test (ipGTT). IpGTT revealed that the elevation of blood glucose levels was significantly lower in atATGL-KO TAC-operated compared to WT TAC-operated mice (**Figure 4.12** A and B). The analysis of the area under the curve (AUC) showed that atATGL-KO after TAC had a significantly improved glucose tolerance compared to WT after TAC (mean±SEM; WT-TAC 35775±1680 vs. atATGL-KO-TAC 25729±630, p<0.001) (**Figure 4.12** C). Sham-operated WT and atATGL-KO mice did not differ regarding glucose tolerance.

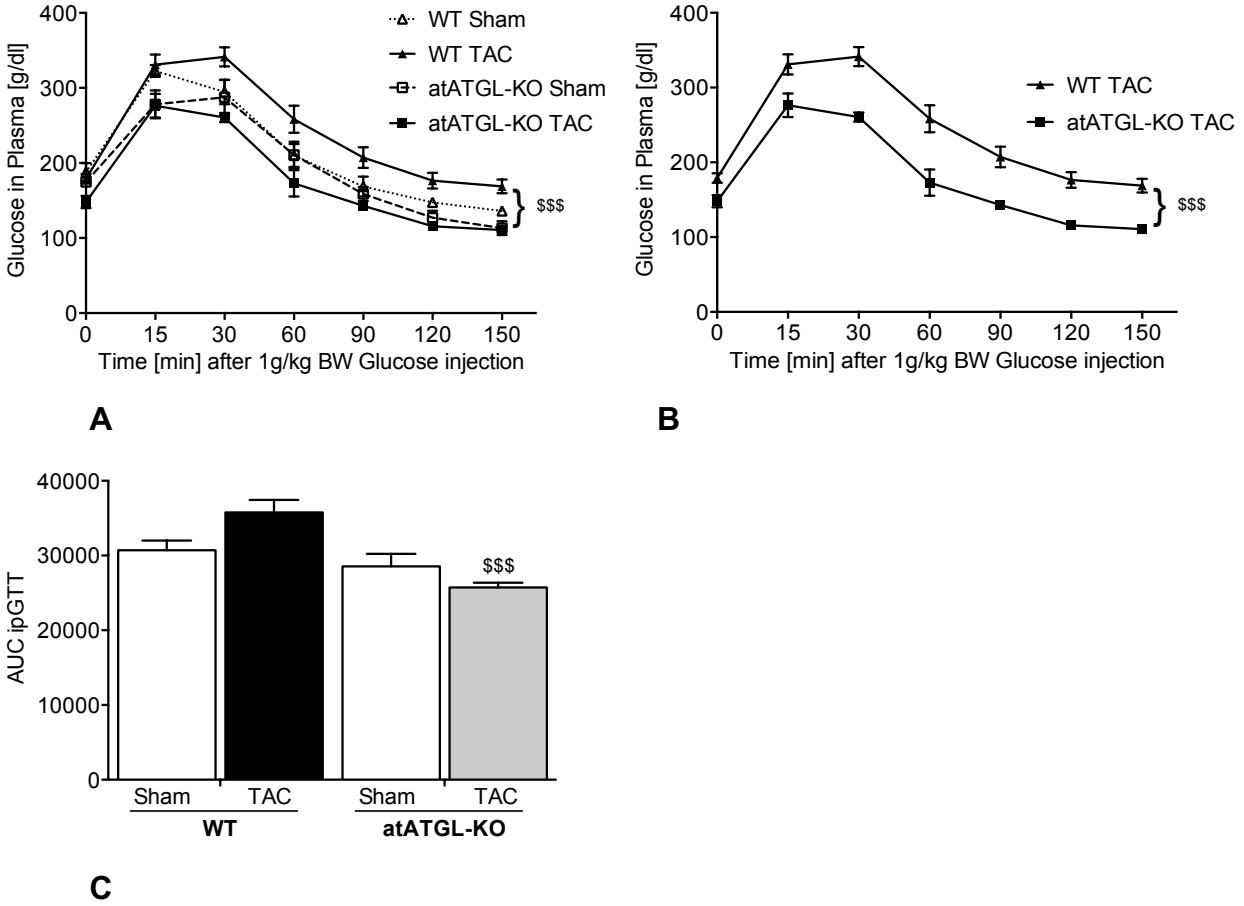

Figure 4.12 Glucose Tolerance Test 11 weeks after TAC/Sham-surgery

A Intraperitoneal Glucose Tolerance Test (ipGTT) of all groups. Indications for significant differences are from differences of the area under the curve (AUC) between groups. **B** IpGTT in TAC groups only. Indications for significant differences are from differences in AUC between groups. **C** Area under the curve (AUC) of ipGTT; n = 4-5, $^{\$\$\$}$p<0.001 vs. WT TAC; T-test.

4.2.2.4 Intraperitoneal Insulin Tolerance Test

Intraperitoneal Insulin Tolerance Test (ipITT) was performed 11 weeks after TAC/Sham-surgery just before sacrificing mice. AUC-values of all groups were compared (**Figure 4.13** C). IpITT revealed that insulin sensitivity in atATGL-KO Sham-operated mice was significantly improved compared to WT Sham-operated mice ($p<0.01$) (**Figure 4.13** A). In addition, insulin sensitivity was significantly improved in atATGL-KO after TAC-surgery compared to WT post-TAC ($p<0.05$) (**Figure 4.13** B).

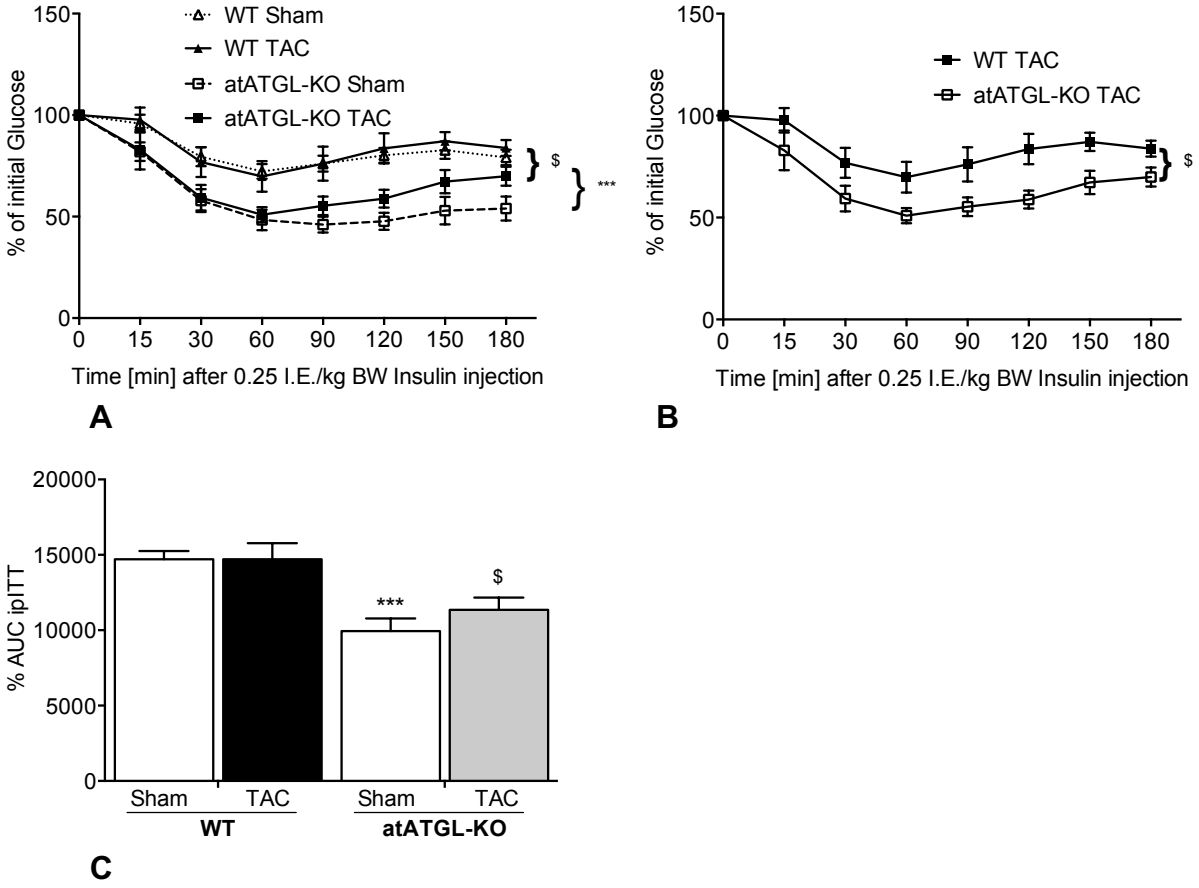

Figure 4.13 Insulin Tolerance Test 11 weeks after TAC/Sham-surgery

A Intraperitoneal Insulin Tolerance Test (ipITT) of all groups. Indications for significant differences are from differences of the area under the curve (AUC) between groups. **B** IpITT of TAC only. Indications for significant differences are from differences in AUC between groups. **C** Area under the curve (AUC) of ipITT. n = 7 - 8, ***$p<0.001$ vs. WT Sham, $^{\$}p<0.05$ vs. WT TAC.

4.2.2.5 Organ weights and organ / body weight ratio 11 weeks after TAC/Sham-surgery

Animals were sacrificed 11 weeks after TAC/Sham-surgery and organs were weighed. There were significant differences in BW on the day of organ harvesting (**Table 4.11**). Also, there were significant differences in BW between the groups before NMR was performed (**Table 4.9**). Heart weight to BW ratios are shown in **Figure 4.1** B. Perirenal adipose tissue (PAT) to BW ratio was significantly higher in atATGL-KO Sham-operated mice compared to WT Sham-operated mice ($p<0.001$). In addition, PAT/BW of atATGL-KO mice after TAC was significantly lower compared to atATGL-KO Sham controls ($p<0.05$) (**Figure 4.14** A). Liver to BW ratio was significantly lower in atATGL-KO mice compared to WT mice for both interventions (**Figure 4.14** B). While there were no significant differences in lung weights to BW ratios, the results indicated lung / BW ratio was slightly higher in WT mice after TAC compared to atATGL-KO mice after TAC (**Figure 4.14** C). However, there were no differences in epididymal adipose tissue weight / BW ratio (EAT/BW) between the four groups 11 weeks after TAC/Sham-surgery (**Table 4.11**).

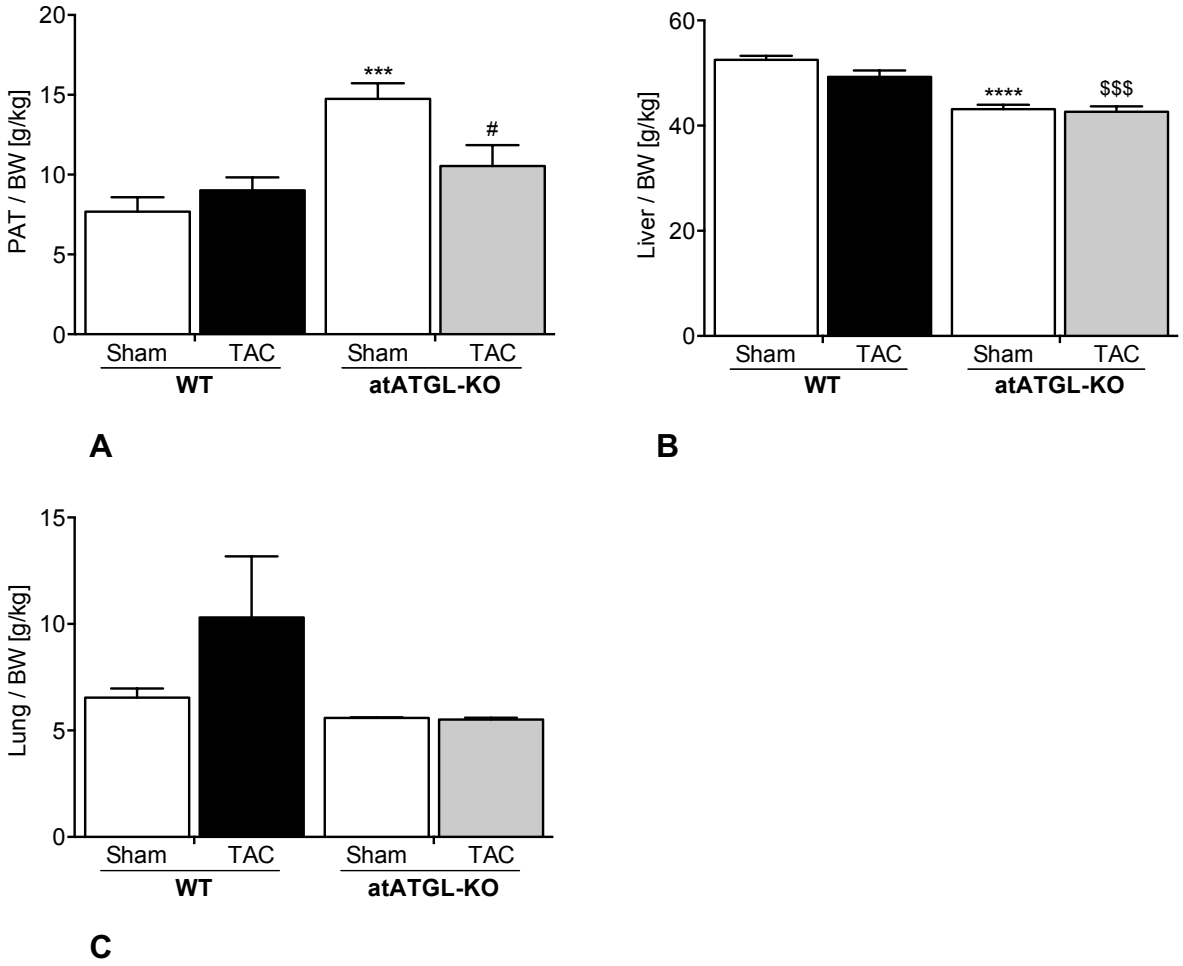

Figure 4.14 Perirenal Adipose Tissue, Lung and Liver to Body weight ratios 11 weeks after TAC/Sham-surgery

A Perirenal Adipose Tissue to Body weight ratio (PAT/BW). **B** Lung weight to Body weight ratio (Lung/BW). **C** Liver weight to Body weight ratio (Liver/BW). PAT/BW and Liver/BW: n (WT Sham) = 9, n (WT TAC) = 11, n (atATGL-KO Sham) = 8, n (atATGL-KO TAC) = 8 ***p<0.001 / ****p<0.0001 vs. WT Sham, $^{\$\$\$}$p<0.001 vs. WT TAC, $^{\#}$p<0.05 vs. atATGL-KO Sham; Lung weight/BW: n (WT Sham) = 4, n (WT TAC) = 5, n (atATGL-KO Sham) = 2, n (atATGL-KO TAC) = 3; 2-way ANOVA (Bonferroni posttest).

Table 4.11 Body weight and organ/body weight ratios 11 weeks after TAC/Sham-surgery.

	WT Sham	WT TAC	atATGL-KO Sham	atATGL-KO TAC
BW [g]	30.58 ± 0.44	31.13 ± 0.58	30.05 ± 0.34	28.88 ± 0,58$^{\$}$
HW/BW [g/kg]	4.12 ± 0.10	6.48 ± 0.32****	4.00 ± 0.24	5.27 ± 0.36$^{\#\ \$}$
PAT/BW [g/kg]	7.68 ± 0.91	9.02 ± 0.81	14.75 ± 0.98***	10.54 ± 1.32$^{\#}$
EAT/BW [g/kg]		21.01 ± 1.42	19.61 ± 1.48	16.83 ± 1.78
Liver/BW [g/kg]	52.51 ± 0.77	49.26 ± 1.22	43.12 ± 0.84****	42.63 ± 1.03$^{\$\$\$}$
Lung/BW [g/kg]	6.54 ± 0,44	10.30 ± 2.88	5.59 ± 0.03	5.51 ± 0.09

Body weight (BW) and Heart weight to Body weight ratio (HW/BW); n (WT Sham) = 5, n (WT TAC) = 6, n (atATGL-KO Sham) = 6, n (atATGL-KO TAC) = 5; Perirenal Adipose Tissue weight to Body weight ratio (PAT/BW), Epididymal Adipose Tissue weight to Body weight ratio (EAT/BW) and Liver weight to Body weight ratio (Liver/BW). Mean ± SEM; BW, HW/BW, PAT/BW, EAT/BW and Liver/BW; n (WT Sham) = 9, n (WT TAC) = 11, n (atATGL-KO Sham) = 8, n (atATGL-KO TAC) = 8, ****p<0.0001 vs. WT Sham, $^{\$\$}$p<0.01 / $^{\$\$\$}$p<0.001 vs. WT TAC, $^{\#}$p<0.05 vs. atATGL-KO Sham; Lung weight/BW: n (WT Sham) = 4, n (WT TAC) = 5, n (atATGL-KO Sham) = 2, n (atATGL-KO TAC) = 3; 2-way ANOVA (Bonferroni posttest).

4.2.2.6 Fatty Acid (FA) levels in blood serum

Blood samples taken 11 weeks after surgery were used to measure FA levels in mice. FA levels were lower in atATGL-KO (**Figure 4.15**). In particular, FA levels in atATGL-KO TAC-operated mice were significantly lower in comparison to WT TAC-operated mice (mean±SEM; atATGL-KO TAC: 0.50±0.036mmol/l vs. WT TAC: 0.97±0.086, p<0.001). However, there were no significant differences between WT and atATGL-KO Sham-operated animals. There were no significant differences between Sham and TAC intervention in between the two genotypes either.

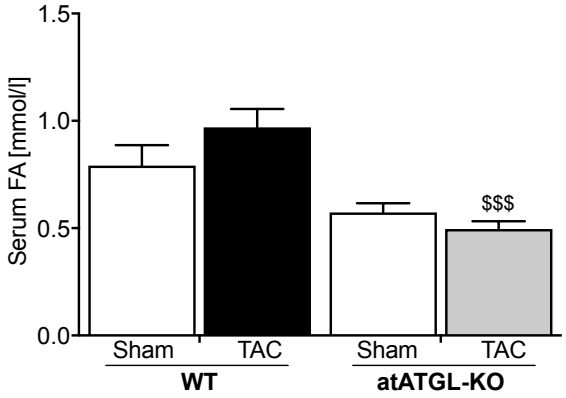

Figure 4.15 Fatty Acid levels in blood serum

Fatty Acid (FA) levels in serum were measured 11 weeks after surgery; n = 5-6, $^{\$\$\$}$p<0.001 vs. WT TAC; 2-way ANOVA (Bonferroni posttest).

4.2.2.7 Fatty Acid Profiling

While total FA levels were significantly lower in atATGL-KO-TAC animals compared to WT-TAC (**Figure 4.16**), HPLC-MS analysis of FA-species in the blood circulation was performed (as described in 3.2.22). Five different FAs could be identified, which were significantly reduced ($p<0.05$) in blood circulation of atATGL-KO TAC mice compared to WT TAC mice (**Figure 4.16**); C16:0 (Palmitic acid), C16:1 (Palmitoleic acid), C18:1 (Oleic acid), C18:2 (Linoleic acid) and C20:5 (Eicosapentaenoic acid).

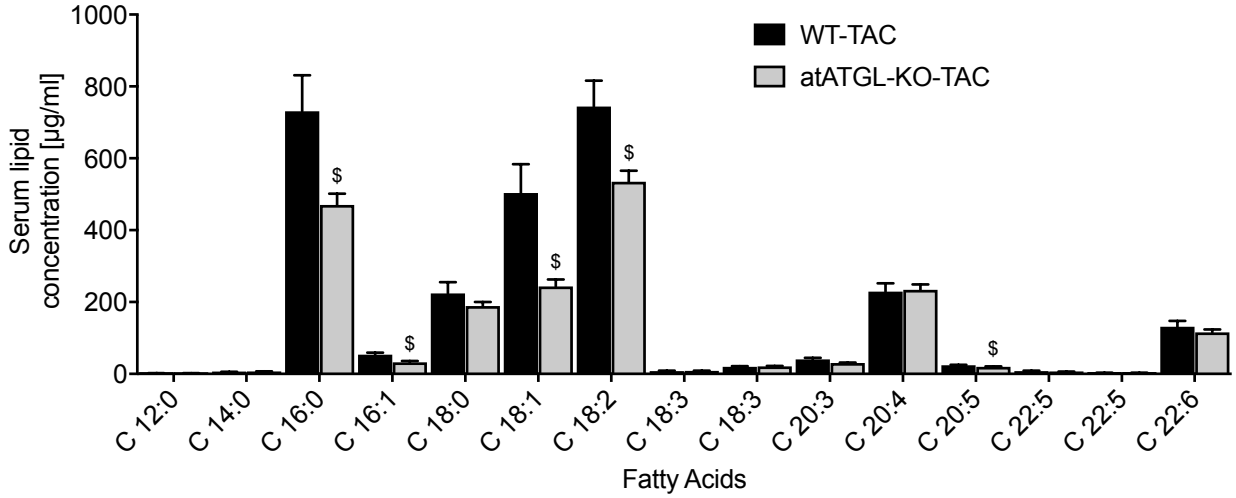

Figure 4.16 Fatty Acid Profiling performed by coupled HPLC-MS

Lipid Profiling was performed with blood samples taken from mice 11 weeks after TAC/Sham-surgery; n = 5-6, $^{\$}p<0.001$ vs. WT TAC; T-Test.

5 Discussion

5.1 Transverse Aortic Constriction induced pressure overload cardiac hypertrophy 5 weeks after surgery

An important aim of this study was to investigate if adipose tissue-specific ATGL (atATGL) influences differences in the development of cardiac hypertrophy, in particular left ventricular hypertrophy (LVH) and heart failure (HF) using transverse aortic constriction (TAC) in atATGL-KO mice.

TAC is one of the most frequently applied, highly reproducible microsurgical techniques used to induce LVH and HF (deAlmeida et al., 2010; Nakamura et al., 2001; Rockman et al., 1991). In this study, only male mice were used, because male mice develop a higher degree of cardiac hypertrophy induced by TAC (Fliegner et al., 2010; Skavdahl et al., 2005). In our study, atATGL-KO and WT mice developed significantly greater thickness of the heart after TAC compared to Sham-surgery already 5 weeks after TAC/Sham-surgery, measured using echocardiography (**Table 4.3**). The wall thickness is represented by IVS-d and LVPW-d in the diastole. An increase of IVS-d and LVPW-d caused a significant increase in LVM after TAC when compared to Sham-operated mice (**Table 4.2**), which is in line with previous studies (Fliegner et al., 2010; Grune et al., 2016). However, LVID-d did not vary among the four groups 5 weeks after TAC/Sham-surgery (**Table 4.3**). These results indicate that male mice of both genotypes develop concentric cardiac hypertrophy after TAC-surgery. Concentric hypertrophy is characterized by the growth of ventricular walls and the interventricular septum, observed without change of ventricular chamber diameter (Heineke and Molkentin, 2006). Moreover, 5 weeks after TAC-surgery mice developed LVH without cardiac function being reduced. The ejection fraction (EF%) and the fractional shortening (FS%) were similar in all four groups (**Table 4.4**). Cardiac hypertrophy with preserved LVID and EF% 5 weeks after TAC-surgery was confirmed in previous mouse studies (Hill et al., 2000). In fact, the development of HF with reduced EF% (HFrEF) and an increase in LVID after TAC-surgery by using a 26.0 Gauge needle for aortic ligation, has been described in previous studies occurring only after 9 weeks (Westphal et al., 2012).

Interestingly, adipose tissue-specific deletion of ATGL in mice led to the development of a different cardiac phenotype than that observed in global ATGL-KO mice. The global absence of ATGL in mice resulted in a lipolytic defect also in cardiomyocytes, which led to severe lipid accumulation, cardiac dysfunction, and shorter life expectancy when

compared to the control group (Haemmerle et al., 2006; Schoiswohl et al., 2010). In this study, we showed that atATGL-KO mice had a preserved cardiac function 5 weeks after Sham- (baseline) and TAC-surgery. Moreover, cardiomyocyte-specific ATGL-KO mice developed pathological hypertrophy and fibrotic cardiomyopathy (Kienesberger et al., 2013), a process that could not be found in this study, since ATGL was still present in the heart. Similar to our results, adipocyte-specific ATGL-KO mice, investigated by other research groups revealed no differences in heart weight between atATGL-KO and the control group without pressure-induced hypertrophy (Ahmadian et al., 2011; Wu et al., 2012).

In summary, 5 weeks after TAC-surgery male mice develop cardiac hypertrophy, but there are no significant differences between WT and atATGL-KO mice in the degree of hypertrophy.

5.2 atATGL-KO mice were resistant to TAC-mediated heart failure

In this study, we investigated HF occurring 11 weeks after TAC-surgery. IVS-d and LVPW-d were significantly larger in TAC-operated male mice compared to Sham-operated controls in both genotypes (**Figure 4.3** A and B). However, there were no significant differences in IVS-d and LVPW-d between the genotypes. Surprisingly, LVID-d, as a measurement of the left ventricular dilatation, was significantly larger in WT compared to atATGL-KO mice (**Figure 4.3** C). This was linked with a significant reduction in the EF% and the FS% in WT mice after TAC-surgery compared to atATGL-KO after TAC-surgery, leading to a reduction in cardiac function (**Figure 4.5**). We showed for the first time that adipose tissue-specific ATGL-KO mice were protected from TAC-mediated HF. In a previous study, atATGL-KO mice were challenged with frequent treadmill training, to investigate the importance of WAT-lipolytic activity and WAT-derived lipid species released into the circulation during the development of exercice-induced/physiological cardiac hypertrophy (Foryst-Ludwig et al., 2015). atATGL-KO showed reduced FFA release into the blood circulation and attenuated myocardial uptake of FFA uptake. This resulted in a reduced ability of these mice to develop adaptive LVH after training, when compared to WT control mice (Foryst-Ludwig et al., 2015). Interestingly, atATGL-KO male mice developed a reduced cardiac hypertrophy due to aortic constriction in pathological LVH, as shown in this study, even though the pathophysiological mechanisms are quite different.

Kienesberger and colleagues focused on the importance of myocardial ATGL. In cardiomyocyte-specific ATGL overexpressing mice, they observed less cardiac lipid accumulation, improved cardiac function at baseline and maintained cardiac function after TAC (Kienesberger et al., 2012). Consistent with those results is the cardiomyocyte-specific ATGL-deficiency model, resulting in pathological hypertrophy and cardiac fibrosis, which led to cardiac dysfunction (Kienesberger et al., 2013). Haemmerle and colleagues showed that cardiac muscle-specific ATGL-deficiency results in reduced expression levels of PPAR-α and PPAR-δ target genes and leads to massive inhibition of β-oxidation, followed by lipid accumulation, mitochondrial defects and cardiac dysfunction (Haemmerle et al., 2011). Studies performed on cardiomyocyte-specific ATGL-deficiency conclude that the impaired cardiac function does not correlate with FFA release from WAT and lipid availability to the heart. Our results on TAC-operated adipose tissue-specific ATGL-KO mice stand in contrast to findings derived from the studies on global ATGL-deficiency and cardiomyocyte-specific ATGL-KO. In our study, local effects of ATGL activity in WAT directly modulate cardiac function, independent of the myocardial ATGL activity, which is preserved in the heart of our mice. atATGL-KO caused preserved cardiac function in TAC-operated mice. Hence, it seems that ATGL, while expressed in multiple organs, influences the cardiac function in an organ-specific manner.

Previous studies described an increase in lung weights due to TAC-mediated systolic pressure overload in mice, as a hallmark of HF in mice (Chen et al., 2012; Liu et al., 2014). Chen and colleagues could identify lung fibrosis, vascular remodeling and leukocyte infiltration as causes for the increase in lung weights (Chen et al., 2012). Also in the current study, lung weight/BW ratios were greater in WT mice after TAC compared to all other groups, even though there was no significant difference (**Figure 4.14** C). However, Chen and colleagues observed a significant increase in lung weight/BW ratio 4 weeks after TAC-surgery using a 26 Gauge needle. While WT mice after TAC-surgery developed an increased ratio of lung weights to BW 11 weeks after TAC-surgery, the current study could not confirm such a large increase in lung weights due to the TAC-surgery. These could be explained – at least in part – by the small sample size of lungs included in this study. A higher sample size might have resulted in a significant difference in the ratio of lung weight to BW between WT Sham- and TAC-operated mice.

Collectively, this study reveals first evidence that adipose tissue-specific ATGL influences the development of HF in male mice. While in previous studies the effect of cardiomyocyte-specific and global ATGL on the cardiac phenotype and function have been investigated, the present study indicates an interaction between white adipose tissue and heart mediated by atATGL.

5.3 Histological and gene expression analysis confirm differences in TAC-mediated cardiac changes between WT and atATGL-KO mice

Cross-sections of hearts were stained with HE and myocardial areas were measured 11 weeks after TAC-surgery. Histological analysis revealed that WT mice after TAC-surgery had the largest myocardial cross-section area of all four groups (**Figure 4.6** A and B). The myocardial cross-section area of atATGL-KO mice 11 weeks after TAC-surgery were also significant larger compared to atATGL-KO Sham-operated mice, but the increase was not as impressive as in WT mice. An increase in myocardial cross-sectional area after TAC-surgery was described in previous studies (van Eickels et al., 2001). Importantly, these histological analyses support the echocardiography data by revealing that WT mice had an increase in myocardial cross-section area after TAC compared to atATGL-KO mice.

Previous studies showed that gene expression levels of ANF, BNP and β-MyHC in myocardium correlate directly to an increased ratio of LVM/TL and a reduced EF% (Gitau et al., 2015; Han et al., 2015; Westphal et al., 2012). The re-expression of the fetal β-MyHC has been associated with reduced cardiac contractility (Tardiff et al., 2000). In addition, the expression of ANF and BNP indicates atrial and ventricular overload and dysfunction (Yasue et al., 1994; Yoshimura et al., 1993). In this study, ANF expression levels increased significantly in WT mice 11 weeks after TAC-surgery compared to Sham-surgery (**Figure 4.9** A). While ANF expression levels were higher in atATGL-KO mice after TAC compared to Sham, they were not significantly different due to a wide variation. BNP expression levels in WT and atATGL-KO mice increased to a similar extent due to TAC-surgery (**Figure 4.9** B). Obese individuals have lower NP levels compare to individuals with normal BMI (Gruden et al., 2014; Wang et al., 2004). atATGL-KO mice 11 weeks after TAC/Sham-surgery developed higher perirenal adipose tissue / BW ratios (PAT/BW) compared to WT mice. Excess body fat mass is a hallmark of obesity (Despres, 2012). Natriuretic peptide clearance receptors (NPR-C) are expressed in adipocytes, which participate in NP removal from circulation (Morigny

et al., 2016; Sarzani et al., 1995). Therefore the slightly reduced expression of ANF and BNP in atATGL-KO mice compared to WT mice after TAC-surgery might also be related to increased NPR-C expression in adipocytes of atATGL-KO mice.

The gene expression levels of β-MyHC increased significantly only in WT mice after TAC-surgery (**Figure 4.9** C). β-MyHC expression levels of atATGL-KO mice after Sham- and TAC-surgery were similar. In other studies, increased β-MyHC-expression in the myocardium was associated with HF and cardiac hypertrophy (Pandya et al., 2006) and an impaired function of the hypertrophied ventricle (Tardiff et al., 2000). In addition, cardiac β-MyHC-expression seems to be specifically increased in the fibrotic tissue (Pandya and Smithies, 2011).

In our study, it could be confirmed that WT mice after TAC-surgery are characterized by reduced cardiac function and elevated cardiac fibrosis (**Figure 4.5** A and B; **Figure 4.7** A and B) and express significantly higher levels of β-MyHC compared to atATGL-KO mice.

5.4 atATGL-deficiency does not influence cardiac fibrosis

Cardiac fibrosis in WT mice after TAC-surgery was significantly more prominent compared to WT Sham-operated mice (**Figure 4.7** A and B). However, there were no significant differences in the degree of cardiac fibrosis between atATGL-KO and WT mice after TAC-surgery. Semiquantitative analysis of MAC387 using immunohistochemical staining of heart tissue section from mice 11 weeks after TAC/Sham-surgery also revealed no differences among the four groups (**Figure 4.8** A and B). Infiltration of macrophages in cardiac tissue is essential for inflammation and fibrosis (Shen et al., 2014). In the present study, cardiac fibrosis due to TAC-surgery in WT mice could not be directly linked to infiltration of macrophages. It could be explained – at least in part – by the different time frame, in which macrophages are actively attracted to the cardiac tissue, priming cardiac inflammation in the early stage of HF, and the later stage linked with fibrotic processes, mediated mostly by re-differentiating fibroblast, observed 11 weeks after surgery.

TAC-surgery has been used in previous studies to induce cardiac fibrosis in mice (Eclov et al., 2015; Luo et al., 2015; Westphal et al., 2012). Interestingly, Haemmerle and colleagues observed increased cardiac fibrosis in global ATGL-KO mice (Haemmerle et al., 2006). Exercise-induced physiological hypertrophy in atATGL-KO mice did not result in infiltration of macrophages or cardiac fibrosis (Foryst-Ludwig et al., 2015). However,

ATGL-deficiency in adult cardiomyocytes was linked with increased fibrosis, processing in cardiac dysfunction (Kienesberger et al., 2013). In this mouse model cardiac dysfunction was explained with an increase in triglyceride accumulation and fibrosis, accompanied by an increase in cardiac mRNA expression of collagen type I and transforming-growth-factor-β (Kienesberger et al., 2013). It was demonstrated that connective tissue growth factor (CTGF) causes cardiac fibrosis in the heart, resulting in accumulation of extracellular matrix. Wang and colleagues demonstrated that FFAs induce CTGF-activity, leading to the development of cardiac fibrosis in rats (Wang et al., 2009b). However, other studies in mice and rats using TAC-surgery combined with a high-fat diet (HFD) feeding promoted myocardial lipid accumulation, but did not alter cardiac function due to fibrosis (Chess et al., 2009; Rennison et al., 2009). In this study, WT mice with higher FA levels in blood circulation (**Figure 4.15**) developed slightly more cardiac fibrosis after TAC-surgery compared to atATGL-KO mice (**Figure 4.7** A and B). However, in comparison to findings by Wang and colleagues cardiac fibrosis analyzed in our study, was not as prominent. The question raises whether TAC-surgery is the appropriate model to study cardiac fibrosis in mice, at least in this setting.

It can be summarized that while the model of TAC-surgery resulted in cardiac fibrosis, independent of infiltration of macrophages and inflammation, the genotype did not influence the cardiac fibrosis.

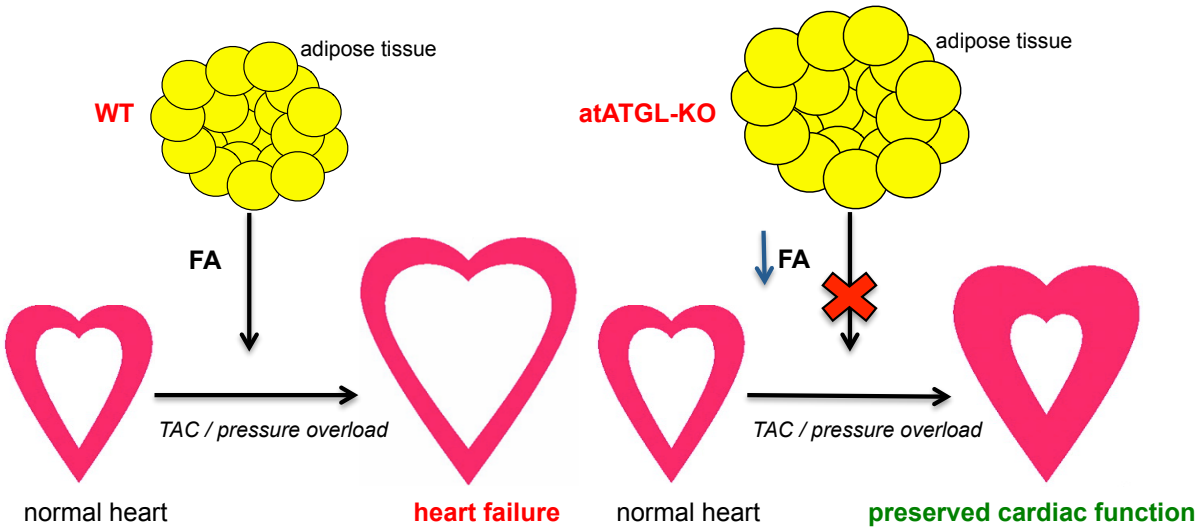

Figure 5.1 Results of cardiac phenotype 11 weeks after TAC/Sham-surgery

WT – wild type; atATGL-KO - adipose tissue-specific Adipose Triglyceride Lipase Knock-out; FA –fatty acids

5.5 atATGL-KO results in reduced liver weights

In the current study, 5 and 10 weeks after TAC/Sham-surgery, liver weights / BW ratio were significantly lower in atATGL-KO mice compared to WT mice (**Figure 4.11** C and **Figure 4.14** B). This was independent of intervention. Previous studies confirm these findings (Schoiswohl et al., 2015). Schoiswohl and colleagues revealed that liver weights were significantly reduced in Adipoq-atATGL-KO mice compared to control mice, even in mice fed with HFD. Wu and colleagues demonstrated that atATGL-deficiency results in reduced glycogen and triacylglycerol content in the liver when compared to controls (Wu et al., 2012). Interestingly, in fasting atATGL-KO mice liver glycogen levels decreased more dramatically compared to control mice in fasting. It has been suggested that the reduced FFA supply from adipose tissue lipolysis causes glycogen reserves to be exhausted (Wu et al., 2012).

While atATGL-KO mice showed a reduction in liver weights, liver-specific ATGL-KO mice developed a significant increase in liver weights (Ong et al., 2011). In addition, liver-specific ATGL-KO mice had marked hepatic steatosis with higher TAG content in liver (Ong et al., 2011; Wu et al., 2011). Also, the global ATGL-KO resulted in increased liver weights (Haemmerle et al., 2006) and enhanced hepatic inflammation with steatosis (Jha et al., 2014). Jha and colleagues argue that ATGL is required for hepatic lipid metabolism and anti-inflammatory effects due to the activation of PPAR-α. Interestingly, the overexpression of adipocyte-specific ATGL in mice also causes a reduction of liver weights and TAG in the liver. That results in improved hepatic insulin sensitivity and decreased hepatic steatosis (Ahmadian et al., 2009). In the current study, a reduction in liver weights could be confirmed. In general, the impaired adipose tissue lipolysis correlated with increased gluconeogenesis and, in parallel, with enhanced proteolysis (Wu et al., 2012). Increased hepatic gluconeogenesis and subsequently increased glucose levels in the circulation could be relevant for the cardiac metabolism in HF. While changes in cardiac glucose utilization in HF are still controversial discussed, glycolysis requires less oxygen than FAO and might be beneficial in HF (Korvald et al., 2000).

In summary, adipose tissue-specific ATGL-deficiency results in reduced liver weights, likely a result of reduced hepatic glycogen content. These data support the notion that atATGL-KO mice are predominantly reliant on glucose as an energy source.

5.6 atATGL-KO show different adipose tissue distribution

NMR measurements revealed that 5 weeks after TAC/Sham-surgery, atATGL-KO mice had a significantly higher ratio of total Fat mass to BW ratio compared to WT (**Figure 4.10** A). Consistent with the higher Fat mass/BW ratio is the lower Lean mass/BW ratio 5 weeks after TAC/Sham-surgery in atATGL-KO mice compared to WT mice (**Figure 4.10** B). Increased weights of Perirenal Adipose Tissue (PAT) 5 weeks after TAC/Sham-surgery in atATGL-KO mice support the NMR findings (**Figure 4.11** B). Ahmadian and colleagues demonstrated an increase in fat pad weights in atATGL-KO mice on chow diet and, even more prominent, in animals fed with HFD at the age of 12-14 weeks (Ahmadian et al., 2011). In addition, Wu and colleagues revealed that 12-16 weeks old atATGL-KO male mice have a significantly larger ratio of total fat mass to BW compared to WT controls (Wu et al., 2012). Findings from our study can confirm these previous results. 5 weeks after TAC/Sham-surgery mice were 13-14 weeks old and therefore comparable with the mice used in studies by Wu and colleagues. However, the ratio of Epididymal Adipose Tissue to BW (EAT/BW) did not differ between the four groups 5 weeks after TAC/Sham-surgery (**Table 4.8**). This stands in contrast to findings in the work by Ahmadian et. al, who demonstrated an increase in Gonadal Adipose Tissue in atATGL-KO mice (Ahmadian et al., 2011).

11 weeks after TAC/Sham-surgery NMR measurements revealed that Fat Mass and Lean Mass/BW ratio did not differ between the four groups (**Table 4.9**). PAT/BW was still larger in atATGL-KO mice 11 after TAC- and Sham-surgery compared to WT mice (**Figure 4.14** A), but not as significant as 5 weeks after TAC/Sham-surgery. Total Fat mass increased in WT mice from week 5 to week 11 after TAC/Sham-surgery, but not in atATGL-KO mice. It has been well described that body weight and visceral adipose tissue increase with aging in mice (Shin et al., 2015). Hence, it is unexpected that atATGL-KO mice show a reduced increase in adipose tissue mass with aging in comparison to WT mice.

Regarding results in mice 11 weeks after TAC/Sham-surgery, Schoiswohl and colleagues demonstrated similar results in 24 weeks old adipocytes-specific ATGL-KO male mice using Adipoq-promoter (Adipoq-AAKO mice). Fat mass was similar in Adipoq-AAKO mice compared to WT mice on chow diet and HFD (Schoiswohl et al., 2015). In addition, metabolic studies in humans with ATGL-deficiency (neutral lipid storage disease with myopathy) also showed only a small increase in body weight and total fat mass (Natali et al., 2013; Reilich et al., 2011). Schoiswohl and colleagues

indicated that the reduction in fat mass is caused by a down-regulation of adipocyte lipid uptake and lipid synthesis (Schoiswohl et al., 2015). One could argue that the Adipoq-Cre-model shows significant differences compared to the aP2-Cre-model in terms of fat distribution and fat mass. However, as shown in the present study, there might be an age-dependent change in adipose tissue distribution in atATGL-KO mice. Additional studies, comparing fat mass distribution at different ages in mice, are required to further characterize this reduced increase in fat mass in atATGL-KO mice.

Collectively, atATGL-KO mice had significantly higher Fat mass/BW and PAT/BW ratios in comparison to WT mice 5 weeks after Sham- and TAC-surgery. Also 11 weeks after Sham-surgery PAT/BW ratio were larger in atATGL-KO mice compared to WT control mice. The larger accumulation of WAT in adipose tissue-specific ATGL-KO mice indicates a reduction in FA mobilization caused by decreased lipolysis.

5.7 atATGL-KO mice develop improved insulin sensitivity and glucose tolerance when compared to WT

Intraperitoneal insulin tolerance test (ipITT) revealed that atATGL-KO 11 weeks after TAC-surgery had a higher insulin sensitivity compared to WT after TAC-surgery (**Figure 4.13** C). Moreover, atATGL-KO after Sham-surgery had a significantly higher insulin sensitivity compared to WT mice after Sham-surgery (**Figure 4.13** A). The reduced availability of FFA from the adipose tissue in atATGL-KO mice led to an increased glucose utilization, resulting in a higher insulin sensitivity compared to WT mice. Randle and colleagues demonstrated a reciprocal relationship between glucose- and FA-metabolism in 1963. The Randle-cycle controls substrate supply and demand in adipose tissue and muscle (Randle et al., 1963). A higher uptake of glucose and an increase in glucose oxidation results in higher levels of acetyl-CoA, which can be converted to malonyl-CoA by acetyl-CoA carboxylase. Malonyl-CoA inhibits CPT-1 and therefore promotes the formation of TAGs in the cytosol (Beauloye et al., 2011). The results of this study support this idea and are comparable with previous studies using global ATGL-KO mice (Haemmerle et al., 2006). Haemmerle and colleagues demonstrated that global ATGL-KO mice develop an increased glucose tolerance and increased insulin sensitivity. Also, Wu and colleagues found higher insulin sensitivity in atATGL-KO mice, but higher blood glucose levels in the fasting state. The group argues that lower insulin levels caused higher blood glucose levels in these mice (Wu et al., 2012). In Adipoq-AAKO mice, higher insulin sensitivity and lower glucose levels in GTTs

were observed (Schoiswohl et al., 2015). The results of the present study confirm previous findings that adipose tissue-specific ATGL-deficiency causes higher insulin sensitivity, higher glucose uptake, and improved glucose homeostasis.

HF is associated with insulin resistance and higher glucose levels (Riehle and Abel, 2016; Shimizu et al., 2012). Shimizu and colleagues revealed that insulin sensitivity and glucose tolerance were impaired in mice 4-6 weeks after TAC-surgery. Furthermore, they demonstrated that lipolytic activity in adipose tissue, induced by TAC-surgery, is mediated via the sympathetic nervous system. That leads to the upregulation of p53 tumor suppressor pathway and resulted in adipose tissue inflammation and insulin resistance (Shimizu et al., 2012). Shimizu and colleagues demonstrated that inhibiting p53 with pifithrin-α normalized insulin sensitivity after TAC-surgery. In this study, pressure overload via TAC did not induce insulin resistance or higher glucose levels (**Figure 4.12** A and **Figure 4.13** A). This result was unexpected. However, recent studies revealed that HF in humans is associated with increased myocardial levels of ceramide and DAG, but not TAG (Chokshi et al., 2012; Schulze et al., 2016). Furthermore, increased ceramide levels were accompanied with insulin resistance in patients with HF (Chokshi et al., 2012). Further experiments performed by our group regarding this study, revealed that myocardial ceramide levels were slightly reduced in mice after TAC-surgery (data not shown here). The reduced ceramide levels might be linked to the preserved insulin sensitivity in mice after pressure overload-induced HF.

Interestingly, TAC-operated atATGL-KO mice developed higher insulin sensitivity compared to WT mice after TAC, similar to the effect of pifithrin-α inhibiting p53 in adipose tissue (**Figure 4.13** B and C). ATGL-deficiency in adipose tissue improves metabolic abnormalities after the development of HF in mice. Further studies are required to investigate if a reduced inflammatory process in adipose tissue might be responsible for improved metabolic abnormalities.

5.8 Systemic effects of reduced FA levels in atATGL-KO mice

In the present study, we observed a reduction of FA concentration in the blood circulation of atATGL-KO mice (**Figure 4.15**). That was linked with the reduced lipolytic rate in WAT. This result is comparable with previous studies (Haemmerle et al., 2006; Schoiswohl et al., 2015; Wu et al., 2012).

Wu and colleagues demonstrated that atATGL-KO mice suffer from hypothermia when exposed to cold and hypomobility (Wu et al., 2012). In our study, hypomobility of atATGL-KO mice compared to WT mice could not be confirmed (**Table 4.10**). However, hypomobility and hypothermia in the study by Wu and colleagues were only observed after food removal, which was not investigated in the present study.

Taken the reduced FA-levels in serum and the increased insulin sensitivity in atATGL-KO mice, one would expect a higher respiratory quotient (RQ) compared to WT mice. However, RQ-values of all four groups were similar (**Table 4.10**). Haemmerle and colleagues investigated RQ-values in feeding and fasting state of global ATGL-KO mice. While there were no differences in RQ-values in feeding states, RQ-values decreased with increasing fasting time in WT mice compared to atATGL-KO mice. Constant or even increased RQ-values in fasting state in atATGL-KO mice were also confirmed in other studies (Schoiswohl et al., 2015; Wu et al., 2012). However, in our study, RQ-values were not investigated in the fasting state.

5.9 Individual FA mediate cardiac function

By performing FA profiling using high-performance liquid chromatography coupled with mass spectrometer (HPLC-MS), 5 FFAs (C16:0, C16:1, C18:1, C18:2 and C20:5) could be identified which were reduced in blood circulation of atATGL-KO mice compared to WT mice after TAC-surgery (**Figure 4.16**).

The WHO “Diet, Nutrition and the Prevention of Chronic Diseases” report stated that there is convincing evidence that palmitic acid (C16:0) and myristic acid (C14:0) increase the risk of cardiovascular disease (CVD) (WHO, 2003). However, a recently published review summarizes that there is no clear evidence of a negative role of palm oil, which consists of 44% palmitic acid, for health (Fattore and Fanelli, 2013).

Palmitoleic acid (C16:1) has been identified as a pro-hypertrophic metabolic in the model of Burmese python (Riquelme et al., 2011) as well as in mice challenged with treadmill running and in male athletes (Foryst-Ludwig et al., 2015). Those models investigated the effect of palmitoleic acid (C16:1) in physiological cardiac hypertrophy.

However, palmitoleic acid could also be identified as a risk factor for HF in the Physicians' Health Study (Djousse et al., 2012). To investigate the importance of palmitoleic acid (C16:1) for the physiological in comparison to the pathological cardiac hypertrophy, additional studies are required.

In contrast to the adverse effect on the cardiovascular system of palmitic acid (C16:0) and the pro-hypertrophic adaptive effects of palmitoleic acid (C16:1), oleic acid (C18:1), is considered to decrease the risk of CVD (WHO, 2003). In addition, Estruch and colleagues demonstrated in a multicenter trial that olive oil, which contains around 71% oleic acid (Strayer et al., 2006), lowers the incidence of cardiovascular events (myocardial infarction, stroke, and death due to cardiovascular disease) in the setting of a Mediterranean diet (Estruch et al., 2013). Moreover, elevated consumption of the native olive oil (oleic acid (C18:1)) has been linked to lower blood pressure values in that population (Teres et al., 2008). In comparison to palmitoleic acid, oleic acid (C18:1) is not associated with risk of HF in man (Djousse et al., 2012).

In recent meta-analysis and systemic review linoleic acid (C18:2) could also be identified as cardio-protective FFA. According to a recent study, a 5% increase in energy from linoleic acid (C18:2) (replacing saturated fatty acids) results in a 9% reduced risk of CAD and 13% lower risk of CAD deaths (Farvid et al., 2014). Linoleic acid (C18:2) is needed for the biosynthesis of arachidonic acid, which is a precursor of prothrombotic and inflammatory leukotrienes, correlating with plaque instability (Farvid et al., 2014; Qiu et al., 2006). However, an increased uptake of linoleic acid (C18:2) does not correlate with an increase in inflammatory markers (Johnson and Fritsche, 2012) or the risk of myocardial infarction (Nielsen et al., 2013).

In addition to oleic (C18:1) and linoleic acid (C18:2), eicosapentaenoic acid (C20:5) decreases the risk of CAD by 36% and total death by 17% (Mozaffarian and Rimm, 2006). Eicosapentaenoic acid (C20:5) is an omega-3 fatty acid, which can be found in fatty fish. The American Heart Association recommends diet rich in omega-3 for patients with CAD (Kris-Etherton et al., 2003). Furthermore, eicosapentaenoic acid (C20:5) could be identified to attenuate atrial remodeling and development of atrial fibrillation (AF) in the model of ventricular tachypacing-induced AF in rabbits. The authors conclude that eicosapentaenoic acid (C20:5) might be useful in preventing AF associated HF (Kitamura et al., 2011).

Due to reduced lipolysis in WAT of atATGL-KO mice 11 weeks after TAC palmitic acid (C16:0), associated with a higher risk of CAD or a pro-hypertrophic effect, as well as the

cardiac-protective FFAs oleic acid (C18:1), linoleic acid (C18:2) and eicosapentaenoic acid (C20:5) were reduced in plasma (**Figure 4.16**). However, the effect of palmitic acid (C16:0) on the heart seems to be unclear to this point (Fattore and Fanelli, 2013). Palmitoleic acid (C16:1) has been identified as a mediator for beneficial physiological cardiac hypertrophy (Foryst-Ludwig et al., 2015; Riquelme et al., 2011). We are performing additional studies to further investigate palmitoleic acid (C16:1) as a potential mediator for physiological cardiac hypertrophy and its role for pathological cardiac hypertrophy.

In addition, we performed mass spectrometry of lipid extraction and left ventricles of mice to analyze lipid classes and species in more detail. Here, we found that in particular the phosphatidylethanolamines (PE) with several PE-species were upregulated in heart tissue of WT mice after TAC-surgery compared to Sham-surgery. However, in HF-induced atATGL-KO mice this increase of cardiac PE-species was diminished (data not shown here). Hence, the reduction of circulating FAs, due to a downregulation of lipolysis in WAT, results in changes of the cardiac lipidome causing improved cardiac function.

Clearly, additional studies are required investigating a possible molecular mechanism of the lipid classes and species released from WAT on the cardiac phenotype and function in the setting of heart failure.

5.10 Limitations of the study

Certainly, the study shows limitations especially concerning the TAC method and the genetic background of the mice.

It has been known, that the genetic background of mice can significantly influence the cardiac response to TAC-surgery (Barrick et al., 2007). While the mouse strains C57BL/6J mice and 129S1/SvImJ are frequently used, Barrick and colleagues performed echocardiographic studies to evaluate the cardiac phenotype up to 8 weeks after TAC-surgery. C57BL/6J mice developed a reduced contractile function, LV dilatation, extensive heart fibrosis and inflammation 5 weeks after TAC-surgery. 129S1/SvImJ mice, on the other hand, developed a larger LVM, greater wall thickness and a decreased LVID. The C57BL/6J mice experienced an earlier development of decompensated HF and higher gene expression for hypertrophy markers (Barrick et al., 2007).

Furthermore, in this study, an adipocyte-specific inactivation of ATGL was created using the promoter adipose Protein 2 (aP2, also known as fatty acid binding protein 4, FABP4) and the Cre/loxP system. Two lines of aP2-Cre mice are frequently published, one by Barabara Kahn`s lab (Abel et al., 2001) and the other one by Ronald Evan´s lab (He et al., 2003). In this study, we have used aP2-Cre mice by Ronald Evan’s lab. In both aP2-Cre mice lines, Cre is expressed in white and brown adipose tissue. However, Urs and colleagues showed aP2-Cre expression also in trigeminal ganglia, dorsal root ganglia, cartilage primordia and vertebrae (Urs et al., 2006). aP2-Cre activity was also found in ganglia of peripheral nervous system, in adrenal medulla and some parts of the central nervous system such as the cortex, hippocampus, hypothalamus and cerebellum (Martens et al., 2010). Zhang and colleagues demonstrated aP2-Cre activity in the hindbrain and the vertebrae of mice embryos and even report an aP2-Cre induced inactivation of von Hippel-Lindau gene in brain and liver of mice causing hemorrhages in the named organs (Zhang et al., 2012).

Also, aP2 is expressed in macrophages and critical for the development of arteriosclerosis (Makowski et al., 2001). In macrophages, aP2 causes an increase of cholesterol and inflammatory processes via NF-kappaB (Makowski et al., 2005). Recent studies identified aP2 in macrophages as an important mediator for the development of arteriosclerosis, insulin resistance and diabetes mellitus (Furuhashi et al., 2014).

As shown in a previous study of our group, atATGL-KO mice lacked ATGL expression in WAT. However, ATGL expression was not reduced in bone marrow-derived

macrophages and heart (Foryst-Ludwig et al., 2015). The expression of aP2-Cre in the hypothalamus was measured as well, which was elevated (data not shown). In this study, significant changes in cardiac function and metabolism of atATGL-KO mice were found. However, it seems unlikely that the aP2-Cre expression, and therefore ATGL, in the hypothalamus is linked to the preserved cardiac function in atATGL-KO mice. However, there are currently no data available connecting ATGL in the hypothalamus to CAD or heart failure. Hence, it seems unlikely that lacking ATGL in hypothalamus influences pathological LVH and HF.

Furthermore, it is important to emphasize that the results of this study have been found in mouse. The mouse is one of the most frequently used organism for human disease research (Justice et al., 2011). Mice and humans share around 99% of their genes and disease such as heart disease, hypertension and obesity (Peters et al., 2007). However, it remains challenging to predict how the observed results in mice might relate to humans.

6 Conclusion and Prospects

In the present study, we investigated for the first time the effect of adipose tissue-specific ATGL on the development of pressure overload-induced LVH and HF in a mouse model.

The results revealed that atATGL does not influence LVH compared to control group 5 weeks after TAC/Sham-surgery. However, the study showed that atATGL is crucial for the development of HF 11 weeks after TAC/Sham-surgery. AtATGL-deficiency resulted in a preserved cardiac function compared to control group, which developed heart failure.

Furthermore, atATGL-deficiency caused significant metabolic changes such as reduced liver weights, increased fat mass, higher insulin sensitivity and reduced serum FFA levels. Interestingly, atATGL-KO resulted in reduced plasma levels of the following FFA; C16:0, C16:1, C18:1, C18:2 and C20:5 (**Figure 6.1**). Palmitoleic acid (C16:1) has been identified as a mediator for physiological cardiac hypertrophy in previous studies of our group (Foryst-Ludwig et al., 2015). However, additional research is required to identify, which FFA is responsible for the improved cardiac phenotype in the setting of pressure overload-induced HF.

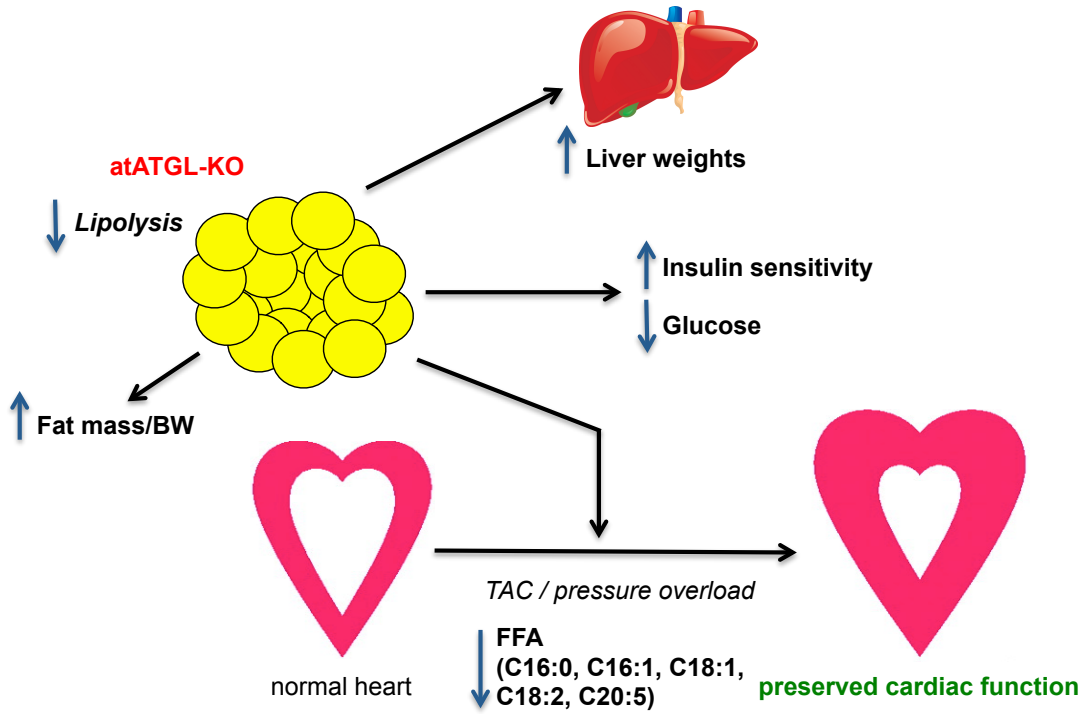

Figure 6.1 Summary of atATGL-KO effects

atATGL-KO - adipose tissue-specific Adipose Triglyceride Lipase Knock-out; FFA – free fatty acids; C16:0 – palmitic acid; C16:1 – palmitoleic acid; C18:1 – oleic acid; C18:2 – linoleic acid; C20:5 – eicosapentaenoic acid

The results clearly show an improved cardiac phenotype due to the reduction of lipolysis in adipose tissue and the subsequent lower circulating FA levels. HF is still one the greatest challenges in our health system worldwide, even though new pharmacological treatments have shown to improve mortality and morbidity in HF patients.

Specific FAs need to be identified interacting with cardiomyocytes in the development of HF. Furthermore, HF patients need to be investigated to determine which FAs might cause similar effects as in mice.

Parts of this work will be used for publication in a peer-reviewed journal.

7 References

1 Abel, E.D. (2004). Glucose transport in the heart. Frontiers in bioscience : a journal and virtual library, 9, 201-215.

2 Abel, E.D., and Doenst, T. (2011). Mitochondrial adaptations to physiological vs. pathological cardiac hypertrophy. Cardiovascular research, 90(2), 234-242. doi: 10.1093/cvr/cvr015

3 Abel, E.D., Peroni, O., Kim, J.K., Kim, Y.B., Boss, O., Hadro, E., Minnemann, T., Shulman, G.I., and Kahn, B.B. (2001). Adipose-selective targeting of the GLUT4 gene impairs insulin action in muscle and liver. Nature, 409(6821), 729-733. doi: 10.1038/35055575

4 Aerni-Flessner, L., Abi-Jaoude, M., Koenig, A., Payne, M., and Hruz, P.W. (2012). GLUT4, GLUT1, and GLUT8 are the dominant GLUT transcripts expressed in the murine left ventricle. Cardiovascular diabetology, 11, 63. doi: 10.1186/1475-2840-11-63

5 Agilent Technologies, I. HPLC Basics (http://polymer.ustc.edu.cn/xwxx_20/xw/201109/P020110906263097048536.pdf: Agilent Technologies), pp. Fundamentals of Liquid Chromatography (HPLC).

6 AHA (2015). About Heart Failure (American Heart Association).

7 Ahmadian, M., Abbott, M.J., Tang, T., Hudak, C.S., Kim, Y., Bruss, M., Hellerstein, M.K., Lee, H.Y., Samuel, V.T., Shulman, G.I., Wang, Y., Duncan, R.E., Kang, C., and Sul, H.S. (2011). Desnutrin/ATGL is regulated by AMPK and is required for a brown adipose phenotype. Cell metabolism, 13(6), 739-748. doi: 10.1016/j.cmet.2011.05.002

8 Ahmadian, M., Duncan, R.E., Varady, K.A., Frasson, D., Hellerstein, M.K., Birkenfeld, A.L., Samuel, V.T., Shulman, G.I., Wang, Y., Kang, C., and Sul, H.S. (2009). Adipose overexpression of desnutrin promotes fatty acid use and attenuates diet-induced obesity. Diabetes, 58(4), 855-866. doi: 10.2337/db08-1644

9 Ahmadian, M., Wang, Y., and Sul, H.S. (2010). Lipolysis in adipocytes. The international journal of biochemistry & cell biology, 42(5), 555-559. doi: 10.1016/j.biocel.2009.12.009

10 Akki, A., Smith, K., and Seymour, A.M. (2008). Compensated cardiac hypertrophy is characterised by a decline in palmitate oxidation. Molecular and cellular biochemistry, 311(1-2), 215-224. doi: 10.1007/s11010-008-9711-y

11 Alberti, K.G., Zimmet, P., and Shaw, J. (2005). The metabolic syndrome--a new worldwide definition. Lancet (London, England), 366(9491), 1059-1062. doi: 10.1016/s0140-6736(05)67402-8

12 Allard, M.F., Schonekess, B.O., Henning, S.L., English, D.R., and Lopaschuk, G.D. (1994). Contribution of oxidative metabolism and glycolysis to ATP

production in hypertrophied hearts. The American journal of physiology, 267(2 Pt 2), H742-750.

13 Anand, I.S., Fisher, L.D., Chiang, Y.T., Latini, R., Masson, S., Maggioni, A.P., Glazer, R.D., Tognoni, G., and Cohn, J.N. (2003). Changes in brain natriuretic peptide and norepinephrine over time and mortality and morbidity in the Valsartan Heart Failure Trial (Val-HeFT). Circulation, 107(9), 1278-1283.

14 Anthonsen, M.W., Ronnstrand, L., Wernstedt, C., Degerman, E., and Holm, C. (1998). Identification of novel phosphorylation sites in hormone-sensitive lipase that are phosphorylated in response to isoproterenol and govern activation properties in vitro. The Journal of biological chemistry, 273(1), 215-221.

15 Armstrong, A.C., Gidding, S., Gjesdal, O., Wu, C., Bluemke, D.A., and Lima, J.A. (2012). LV mass assessed by echocardiography and CMR, cardiovascular outcomes, and medical practice. JACC Cardiovascular imaging, 5(8), 837-848. doi: 10.1016/j.jcmg.2012.06.003

16 Balaban, R.S. (2002). Cardiac energy metabolism homeostasis: role of cytosolic calcium. Journal of molecular and cellular cardiology, 34(10), 1259-1271.

17 Banerji, S., and Flieger, A. (2004). Patatin-like proteins: a new family of lipolytic enzymes present in bacteria? Microbiology (Reading, England), 150(Pt 3), 522-525. doi: 10.1099/mic.0.26957-0

18 Barlow, C., Schroeder, M., Lekstrom-Himes, J., Kylefjord, H., Deng, C.X., Wynshaw-Boris, A., Spiegelman, B.M., and Xanthopoulos, K.G. (1997). Targeted expression of Cre recombinase to adipose tissue of transgenic mice directs adipose-specific excision of loxP-flanked gene segments. Nucleic acids research, 25(12), 2543-2545.

19 Barrick, C.J., Rojas, M., Schoonhoven, R., Smyth, S.S., and Threadgill, D.W. (2007). Cardiac response to pressure overload in 129S1/SvImJ and C57BL/6J mice: temporal- and background-dependent development of concentric left ventricular hypertrophy. American journal of physiology Heart and circulatory physiology, 292(5), H2119-2130. doi: 10.1152/ajpheart.00816.2006

20 Bartz, R., Zehmer, J.K., Zhu, M., Chen, Y., Serrero, G., Zhao, Y., and Liu, P. (2007). Dynamic activity of lipid droplets: protein phosphorylation and GTP-mediated protein translocation. Journal of proteome research, 6(8), 3256-3265. doi: 10.1021/pr070158j

21 Beauloye, C., Bertrand, L., Horman, S., and Hue, L. (2011). AMPK activation, a preventive therapeutic target in the transition from cardiac injury to heart failure. Cardiovascular research, 90(2), 224-233. doi: 10.1093/cvr/cvr034

22 Beigneux, A.P., Gin, P., Davies, B.S., Weinstein, M.M., Bensadoun, A., Ryan, R.O., Fong, L.G., and Young, S.G. (2008). Glycosylation of Asn-76 in mouse GPIHBP1 is critical for its appearance on the cell surface and the binding of

chylomicrons and lipoprotein lipase. Journal of lipid research, 49(6), 1312-1321. doi: 10.1194/jlr.M700593-JLR200

23 Bernardo, B.C., Weeks, K.L., Pretorius, L., and McMullen, J.R. (2010). Molecular distinction between physiological and pathological cardiac hypertrophy: experimental findings and therapeutic strategies. Pharmacology & therapeutics, 128(1), 191-227. doi: 10.1016/j.pharmthera.2010.04.005

24 Berrington de Gonzalez, A., Hartge, P., Cerhan, J.R., Flint, A.J., Hannan, L., MacInnis, R.J., Moore, S.C., Tobias, G.S., Anton-Culver, H., Freeman, L.B., Beeson, W.L., Clipp, S.L., English, D.R., Folsom, A.R., Freedman, D.M., Giles, G., Hakansson, N., Henderson, K.D., Hoffman-Bolton, J., Hoppin, J.A., Koenig, K.L., Lee, I.M., Linet, M.S., Park, Y., Pocobelli, G., Schatzkin, A., Sesso, H.D., Weiderpass, E., Willcox, B.J., Wolk, A., Zeleniuch-Jacquotte, A., Willett, W.C., and Thun, M.J. (2010). Body-mass index and mortality among 1.46 million white adults. The New England journal of medicine, 363(23), 2211-2219. doi: 10.1056/NEJMoa1000367

25 Bezaire, V., and Langin, D. (2009). Regulation of adipose tissue lipolysis revisited. The Proceedings of the Nutrition Society, 68(4), 350-360. doi: 10.1017/s0029665109990279

26 Bezaire, V., Mairal, A., Ribet, C., Lefort, C., Girousse, A., Jocken, J., Laurencikiene, J., Anesia, R., Rodriguez, A.M., Ryden, M., Stenson, B.M., Dani, C., Ailhaud, G., Arner, P., and Langin, D. (2009). Contribution of adipose triglyceride lipase and hormone-sensitive lipase to lipolysis in hMADS adipocytes. The Journal of biological chemistry, 284(27), 18282-18291. doi: 10.1074/jbc.M109.008631

27 Birkenfeld, A.L., Boschmann, M., Moro, C., Adams, F., Heusser, K., Franke, G., Berlan, M., Luft, F.C., Lafontan, M., and Jordan, J. (2005). Lipid mobilization with physiological atrial natriuretic peptide concentrations in humans. The Journal of clinical endocrinology and metabolism, 90(6), 3622-3628. doi: 10.1210/jc.2004-1953

28 Birkenfeld, A.L., Boschmann, M., Moro, C., Adams, F., Heusser, K., Tank, J., Diedrich, A., Schroeder, C., Franke, G., Berlan, M., Luft, F.C., Lafontan, M., and Jordan, J. (2006). Beta-adrenergic and atrial natriuretic peptide interactions on human cardiovascular and metabolic regulation. The Journal of clinical endocrinology and metabolism, 91(12), 5069-5075. doi: 10.1210/jc.2006-1084

29 Bjorntorp, P. (1992). Metabolic abnormalities in visceral obesity. Annals of medicine, 24(1), 3-5.

30 Bluher, M. (2008). The inflammatory process of adipose tissue. Pediatric endocrinology reviews : PER, 6(1), 24-31.

31 Boden, G., and Shulman, G.I. (2002). Free fatty acids in obesity and type 2 diabetes: defining their role in the development of insulin resistance and beta-cell dysfunction. European journal of clinical investigation, 32 Suppl 3, 14-23.

32 Bolger, A.P., Sharma, R., Li, W., Leenarts, M., Kalra, P.R., Kemp, M., Coats, A.J., Anker, S.D., and Gatzoulis, M.A. (2002). Neurohormonal activation and the chronic heart failure syndrome in adults with congenital heart disease. Circulation, 106(1), 92-99.

33 Bolsoni-Lopes, A., and Alonso-Vale, M.I. (2015). Lipolysis and lipases in white adipose tissue - An update. Archives of endocrinology and metabolism, 59(4), 335-342. doi: 10.1590/2359-3997000000067

34 Bordicchia, M., Liu, D., Amri, E.Z., Ailhaud, G., Dessi-Fulgheri, P., Zhang, C., Takahashi, N., Sarzani, R., and Collins, S. (2012). Cardiac natriuretic peptides act via p38 MAPK to induce the brown fat thermogenic program in mouse and human adipocytes. The Journal of clinical investigation, 122(3), 1022-1036. doi: 10.1172/jci59701

35 Broberg, C.S., and Burchill, L.J. (2015). Myocardial factor revisited: The importance of myocardial fibrosis in adults with congenital heart disease. International journal of cardiology, 189, 204-210. doi: 10.1016/j.ijcard.2015.04.064

36 Bugger, H., Schwarzer, M., Chen, D., Schrepper, A., Amorim, P.A., Schoepe, M., Nguyen, T.D., Mohr, F.W., Khalimonchuk, O., Weimer, B.C., and Doenst, T. (2010). Proteomic remodelling of mitochondrial oxidative pathways in pressure overload-induced heart failure. Cardiovascular research, 85(2), 376-384. doi: 10.1093/cvr/cvp344

37 Bundesamt, S. (2014). Todesursachen in Deutschland. In Gesundheit (Wiesbaden: Statistisches Bundesamt).

38 Burchfield, J.S., Xie, M., and Hill, J.A. (2013). Pathological ventricular remodeling: mechanisms: part 1 of 2. Circulation, 128(4), 388-400. doi: 10.1161/circulationaha.113.001878

39 Cacciapuoti, F. (2011). Molecular mechanisms of left ventricular hypertrophy (LVH) in systemic hypertension (SH)-possible therapeutic perspectives. Journal of the American Society of Hypertension : JASH, 5(6), 449-455. doi: 10.1016/j.jash.2011.08.006

40 Cannon, B., and Nedergaard, J. (2004). Brown adipose tissue: function and physiological significance. Physiological reviews, 84(1), 277-359. doi: 10.1152/physrev.00015.2003

41 Cao, W., Daniel, K.W., Robidoux, J., Puigserver, P., Medvedev, A.V., Bai, X., Floering, L.M., Spiegelman, B.M., and Collins, S. (2004). p38 mitogen-activated protein kinase is the central regulator of cyclic AMP-dependent transcription of the brown fat uncoupling protein 1 gene. Molecular and cellular biology, 24(7), 3057-3067.

42 Cao, W., Medvedev, A.V., Daniel, K.W., and Collins, S. (2001). beta-Adrenergic activation of p38 MAP kinase in adipocytes: cAMP induction of the uncoupling protein 1 (UCP1) gene requires p38 MAP kinase. The Journal of biological chemistry, 276(29), 27077-27082. doi: 10.1074/jbc.M101049200

43 Chaggar, P.S., Malkin, C.J., Shaw, S.M., Williams, S.G., and Channer, K.S. (2009). Neuroendocrine effects on the heart and targets for therapeutic manipulation in heart failure. Cardiovascular therapeutics, 27(3), 187-193. doi: 10.1111/j.1755-5922.2009.00094.x

44 Chakrabarti, P., English, T., Shi, J., Smas, C.M., and Kandror, K.V. (2010). Mammalian target of rapamycin complex 1 suppresses lipolysis, stimulates lipogenesis, and promotes fat storage. Diabetes, 59(4), 775-781. doi: 10.2337/db09-1602

45 Chakrabarti, P., and Kandror, K.V. (2009). FoxO1 controls insulin-dependent adipose triglyceride lipase (ATGL) expression and lipolysis in adipocytes. The Journal of biological chemistry, 284(20), 13296-13300. doi: 10.1074/jbc.C800241200

46 Chandler, M.P., Kerner, J., Huang, H., Vazquez, E., Reszko, A., Martini, W.Z., Hoppel, C.L., Imai, M., Rastogi, S., Sabbah, H.N., and Stanley, W.C. (2004). Moderate severity heart failure does not involve a downregulation of myocardial fatty acid oxidation. American journal of physiology Heart and circulatory physiology, 287(4), H1538-1543. doi: 10.1152/ajpheart.00281.2004

47 Chen, Y., Guo, H., Xu, D., Xu, X., Wang, H., Hu, X., Lu, Z., Kwak, D., Xu, Y., Gunther, R., Huo, Y., and Weir, E.K. (2012). Left ventricular failure produces profound lung remodeling and pulmonary hypertension in mice: heart failure causes severe lung disease. Hypertension, 59(6), 1170-1178. doi: 10.1161/hypertensionaha.111.186072

48 Chess, D.J., Khairallah, R.J., O'Shea, K.M., Xu, W., and Stanley, W.C. (2009). A high-fat diet increases adiposity but maintains mitochondrial oxidative enzymes without affecting development of heart failure with pressure overload. American journal of physiology Heart and circulatory physiology, 297(5), H1585-1593. doi: 10.1152/ajpheart.00599.2009

49 Chokshi, A., Drosatos, K., Cheema, F.H., Ji, R., Khawaja, T., Yu, S., Kato, T., Khan, R., Takayama, H., Knoll, R., Milting, H., Chung, C.S., Jorde, U., Naka, Y., Mancini, D.M., Goldberg, I.J., and Schulze, P.C. (2012). Ventricular assist device implantation corrects myocardial lipotoxicity, reverses insulin resistance, and normalizes cardiac metabolism in patients with advanced heart failure. Circulation, 125(23), 2844-2853. doi: 10.1161/circulationaha.111.060889

50 Christe, M.E., and Rodgers, R.L. (1994). Altered glucose and fatty acid oxidation in hearts of the spontaneously hypertensive rat. Journal of molecular and cellular cardiology, 26(10), 1371-1375. doi: 10.1006/jmcc.1994.1155

51 Chrostowska, M., Szyndler, A., Hoffmann, M., and Narkiewicz, K. (2013). Impact of obesity on cardiovascular health. Best practice & research Clinical endocrinology & metabolism, 27(2), 147-156. doi: 10.1016/j.beem.2013.01.004

52 Cinti, S. (2011). Between brown and white: novel aspects of adipocyte differentiation. Annals of medicine, 43(2), 104-115. doi: 10.3109/07853890.2010.535557

53 Cinti, S., Zancanaro, C., Sbarbati, A., Cicolini, M., Vogel, P., Ricquier, D., and Fakan, S. (1989). Immunoelectron microscopical identification of the uncoupling protein in brown adipose tissue mitochondria. Biology of the cell / under the auspices of the European Cell Biology Organization, 67(3), 359-362.

54 Cohn, J.N., Levine, T.B., Olivari, M.T., Garberg, V., Lura, D., Francis, G.S., Simon, A.B., and Rector, T. (1984). Plasma norepinephrine as a guide to prognosis in patients with chronic congestive heart failure. The New England journal of medicine, 311(13), 819-823. doi: 10.1056/nejm198409273111303

55 Collins, K.A., Korcarz, C.E., and Lang, R.M. (2003). Use of echocardiography for the phenotypic assessment of genetically altered mice. Physiological genomics, 13(3), 227-239. doi: 10.1152/physiolgenomics.00005.2003

56 Collins, S. (2014). A heart-adipose tissue connection in the regulation of energy metabolism. Nature reviews Endocrinology, 10(3), 157-163. doi: 10.1038/nrendo.2013.234

57 Contreras, C., Gonzalez, F., Ferno, J., Dieguez, C., Rahmouni, K., Nogueiras, R., and Lopez, M. (2015). The brain and brown fat. Annals of medicine, 47(2), 150-168. doi: 10.3109/07853890.2014.919727

58 Cornaciu, I., Boeszoermenyi, A., Lindermuth, H., Nagy, H.M., Cerk, I.K., Ebner, C., Salzburger, B., Gruber, A., Schweiger, M., Zechner, R., Lass, A., Zimmermann, R., and Oberer, M. (2011). The minimal domain of adipose triglyceride lipase (ATGL) ranges until leucine 254 and can be activated and inhibited by CGI-58 and G0S2, respectively. PLoS One, 6(10), e26349. doi: 10.1371/journal.pone.0026349

59 Cox, E.J., and Marsh, S.A. (2014). A systematic review of fetal genes as biomarkers of cardiac hypertrophy in rodent models of diabetes. PLoS One, 9(3), e92903. doi: 10.1371/journal.pone.0092903

60 Curry, C.W., Nelson, G.S., Wyman, B.T., Declerck, J., Talbot, M., Berger, R.D., McVeigh, E.R., and Kass, D.A. (2000). Mechanical dyssynchrony in dilated cardiomyopathy with intraventricular conduction delay as depicted by 3D tagged magnetic resonance imaging. Circulation, 101(1), E2.

61 Davila-Roman, V.G., Vedala, G., Herrero, P., de las Fuentes, L., Rogers, J.G., Kelly, D.P., and Gropler, R.J. (2002). Altered myocardial fatty acid and glucose metabolism in idiopathic dilated cardiomyopathy. Journal of the American College of Cardiology, 40(2), 271-277.

62 de Bold, A.J. (1985). Atrial natriuretic factor: a hormone produced by the heart. Science, 230(4727), 767-770.

63 de Koning, L., Merchant, A.T., Pogue, J., and Anand, S.S. (2007). Waist circumference and waist-to-hip ratio as predictors of cardiovascular events: meta-regression analysis of prospective studies. Eur Heart J, 28(7), 850-856. doi: 10.1093/eurheartj/ehm026

64 deAlmeida, A.C., van Oort, R.J., and Wehrens, X.H. (2010). Transverse aortic constriction in mice. Journal of visualized experiments : JoVE(38). doi: 10.3791/1729

65 Degerman, E., Smith, C.J., Tornqvist, H., Vasta, V., Belfrage, P., and Manganiello, V.C. (1990). Evidence that insulin and isoprenaline activate the cGMP-inhibited low-Km cAMP phosphodiesterase in rat fat cells by phosphorylation. Proc Natl Acad Sci U S A, 87(2), 533-537.

66 Despres, J.P. (2012). Body fat distribution and risk of cardiovascular disease: an update. Circulation, 126(10), 1301-1313. doi: 10.1161/circulationaha.111.067264

67 Dietz, J., and Schwartz, J. (1991). Growth hormone alters lipolysis and hormone-sensitive lipase activity in 3T3-F442A adipocytes. Metabolism: clinical and experimental, 40(8), 800-806.

68 Djousse, L., Weir, N.L., Hanson, N.Q., Tsai, M.Y., and Gaziano, J.M. (2012). Plasma phospholipid concentration of cis-palmitoleic acid and risk of heart failure. Circulation Heart failure, 5(6), 703-709. doi: 10.1161/circheartfailure.112.967802

69 Dobaczewski, M., Gonzalez-Quesada, C., and Frangogiannis, N.G. (2010). The extracellular matrix as a modulator of the inflammatory and reparative response following myocardial infarction. Journal of molecular and cellular cardiology, 48(3), 504-511. doi: 10.1016/j.yjmcc.2009.07.015

70 Doenst, T., Nguyen, T.D., and Abel, E.D. (2013). Cardiac metabolism in heart failure: implications beyond ATP production. Circulation research, 113(6), 709-724. doi: 10.1161/circresaha.113.300376

71 Doenst, T., Pytel, G., Schrepper, A., Amorim, P., Farber, G., Shingu, Y., Mohr, F.W., and Schwarzer, M. (2010). Decreased rates of substrate oxidation ex vivo predict the onset of heart failure and contractile dysfunction in rats with pressure overload. Cardiovascular research, 86(3), 461-470. doi: 10.1093/cvr/cvp414

72 Dolgin, M. (1994). The Criteria Committee of the New York Heart Association. Nomenclature and Criteria for Diagnosis of Diseases of the Heart and Great Vessels, 253–256.

73 Don-Wauchope, A.C., and McKelvie, R.S. (2015). Evidence based application of BNP/NT-proBNP testing in heart failure. Clinical biochemistry, 48(4-5), 236-246. doi: 10.1016/j.clinbiochem.2014.11.002

74 Dorn, G.W., 2nd. (2009). Novel pharmacotherapies to abrogate postinfarction ventricular remodeling. Nature reviews Cardiology, 6(4), 283-291. doi: 10.1038/nrcardio.2009.12

75 Douglass, J.D., Zhou, Y.X., Wu, A., Zadrogra, J.A., Gajda, A.M., Lackey, A.I., Lang, W., Chevalier, K.M., Sutton, S.W., Zhang, S.P., Flores, C.M., Connelly, M.A., and Storch, J. (2015). Global deletion of MGL in mice delays lipid absorption and alters energy homeostasis and diet-induced obesity. Journal of lipid research, 56(6), 1153-1171. doi: 10.1194/jlr.M058586

76 Duncan, R.E., Wang, Y., Ahmadian, M., Lu, J., Sarkadi-Nagy, E., and Sul, H.S. (2010). Characterization of desnutrin functional domains: critical residues for triacylglycerol hydrolysis in cultured cells. Journal of lipid research, 51(2), 309-317. doi: 10.1194/jlr.M000729

77 Eclov, J.A., Qian, Q., Redetzke, R., Chen, Q., Wu, S.C., Healy, C.L., Ortmeier, S.B., Harmon, E., Shearer, G.C., and O'Connell, T.D. (2015). EPA, not DHA, prevents fibrosis in pressure overload-induced heart failure: potential role of free fatty acid receptor 4. Journal of lipid research, 56(12), 2297-2308. doi: 10.1194/jlr.M062034

78 Ellong, E.N., Soni, K.G., Bui, Q.T., Sougrat, R., Golinelli-Cohen, M.P., and Jackson, C.L. (2011). Interaction between the triglyceride lipase ATGL and the Arf1 activator GBF1. PLoS One, 6(7), e21889. doi: 10.1371/journal.pone.0021889

79 Engfeldt, P., Hellmer, J., Wahrenberg, H., and Arner, P. (1988). Effects of insulin on adrenoceptor binding and the rate of catecholamine-induced lipolysis in isolated human fat cells. The Journal of biological chemistry, 263(30), 15553-15560.

80 Estruch, R., Ros, E., Salas-Salvado, J., Covas, M.I., Corella, D., Aros, F., Gomez-Gracia, E., Ruiz-Gutierrez, V., Fiol, M., Lapetra, J., Lamuela-Raventos, R.M., Serra-Majem, L., Pinto, X., Basora, J., Munoz, M.A., Sorli, J.V., Martinez, J.A., and Martinez-Gonzalez, M.A. (2013). Primary prevention of cardiovascular disease with a Mediterranean diet. The New England journal of medicine, 368(14), 1279-1290. doi: 10.1056/NEJMoa1200303

81 Farvid, M.S., Ding, M., Pan, A., Sun, Q., Chiuve, S.E., Steffen, L.M., Willett, W.C., and Hu, F.B. (2014). Dietary linoleic acid and risk of coronary heart disease: a systematic review and meta-analysis of prospective cohort studies. Circulation, 130(18), 1568-1578. doi: 10.1161/circulationaha.114.010236

82 Fattore, E., and Fanelli, R. (2013). Palm oil and palmitic acid: a review on cardiovascular effects and carcinogenicity. International journal of food sciences and nutrition, 64(5), 648-659. doi: 10.3109/09637486.2013.768213

83 Fischer, J., Lefevre, C., Morava, E., Mussini, J.M., Laforet, P., Negre-Salvayre, A., Lathrop, M., and Salvayre, R. (2007). The gene encoding adipose triglyceride lipase (PNPLA2) is mutated in neutral lipid storage disease with myopathy. Nature genetics, 39(1), 28-30. doi: 10.1038/ng1951

84 Fishberg, A. (1937). Heart Failure (Philadelphia: Lea & Febiger).

85 Fliegner, D., Schubert, C., Penkalla, A., Witt, H., Kararigas, G., Dworatzek, E., Staub, E., Martus, P., Ruiz Noppinger, P., Kintscher, U., Gustafsson, J.A., and Regitz-Zagrosek, V. (2010). Female sex and estrogen receptor-beta attenuate cardiac remodeling and apoptosis in pressure overload. American journal of physiology Regulatory, integrative and comparative physiology, 298(6), R1597-1606. doi: 10.1152/ajpregu.00825.2009

86 Foryst-Ludwig, A., and Kintscher, U. (2013). Sex differences in exercise-induced cardiac hypertrophy. Pflugers Archiv : European journal of physiology, 465(5), 731-737. doi: 10.1007/s00424-013-1225-0

87 Foryst-Ludwig, A., Kreissl, M.C., Benz, V., Brix, S., Smeir, E., Ban, Z., Januszewicz, E., Salatzki, J., Grune, J., Schwanstecher, A.K., Blumrich, A., Schirbel, A., Klopfleisch, R., Rothe, M., Blume, K., Halle, M., Wolfarth, B., Kershaw, E.E., and Kintscher, U. (2015). Adipose Tissue Lipolysis Promotes Exercise-Induced Cardiac Hypertrophy Involving the Lipokine C16:1n7-Palmitoleate. The Journal of biological chemistry. doi: 10.1074/jbc.M115.645341

88 Fox, C.S., Massaro, J.M., Hoffmann, U., Pou, K.M., Maurovich-Horvat, P., Liu, C.Y., Vasan, R.S., Murabito, J.M., Meigs, J.B., Cupples, L.A., D'Agostino, R.B., Sr., and O'Donnell, C.J. (2007). Abdominal visceral and subcutaneous adipose tissue compartments: association with metabolic risk factors in the Framingham Heart Study. Circulation, 116(1), 39-48. doi: 10.1161/circulationaha.106.675355

89 Frenz, U. (1999). Whole body calorimetry. In Handbook of Thermal Analysis and Calorimetry, P.B. Kemp, ed. (Amsterdam, Lausanne, New York, Oxford, Shannon, Singapore, Tokyo: Elsevier Science), pp. 511-555.

90 Frey, N., Katus, H.A., Olson, E.N., and Hill, J.A. (2004). Hypertrophy of the heart: a new therapeutic target? Circulation, 109(13), 1580-1589. doi: 10.1161/01.cir.0000120390.68287.bb

91 Fritsche, O. (2013). Physik für Biologen und Mediziner, Vol 1 (Berlin Heidelberg: Springer Spektrum).

92 Fruhbeck, G., Mendez-Gimenez, L., Fernandez-Formoso, J.A., Fernandez, S., and Rodriguez, A. (2014). Regulation of adipocyte lipolysis. Nutrition research reviews, 27(1), 63-93. doi: 10.1017/s095442241400002x

93 Funada, J., Betts, T.R., Hodson, L., Humphreys, S.M., Timperley, J., Frayn, K.N., and Karpe, F. (2009). Substrate utilization by the failing human heart by direct

quantification using arterio-venous blood sampling. PLoS One, 4(10), e7533. doi: 10.1371/journal.pone.0007533

94 Furuhashi, M., Saitoh, S., Shimamoto, K., and Miura, T. (2014). Fatty Acid-Binding Protein 4 (FABP4): Pathophysiological Insights and Potent Clinical Biomarker of Metabolic and Cardiovascular Diseases. Clinical Medicine Insights Cardiology, 8(Suppl 3), 23-33. doi: 10.4137/cmc.s17067

95 Gao, H., Feng, X.J., Li, Z.M., Li, M., Gao, S., He, Y.H., Wang, J.J., Zeng, S.Y., Liu, X.P., Huang, X.Y., Chen, S.R., and Liu, P.Q. (2015). Downregulation of adipose triglyceride lipase promotes cardiomyocyte hypertrophy by triggering the accumulation of ceramides. Archives of biochemistry and biophysics, 565, 76-88. doi: 10.1016/j.abb.2014.11.009

96 Gekle, M. (2014). Energiehaushalt und Kontrolle des Körpergewichts. In Physiologie, H.-C. Pape, A. Kurtz, and S. Silbernagl, eds. (Stuttgart, Germany: Thieme Verlag KG), pp. 555-556.

97 Giri, D. (2015). LaboratoryInfo.com.

98 Girousse, A., and Langin, D. (2012). Adipocyte lipases and lipid droplet-associated proteins: insight from transgenic mouse models. International journal of obesity (2005), 36(4), 581-594. doi: 10.1038/ijo.2011.113

99 Gitau, S.C., Li, X., Zhao, D., Guo, Z., Liang, H., Qian, M., Lv, L., Li, T., Xu, B., Wang, Z., Zhang, Y., Xu, C., Lu, Y., Du, Z., Shan, H., and Yang, B. (2015). Acetyl salicylic acid attenuates cardiac hypertrophy through Wnt signaling. Frontiers of medicine, 9(4), 444-456. doi: 10.1007/s11684-015-0421-z

100 Go, A.S., Mozaffarian, D., Roger, V.L., Benjamin, E.J., Berry, J.D., Borden, W.B., Bravata, D.M., Dai, S., Ford, E.S., Fox, C.S., Franco, S., Fullerton, H.J., Gillespie, C., Hailpern, S.M., Heit, J.A., Howard, V.J., Huffman, M.D., Kissela, B.M., Kittner, S.J., Lackland, D.T., Lichtman, J.H., Lisabeth, L.D., Magid, D., Marcus, G.M., Marelli, A., Matchar, D.B., McGuire, D.K., Mohler, E.R., Moy, C.S., Mussolino, M.E., Nichol, G., Paynter, N.P., Schreiner, P.J., Sorlie, P.D., Stein, J., Turan, T.N., Virani, S.S., Wong, N.D., Woo, D., and Turner, M.B. (2013). Heart disease and stroke statistics--2013 update: a report from the American Heart Association. Circulation, 127(1), e6-e245. doi: 10.1161/CIR.0b013e31828124ad

101 Grahn, T.H., Kaur, R., Yin, J., Schweiger, M., Sharma, V.M., Lee, M.J., Ido, Y., Smas, C.M., Zechner, R., Lass, A., and Puri, V. (2014). Fat-specific protein 27 (FSP27) interacts with adipose triglyceride lipase (ATGL) to regulate lipolysis and insulin sensitivity in human adipocytes. The Journal of biological chemistry, 289(17), 12029-12039. doi: 10.1074/jbc.M113.539890

102 Granneman, J.G., Moore, H.P., Granneman, R.L., Greenberg, A.S., Obin, M.S., and Zhu, Z. (2007). Analysis of lipolytic protein trafficking and interactions in adipocytes. The Journal of biological chemistry, 282(8), 5726-5735. doi: 10.1074/jbc.M610580200

103 Greenberg, A.S., Coleman, R.A., Kraemer, F.B., McManaman, J.L., Obin, M.S., Puri, V., Yan, Q.W., Miyoshi, H., and Mashek, D.G. (2011). The role of lipid droplets in metabolic disease in rodents and humans. The Journal of clinical investigation, 121(6), 2102-2110. doi: 10.1172/jci46069

104 Gribok, A., Hoyt, R., Buller, M., and Rumpler, W. (2013). On the accuracy of instantaneous gas exchange rates, energy expenditure and respiratory quotient calculations obtained from indirect whole room calorimetry. Physiological measurement, 34(6), 737-755. doi: 10.1088/0967-3334/34/6/737

105 Grossman, W., Jones, D., and McLaurin, L.P. (1975). Wall stress and patterns of hypertrophy in the human left ventricle. The Journal of clinical investigation, 56(1), 56-64. doi: 10.1172/jci108079

106 Gruden, G., Landi, A., and Bruno, G. (2014). Natriuretic peptides, heart, and adipose tissue: new findings and future developments for diabetes research. Diabetes care, 37(11), 2899-2908. doi: 10.2337/dc14-0669

107 Grune, J., Benz, V., Brix, S., Salatzki, J., Blumrich, A., Hoft, B., Klopfleisch, R., Foryst-Ludwig, A., Kolkhof, P., and Kintscher, U. (2016). Steroidal and Nonsteroidal Mineralocorticoid Receptor Antagonists Cause Differential Cardiac Gene Expression in Pressure Overload-Induced Cardiac Hypertrophy. Journal of cardiovascular pharmacology. doi: 10.1097/fjc.0000000000000366

108 Guo, Y., Walther, T.C., Rao, M., Stuurman, N., Goshima, G., Terayama, K., Wong, J.S., Vale, R.D., Walter, P., and Farese, R.V. (2008). Functional genomic screen reveals genes involved in lipid-droplet formation and utilization. Nature, 453(7195), 657-661. doi: 10.1038/nature06928

109 Gustafson, T.A., Bahl, J.J., Markham, B.E., Roeske, W.R., and Morkin, E. (1987). Hormonal regulation of myosin heavy chain and alpha-actin gene expression in cultured fetal rat heart myocytes. The Journal of biological chemistry, 262(27), 13316-13322.

110 Haddad, H. (2016). Heart Failure (http://slideplayer.com/slide/9084651/).

111 Haemmerle, G., Lass, A., Zimmermann, R., Gorkiewicz, G., Meyer, C., Rozman, J., Heldmaier, G., Maier, R., Theussl, C., Eder, S., Kratky, D., Wagner, E.F., Klingenspor, M., Hoefler, G., and Zechner, R. (2006). Defective lipolysis and altered energy metabolism in mice lacking adipose triglyceride lipase. Science, 312(5774), 734-737. doi: 10.1126/science.1123965

112 Haemmerle, G., Moustafa, T., Woelkart, G., Buttner, S., Schmidt, A., van de Weijer, T., Hesselink, M., Jaeger, D., Kienesberger, P.C., Zierler, K., Schreiber, R., Eichmann, T., Kolb, D., Kotzbeck, P., Schweiger, M., Kumari, M., Eder, S., Schoiswohl, G., Wongsiriroj, N., Pollak, N.M., Radner, F.P., Preiss-Landl, K., Kolbe, T., Rulicke, T., Pieske, B., Trauner, M., Lass, A., Zimmermann, R., Hoefler, G., Cinti, S., Kershaw, E.E., Schrauwen, P., Madeo, F., Mayer, B., and Zechner, R. (2011). ATGL-mediated fat catabolism regulates cardiac

mitochondrial function via PPAR-alpha and PGC-1. Nature medicine, 17(9), 1076-1085. doi: 10.1038/nm.2439

113 Haemmerle, G., Zimmermann, R., Hayn, M., Theussl, C., Waeg, G., Wagner, E., Sattler, W., Magin, T.M., Wagner, E.F., and Zechner, R. (2002). Hormone-sensitive lipase deficiency in mice causes diglyceride accumulation in adipose tissue, muscle, and testis. The Journal of biological chemistry, 277(7), 4806-4815. doi: 10.1074/jbc.M110355200

114 Haffner, S.M., Stern, M.P., Hazuda, H.P., Pugh, J.A., and Patterson, J.K. (1986). Hyperinsulinemia in a population at high risk for non-insulin-dependent diabetes mellitus. The New England journal of medicine, 315(4), 220-224. doi: 10.1056/nejm198607243150403

115 Hajer, G.R., van Haeften, T.W., and Visseren, F.L. (2008). Adipose tissue dysfunction in obesity, diabetes, and vascular diseases. Eur Heart J, 29(24), 2959-2971. doi: 10.1093/eurheartj/ehn387

116 Hall, J.E. (2011). Methods for Determining Metabolic Utilization of Cardohydrates, Fats and Proteins. In Guyton and Hall Textbook of Medical Physiology (Jackson, Mississippi), pp. 888-889.

117 Han, W., Han, Y., Liu, X., and Shang, X. (2015). Effect of miR-29a inhibition on ventricular hypertrophy induced by pressure overload. Cell biochemistry and biophysics, 71(2), 821-826. doi: 10.1007/s12013-014-0269-x

118 Hassing, H.C., Surendran, R.P., Mooij, H.L., Stroes, E.S., Nieuwdorp, M., and Dallinga-Thie, G.M. (2012). Pathophysiology of hypertriglyceridemia. Biochimica et biophysica acta, 1821(5), 826-832. doi: 10.1016/j.bbalip.2011.11.010

119 Hatem, S.N., Redheuil, A., and Gandjbakhch, E. (2016). Cardiac adipose tissue and atrial fibrillation: the perils of adiposity. Cardiovascular research. doi: 10.1093/cvr/cvw001

120 Hayek, S., and Nemer, M. (2011). Cardiac natriuretic peptides: from basic discovery to clinical practice. Cardiovascular therapeutics, 29(6), 362-376. doi: 10.1111/j.1755-5922.2010.00152.x

121 He, J., Ogden, L.G., Bazzano, L.A., Vupputuri, S., Loria, C., and Whelton, P.K. (2001). Risk factors for congestive heart failure in US men and women: NHANES I epidemiologic follow-up study. Archives of internal medicine, 161(7), 996-1002.

122 He, W., Barak, Y., Hevener, A., Olson, P., Liao, D., Le, J., Nelson, M., Ong, E., Olefsky, J.M., and Evans, R.M. (2003). Adipose-specific peroxisome proliferator-activated receptor gamma knockout causes insulin resistance in fat and liver but not in muscle. Proc Natl Acad Sci U S A, 100(26), 15712-15717. doi: 10.1073/pnas.2536828100

123 Heidenreich PA, A.N., Allen LA, Bluemke DA, Butler J, Fonarow GC, Ikonomidis JS, Khavjou O, Konstam MA, Maddox TM, Nichol G, Pham M, Pina IL, Trogdon

JG. (2013). on behalf of the American Heart Association Advocacy Coordinating Committee, Council on Arteriosclerosis, Thrombosis and Vascular Biology, Council on Cardiovascular Radiology and Intervention, Council on Clinical Cardiology, Council on Epidemiol- ogy and Prevention, and Stroke Council: Forecasting the impact of heart failure in the United States: a policy statement from the American Heart Association. Circ Heart Fail, 6, 606–619.

124 Heineke, J., and Molkentin, J.D. (2006). Regulation of cardiac hypertrophy by intracellular signalling pathways. Nature reviews Molecular cell biology, 7(8), 589-600. doi: 10.1038/nrm1983

125 Hill, J.A., Karimi, M., Kutschke, W., Davisson, R.L., Zimmerman, K., Wang, Z., Kerber, R.E., and Weiss, R.M. (2000). Cardiac hypertrophy is not a required compensatory response to short-term pressure overload. Circulation, 101(24), 2863-2869.

126 Himms-Hagen, J. (1986). Brown adipose tissue and cold-acclimation (Brown Adipose Tissue: Edward Arnold: London).

127 Hirano, K., Ikeda, Y., Zaima, N., Sakata, Y., and Matsumiya, G. (2008). Triglyceride deposit cardiomyovasculopathy. The New England journal of medicine, 359(22), 2396-2398. doi: 10.1056/NEJMc0805305

128 Hjalmarson, A., Goldstein, S., Fagerberg, B., Wedel, H., Waagstein, F., Kjekshus, J., Wikstrand, J., El Allaf, D., Vitovec, J., Aldershvile, J., Halinen, M., Dietz, R., Neuhaus, K.L., Janosi, A., Thorgeirsson, G., Dunselman, P.H., Gullestad, L., Kuch, J., Herlitz, J., Rickenbacher, P., Ball, S., Gottlieb, S., and Deedwania, P. (2000). Effects of controlled-release metoprolol on total mortality, hospitalizations, and well-being in patients with heart failure: the Metoprolol CR/XL Randomized Intervention Trial in congestive heart failure (MERIT-HF). MERIT-HF Study Group. Jama, 283(10), 1295-1302.

129 Hofer, P., Boeszoermenyi, A., Jaeger, D., Feiler, U., Arthanari, H., Mayer, N., Zehender, F., Rechberger, G., Oberer, M., Zimmermann, R., Lass, A., Haemmerle, G., Breinbauer, R., Zechner, R., and Preiss-Landl, K. (2015). Fatty Acid-binding Proteins Interact with Comparative Gene Identification-58 Linking Lipolysis with Lipid Ligand Shuttling. The Journal of biological chemistry, 290(30), 18438-18453. doi: 10.1074/jbc.M114.628958

130 Huijsman, E., van de Par, C., Economou, C., van der Poel, C., Lynch, G.S., Schoiswohl, G., Haemmerle, G., Zechner, R., and Watt, M.J. (2009). Adipose triacylglycerol lipase deletion alters whole body energy metabolism and impairs exercise performance in mice. American journal of physiology Endocrinology and metabolism, 297(2), E505-513. doi: 10.1152/ajpendo.00190.2009

131 Ibrahimi, A., Bonen, A., Blinn, W.D., Hajri, T., Li, X., Zhong, K., Cameron, R., and Abumrad, N.A. (1999). Muscle-specific overexpression of FAT/CD36 enhances fatty acid oxidation by contracting muscle, reduces plasma triglycerides and fatty acids, and increases plasma glucose and insulin. The Journal of biological chemistry, 274(38), 26761-26766.

132 Ingelsson, E., Arnlov, J., Lind, L., and Sundstrom, J. (2006). Metabolic syndrome and risk for heart failure in middle-aged men. Heart (British Cardiac Society), 92(10), 1409-1413. doi: 10.1136/hrt.2006.089011

133 Ingwall, J.S. (2009). Energy metabolism in heart failure and remodelling. Cardiovascular research, 81(3), 412-419. doi: 10.1093/cvr/cvn301

134 Ingwall, J.S., and Weiss, R.G. (2004). Is the failing heart energy starved? On using chemical energy to support cardiac function. Circulation research, 95(2), 135-145. doi: 10.1161/01.RES.0000137170.41939.d9

135 Iqbal, J., and Hussain, M.M. (2009). Intestinal lipid absorption. American journal of physiology Endocrinology and metabolism, 296(6), E1183-1194. doi: 10.1152/ajpendo.90899.2008

136 Iribarren, C., Karter, A.J., Go, A.S., Ferrara, A., Liu, J.Y., Sidney, S., and Selby, J.V. (2001). Glycemic control and heart failure among adult patients with diabetes. Circulation, 103(22), 2668-2673.

137 Irie, H., Krukenkamp, I.B., Brinkmann, J.F., Gaudette, G.R., Saltman, A.E., Jou, W., Glatz, J.F., Abumrad, N.A., and Ibrahimi, A. (2003). Myocardial recovery from ischemia is impaired in CD36-null mice and restored by myocyte CD36 expression or medium-chain fatty acids. Proc Natl Acad Sci U S A, 100(11), 6819-6824. doi: 10.1073/pnas.1132094100

138 Ishibashi, J., and Seale, P. (2010). Medicine. Beige can be slimming. Science, 328(5982), 1113-1114. doi: 10.1126/science.1190816

139 Iwano, H., and Little, W.C. (2013). Heart failure: what does ejection fraction have to do with it? Journal of cardiology, 62(1), 1-3. doi: 10.1016/j.jjcc.2013.02.017

140 Jenkins, C.M., Mancuso, D.J., Yan, W., Sims, H.F., Gibson, B., and Gross, R.W. (2004). Identification, cloning, expression, and purification of three novel human calcium-independent phospholipase A2 family members possessing triacylglycerol lipase and acylglycerol transacylase activities. The Journal of biological chemistry, 279(47), 48968-48975. doi: 10.1074/jbc.M407841200

141 Jha, P., Claudel, T., Baghdasaryan, A., Mueller, M., Halilbasic, E., Das, S.K., Lass, A., Zimmermann, R., Zechner, R., Hoefler, G., and Trauner, M. (2014). Role of adipose triglyceride lipase (PNPLA2) in protection from hepatic inflammation in mouse models of steatohepatitis and endotoxemia. Hepatology (Baltimore, Md), 59(3), 858-869. doi: 10.1002/hep.26732

142 Johnson, E.J., Dieter, B.P., and Marsh, S.A. (2015). Evidence for distinct effects of exercise in different cardiac hypertrophic disorders. Life sciences, 123, 100-106. doi: 10.1016/j.lfs.2015.01.007

143 Johnson, G.H., and Fritsche, K. (2012). Effect of dietary linoleic acid on markers of inflammation in healthy persons: a systematic review of randomized controlled

trials. Journal of the Academy of Nutrition and Dietetics, 112(7), 1029-1041, 1041.e1021-1015. doi: 10.1016/j.jand.2012.03.029

144 Justice, M.J., Siracusa, L.D., and Stewart, A.F. (2011). Technical approaches for mouse models of human disease. Disease models & mechanisms, 4(3), 305-310. doi: 10.1242/dmm.000901

145 Kararigas, G., Fliegner, D., Forler, S., Klein, O., Schubert, C., Gustafsson, J.A., Klose, J., and Regitz-Zagrosek, V. (2014). Comparative proteomic analysis reveals sex and estrogen receptor beta effects in the pressure overloaded heart. Journal of proteome research, 13(12), 5829-5836. doi: 10.1021/pr500749j

146 Kato, T., Niizuma, S., Inuzuka, Y., Kawashima, T., Okuda, J., Tamaki, Y., Iwanaga, Y., Narazaki, M., Matsuda, T., Soga, T., Kita, T., Kimura, T., and Shioi, T. (2010). Analysis of metabolic remodeling in compensated left ventricular hypertrophy and heart failure. Circulation Heart failure, 3(3), 420-430. doi: 10.1161/circheartfailure.109.888479

147 Katz, A.M., and Rolett, E.L. (2016). Heart failure: when form fails to follow function. Eur Heart J, 37(5), 449-454. doi: 10.1093/eurheartj/ehv548

148 Kemp, C.D., and Conte, J.V. (2012). The pathophysiology of heart failure. Cardiovascular pathology : the official journal of the Society for Cardiovascular Pathology, 21(5), 365-371. doi: 10.1016/j.carpath.2011.11.007

149 Kenchaiah, S., Evans, J.C., Levy, D., Wilson, P.W., Benjamin, E.J., Larson, M.G., Kannel, W.B., and Vasan, R.S. (2002). Obesity and the risk of heart failure. The New England journal of medicine, 347(5), 305-313. doi: 10.1056/NEJMoa020245

150 Kershaw, E.E., Hamm, J.K., Verhagen, L.A., Peroni, O., Katic, M., and Flier, J.S. (2006). Adipose triglyceride lipase: function, regulation by insulin, and comparison with adiponutrin. Diabetes, 55(1), 148-157.

151 Kharroubi, I., Ladriere, L., Cardozo, A.K., Dogusan, Z., Cnop, M., and Eizirik, D.L. (2004). Free fatty acids and cytokines induce pancreatic beta-cell apoptosis by different mechanisms: role of nuclear factor-kappaB and endoplasmic reticulum stress. Endocrinology, 145(11), 5087-5096. doi: 10.1210/en.2004-0478

152 Kienesberger, P.C., Lee, D., Pulinilkunnil, T., Brenner, D.S., Cai, L., Magnes, C., Koefeler, H.C., Streith, I.E., Rechberger, G.N., Haemmerle, G., Flier, J.S., Zechner, R., Kim, Y.B., and Kershaw, E.E. (2009). Adipose triglyceride lipase deficiency causes tissue-specific changes in insulin signaling. The Journal of biological chemistry, 284(44), 30218-30229. doi: 10.1074/jbc.M109.047787

153 Kienesberger, P.C., Pulinilkunnil, T., Nagendran, J., Young, M.E., Bogner-Strauss, J.G., Hackl, H., Khadour, R., Heydari, E., Haemmerle, G., Zechner, R., Kershaw, E.E., and Dyck, J.R. (2013). Early structural and metabolic cardiac remodelling in response to inducible adipose triglyceride lipase ablation. Cardiovascular research, 99(3), 442-451. doi: 10.1093/cvr/cvt124

154 Kienesberger, P.C., Pulinilkunnil, T., Sung, M.M., Nagendran, J., Haemmerle, G., Kershaw, E.E., Young, M.E., Light, P.E., Oudit, G.Y., Zechner, R., and Dyck, J.R. (2012). Myocardial ATGL overexpression decreases the reliance on fatty acid oxidation and protects against pressure overload-induced cardiac dysfunction. Molecular and cellular biology, 32(4), 740-750. doi: 10.1128/mcb.06470-11

155 Kim, J.Y., Tillison, K., Lee, J.H., Rearick, D.A., and Smas, C.M. (2006). The adipose tissue triglyceride lipase ATGL/PNPLA2 is downregulated by insulin and TNF-alpha in 3T3-L1 adipocytes and is a target for transactivation by PPARgamma. American journal of physiology Endocrinology and metabolism, 291(1), E115-127. doi: 10.1152/ajpendo.00317.2005

156 Kitamura, K., Shibata, R., Tsuji, Y., Shimano, M., Inden, Y., and Murohara, T. (2011). Eicosapentaenoic acid prevents atrial fibrillation associated with heart failure in a rabbit model. American journal of physiology Heart and circulatory physiology, 300(5), H1814-1821. doi: 10.1152/ajpheart.00771.2010

157 Klopfleisch, R., von Deetzen, M., Weiss, A.T., Weigner, J., Weigner, F., Plendl, J., and Gruber, A.D. (2013). Weigners fixative-an alternative to formalin fixation for histology with improved preservation of nucleic acids. Veterinary pathology, 50(1), 191-199. doi: 10.1177/0300985812441031

158 Klose, P., Weise, C., Bondzio, A., Multhaup, G., Einspanier, R., Gruber, A.D., and Klopfleisch, R. (2011). Is there a malignant progression associated with a linear change in protein expression levels from normal canine mammary gland to metastatic mammary tumors? Journal of proteome research, 10(10), 4405-4415. doi: 10.1021/pr200112q

159 Kobayashi, K., Inoguchi, T., Maeda, Y., Nakashima, N., Kuwano, A., Eto, E., Ueno, N., Sasaki, S., Sawada, F., Fujii, M., Matoba, Y., Sumiyoshi, S., Kawate, H., and Takayanagi, R. (2008). The lack of the C-terminal domain of adipose triglyceride lipase causes neutral lipid storage disease through impaired interactions with lipid droplets. The Journal of clinical endocrinology and metabolism, 93(7), 2877-2884. doi: 10.1210/jc.2007-2247

160 Kolwicz, S.C., Jr., and Tian, R. (2011). Glucose metabolism and cardiac hypertrophy. Cardiovascular research, 90(2), 194-201. doi: 10.1093/cvr/cvr071

161 Kong, P., Christia, P., and Frangogiannis, N.G. (2014). The pathogenesis of cardiac fibrosis. Cellular and molecular life sciences : CMLS, 71(4), 549-574. doi: 10.1007/s00018-013-1349-6

162 Korvald, C., Elvenes, O.P., and Myrmel, T. (2000). Myocardial substrate metabolism influences left ventricular energetics in vivo. American journal of physiology Heart and circulatory physiology, 278(4), H1345-1351.

163 Kris-Etherton, P.M., Harris, W.S., and Appel, L.J. (2003). Omega-3 fatty acids and cardiovascular disease: new recommendations from the American Heart Association. Arteriosclerosis, thrombosis, and vascular biology, 23(2), 151-152.

164 Lafontan, M., and Langin, D. (2009). Lipolysis and lipid mobilization in human adipose tissue. Progress in lipid research, 48(5), 275-297. doi: 10.1016/j.plipres.2009.05.001

165 Lamb, C.A., Yoshimori, T., and Tooze, S.A. (2013). The autophagosome: origins unknown, biogenesis complex. Nature reviews Molecular cell biology, 14(12), 759-774. doi: 10.1038/nrm3696

166 Lamba, S., and Abraham, W.T. (2000). Alterations in adrenergic receptor signaling in heart failure. Heart failure reviews, 5(1), 7-16. doi: 10.1023/a:1009885822076

167 Lass, A., Zimmermann, R., Haemmerle, G., Riederer, M., Schoiswohl, G., Schweiger, M., Kienesberger, P., Strauss, J.G., Gorkiewicz, G., and Zechner, R. (2006). Adipose triglyceride lipase-mediated lipolysis of cellular fat stores is activated by CGI-58 and defective in Chanarin-Dorfman Syndrome. Cell metabolism, 3(5), 309-319. doi: 10.1016/j.cmet.2006.03.005

168 Lass, A., Zimmermann, R., Oberer, M., and Zechner, R. (2011). Lipolysis - a highly regulated multi-enzyme complex mediates the catabolism of cellular fat stores. Progress in lipid research, 50(1), 14-27. doi: 10.1016/j.plipres.2010.10.004

169 Last, R.L., Jones, A.D., and Shachar-Hill, Y. (2007). Towards the plant metabolome and beyond. Nature reviews Molecular cell biology, 8(2), 167-174. doi: 10.1038/nrm2098

170 Lavie, C.J., Patel, D.A., Milani, R.V., Ventura, H.O., Shah, S., and Gilliland, Y. (2014). Impact of echocardiographic left ventricular geometry on clinical prognosis. Progress in cardiovascular diseases, 57(1), 3-9. doi: 10.1016/j.pcad.2014.05.003

171 Lefevre, C., Jobard, F., Caux, F., Bouadjar, B., Karaduman, A., Heilig, R., Lakhdar, H., Wollenberg, A., Verret, J.L., Weissenbach, J., Ozguc, M., Lathrop, M., Prud'homme, J.F., and Fischer, J. (2001). Mutations in CGI-58, the gene encoding a new protein of the esterase/lipase/thioesterase subfamily, in Chanarin-Dorfman syndrome. American journal of human genetics, 69(5), 1002-1012. doi: 10.1086/324121

172 Lei, B., Lionetti, V., Young, M.E., Chandler, M.P., d'Agostino, C., Kang, E., Altarejos, M., Matsuo, K., Hintze, T.H., Stanley, W.C., and Recchia, F.A. (2004). Paradoxical downregulation of the glucose oxidation pathway despite enhanced flux in severe heart failure. Journal of molecular and cellular cardiology, 36(4), 567-576. doi: 10.1016/j.yjmcc.2004.02.004

173 Leimbach, W.N., Jr., Wallin, B.G., Victor, R.G., Aylward, P.E., Sundlof, G., and Mark, A.L. (1986). Direct evidence from intraneural recordings for increased central sympathetic outflow in patients with heart failure. Circulation, 73(5), 913-919.

174 Lettieri Barbato, D., Aquilano, K., Baldelli, S., Cannata, S.M., Bernardini, S., Rotilio, G., and Ciriolo, M.R. (2014). Proline oxidase-adipose triglyceride lipase pathway restrains adipose cell death and tissue inflammation. Cell death and differentiation, 21(1), 113-123. doi: 10.1038/cdd.2013.137

175 Levine, T.B., Francis, G.S., Goldsmith, S.R., Simon, A.B., and Cohn, J.N. (1982). Activity of the sympathetic nervous system and renin-angiotensin system assessed by plasma hormone levels and their relation to hemodynamic abnormalities in congestive heart failure. The American journal of cardiology, 49(7), 1659-1666.

176 Levy, D., Larson, M.G., Vasan, R.S., Kannel, W.B., and Ho, K.K. (1996). The progression from hypertension to congestive heart failure. Jama, 275(20), 1557-1562.

177 Lionetti, V., Stanley, W.C., and Recchia, F.A. (2011). Modulating fatty acid oxidation in heart failure. Cardiovascular research, 90(2), 202-209. doi: 10.1093/cvr/cvr038

178 Liu, X., Kwak, D., Lu, Z., Xu, X., Fassett, J., Wang, H., Wei, Y., Cavener, D.R., Hu, X., Hall, J., Bache, R.J., and Chen, Y. (2014). Endoplasmic reticulum stress sensor protein kinase R-like endoplasmic reticulum kinase (PERK) protects against pressure overload-induced heart failure and lung remodeling. Hypertension, 64(4), 738-744. doi: 10.1161/hypertensionaha.114.03811

179 Loeffler, G. (2014). Lipogenese und Lipolyse - Bildung und Verwertung der Fettspeicher, Vol 9 (Löffler/Petrides Biochemie und Pathobiochemie: Peter C Heinrich, Matthias Müller, Lutz Graeve).

180 Lopez, J.E., Myagmar, B.E., Swigart, P.M., Montgomery, M.D., Haynam, S., Bigos, M., Rodrigo, M.C., and Simpson, P.C. (2011). beta-myosin heavy chain is induced by pressure overload in a minor subpopulation of smaller mouse cardiac myocytes. Circulation research, 109(6), 629-638. doi: 10.1161/circresaha.111.243410

181 Lu, X., Yang, X., and Liu, J. (2010). Differential control of ATGL-mediated lipid droplet degradation by CGI-58 and G0S2. Cell cycle (Georgetown, Tex), 9(14), 2719-2725.

182 Lüllmann, H., Mohr, K., and Hein, L. (2010). Pharmakologie und Toxikologie, Vol 17 (Stuttgart: Georg Thieme Verlag KG).

183 Lüllmann-Rauch, R., and Paulsen, F. (2012). Taschenlehrbuch Histologie, Vol 4 (Kiel und Erlangen: Georg Thieme Verlag).

184 Luo, T., Chen, B., and Wang, X. (2015). 4-PBA prevents pressure overload-induced myocardial hypertrophy and interstitial fibrosis by attenuating endoplasmic reticulum stress. Chemico-biological interactions, 242, 99-106. doi: 10.1016/j.cbi.2015.09.025

185 Maganti, K., Rigolin, V.H., Sarano, M.E., and Bonow, R.O. (2010). Valvular heart disease: diagnosis and management. Mayo Clinic proceedings, 85(5), 483-500. doi: 10.4065/mcp.2009.0706

186 Makowski, L., Boord, J.B., Maeda, K., Babaev, V.R., Uysal, K.T., Morgan, M.A., Parker, R.A., Suttles, J., Fazio, S., Hotamisligil, G.S., and Linton, M.F. (2001). Lack of macrophage fatty-acid-binding protein aP2 protects mice deficient in apolipoprotein E against atherosclerosis. Nature medicine, 7(6), 699-705. doi: 10.1038/89076

187 Makowski, L., Brittingham, K.C., Reynolds, J.M., Suttles, J., and Hotamisligil, G.S. (2005). The fatty acid-binding protein, aP2, coordinates macrophage cholesterol trafficking and inflammatory activity. Macrophage expression of aP2 impacts peroxisome proliferator-activated receptor gamma and IkappaB kinase activities. The Journal of biological chemistry, 280(13), 12888-12895. doi: 10.1074/jbc.M413788200

188 Mancia, G., Fagard, R., Narkiewicz, K., Redon, J., Zanchetti, A., Bohm, M., Christiaens, T., Cifkova, R., De Backer, G., Dominiczak, A., Galderisi, M., Grobbee, D.E., Jaarsma, T., Kirchhof, P., Kjeldsen, S.E., Laurent, S., Manolis, A.J., Nilsson, P.M., Ruilope, L.M., Schmieder, R.E., Sirnes, P.A., Sleight, P., Viigimaa, M., Waeber, B., and Zannad, F. (2014). 2013 ESH/ESC Practice Guidelines for the Management of Arterial Hypertension. Blood pressure, 23(1), 3-16. doi: 10.3109/08037051.2014.868629

189 Mandviwala, T., Khalid, U., and Deswal, A. (2016). Obesity and Cardiovascular Disease: a Risk Factor or a Risk Marker? Current atherosclerosis reports, 18(5), 21. doi: 10.1007/s11883-016-0575-4

190 Martens, K., Bottelbergs, A., and Baes, M. (2010). Ectopic recombination in the central and peripheral nervous system by aP2/FABP4-Cre mice: implications for metabolism research. FEBS letters, 584(5), 1054-1058. doi: 10.1016/j.febslet.2010.01.061

191 Mason, C., and Katzmarzyk, P.T. (2010). Waist circumference thresholds for the prediction of cardiometabolic risk: is measurement site important? European journal of clinical nutrition, 64(8), 862-867. doi: 10.1038/ejcn.2010.82

192 Mauriege, P., Imbeault, P., Langin, D., Lacaille, M., Almeras, N., Tremblay, A., and Despres, J.P. (1999). Regional and gender variations in adipose tissue lipolysis in response to weight loss. Journal of lipid research, 40(9), 1559-1571.

193 McMurray, J.J., Adamopoulos, S., Anker, S.D., Auricchio, A., Bohm, M., Dickstein, K., Falk, V., Filippatos, G., Fonseca, C., Gomez-Sanchez, M.A., Jaarsma, T., Kober, L., Lip, G.Y., Maggioni, A.P., Parkhomenko, A., Pieske, B.M., Popescu, B.A., Ronnevik, P.K., Rutten, F.H., Schwitter, J., Seferovic, P., Stepinska, J., Trindade, P.T., Voors, A.A., Zannad, F., and Zeiher, A. (2012). ESC Guidelines for the diagnosis and treatment of acute and chronic heart failure 2012: The Task Force for the Diagnosis and Treatment of Acute and

Chronic Heart Failure 2012 of the European Society of Cardiology. Developed in collaboration with the Heart Failure Association (HFA) of the ESC. Eur Heart J, 33(14), 1787-1847. doi: 10.1093/eurheartj/ehs104

194 Mensink, G.B., Schienkiewitz, A., Haftenberger, M., Lampert, T., Ziese, T., and Scheidt-Nave, C. (2013). [Overweight and obesity in Germany: results of the German Health Interview and Examination Survey for Adults (DEGS1)]. Bundesgesundheitsblatt, Gesundheitsforschung, Gesundheitsschutz, 56(5-6), 786-794. doi: 10.1007/s00103-012-1656-3

195 Misra, A., Garg, A., Abate, N., Peshock, R.M., Stray-Gundersen, J., and Grundy, S.M. (1997). Relationship of anterior and posterior subcutaneous abdominal fat to insulin sensitivity in nondiabetic men. Obesity research, 5(2), 93-99.

196 Mitaka, C., Kudo, T., Haraguchi, G., and Tomita, M. (2011). Cardiovascular and renal effects of carperitide and nesiritide in cardiovascular surgery patients: a systematic review and meta-analysis. Critical care (London, England), 15(5), R258. doi: 10.1186/cc10519

197 Miyoshi, H., Perfield, J.W., 2nd, Obin, M.S., and Greenberg, A.S. (2008). Adipose triglyceride lipase regulates basal lipolysis and lipid droplet size in adipocytes. Journal of cellular biochemistry, 105(6), 1430-1436. doi: 10.1002/jcb.21964

198 Mootha, V.K., Arai, A.E., and Balaban, R.S. (1997). Maximum oxidative phosphorylation capacity of the mammalian heart. The American journal of physiology, 272(2 Pt 2), H769-775.

199 Morigny, P., Houssier, M., Mouisel, E., and Langin, D. (2016). Adipocyte lipolysis and insulin resistance. Biochimie, 125, 259-266. doi: 10.1016/j.biochi.2015.10.024

200 Moro, C., Galitzky, J., Sengenes, C., Crampes, F., Lafontan, M., and Berlan, M. (2004). Functional and pharmacological characterization of the natriuretic peptide-dependent lipolytic pathway in human fat cells. The Journal of pharmacology and experimental therapeutics, 308(3), 984-992. doi: 10.1124/jpet.103.060913

201 Mozaffarian, D., Benjamin, E.J., Go, A.S., Arnett, D.K., Blaha, M.J., Cushman, M., de Ferranti, S., Despres, J.P., Fullerton, H.J., Howard, V.J., Huffman, M.D., Judd, S.E., Kissela, B.M., Lackland, D.T., Lichtman, J.H., Lisabeth, L.D., Liu, S., Mackey, R.H., Matchar, D.B., McGuire, D.K., Mohler, E.R., 3rd, Moy, C.S., Muntner, P., Mussolino, M.E., Nasir, K., Neumar, R.W., Nichol, G., Palaniappan, L., Pandey, D.K., Reeves, M.J., Rodriguez, C.J., Sorlie, P.D., Stein, J., Towfighi, A., Turan, T.N., Virani, S.S., Willey, J.Z., Woo, D., Yeh, R.W., and Turner, M.B. (2015). Heart disease and stroke statistics--2015 update: a report from the American Heart Association. Circulation, 131(4), e29-322. doi: 10.1161/cir.0000000000000152

202 Mozaffarian, D., and Rimm, E.B. (2006). Fish intake, contaminants, and human health: evaluating the risks and the benefits. Jama, 296(15), 1885-1899. doi: 10.1001/jama.296.15.1885

203 Nakamura, A., Rokosh, D.G., Paccanaro, M., Yee, R.R., Simpson, P.C., Grossman, W., and Foster, E. (2001). LV systolic performance improves with development of hypertrophy after transverse aortic constriction in mice. American journal of physiology Heart and circulatory physiology, 281(3), H1104-1112.

204 Nascimben, L., Ingwall, J.S., Lorell, B.H., Pinz, I., Schultz, V., Tornheim, K., and Tian, R. (2004). Mechanisms for increased glycolysis in the hypertrophied rat heart. Hypertension, 44(5), 662-667. doi: 10.1161/01.HYP.0000144292.69599.0c

205 Natali, A., Gastaldelli, A., Camastra, S., Baldi, S., Quagliarini, F., Minicocci, I., Bruno, C., Pennisi, E., and Arca, M. (2013). Metabolic consequences of adipose triglyceride lipase deficiency in humans: an in vivo study in patients with neutral lipid storage disease with myopathy. The Journal of clinical endocrinology and metabolism, 98(9), E1540-1548. doi: 10.1210/jc.2013-1444

206 Nedergaard, J., Bengtsson, T., and Cannon, B. (2007). Unexpected evidence for active brown adipose tissue in adult humans. American journal of physiology Endocrinology and metabolism, 293(2), E444-452. doi: 10.1152/ajpendo.00691.2006

207 Neubauer, S. (2007). The failing heart--an engine out of fuel. The New England journal of medicine, 356(11), 1140-1151. doi: 10.1056/NEJMra063052

208 Nickel, A., Loffler, J., and Maack, C. (2013). Myocardial energetics in heart failure. Basic research in cardiology, 108(4), 358. doi: 10.1007/s00395-013-0358-9

209 Nielsen, M.S., Schmidt, E.B., Stegger, J., Gorst-Rasmussen, A., Tjonneland, A., and Overvad, K. (2013). Adipose tissue arachidonic acid content is associated with the risk of myocardial infarction: a Danish case-cohort study. Atherosclerosis, 227(2), 386-390. doi: 10.1016/j.atherosclerosis.2012.12.035

210 Nikolaidis, L.A., Sturzu, A., Stolarski, C., Elahi, D., Shen, Y.T., and Shannon, R.P. (2004). The development of myocardial insulin resistance in conscious dogs with advanced dilated cardiomyopathy. Cardiovascular research, 61(2), 297-306.

211 Nishida, K., and Otsu, K. (2015). Autophagy during cardiac remodeling. Journal of molecular and cellular cardiology. doi: 10.1016/j.yjmcc.2015.12.003

212 Nishino, N., Tamori, Y., Tateya, S., Kawaguchi, T., Shibakusa, T., Mizunoya, W., Inoue, K., Kitazawa, R., Kitazawa, S., Matsuki, Y., Hiramatsu, R., Masubuchi, S., Omachi, A., Kimura, K., Saito, M., Amo, T., Ohta, S., Yamaguchi, T., Osumi, T., Cheng, J., Fujimoto, T., Nakao, H., Nakao, K., Aiba, A., Okamura, H., Fushiki, T., and Kasuga, M. (2008). FSP27 contributes to efficient energy storage in murine white adipocytes by promoting the formation of unilocular lipid droplets. The Journal of clinical investigation, 118(8), 2808-2821. doi: 10.1172/jci34090

213 O'Connor, C.M., Starling, R.C., Hernandez, A.F., Armstrong, P.W., Dickstein, K., Hasselblad, V., Heizer, G.M., Komajda, M., Massie, B.M., McMurray, J.J., Nieminen, M.S., Reist, C.J., Rouleau, J.L., Swedberg, K., Adams, K.F., Jr., Anker, S.D., Atar, D., Battler, A., Botero, R., Bohidar, N.R., Butler, J., Clausell, N., Corbalan, R., Costanzo, M.R., Dahlstrom, U., Deckelbaum, L.I., Diaz, R., Dunlap, M.E., Ezekowitz, J.A., Feldman, D., Felker, G.M., Fonarow, G.C., Gennevois, D., Gottlieb, S.S., Hill, J.A., Hollander, J.E., Howlett, J.G., Hudson, M.P., Kociol, R.D., Krum, H., Laucevicius, A., Levy, W.C., Mendez, G.F., Metra, M., Mittal, S., Oh, B.H., Pereira, N.L., Ponikowski, P., Tang, W.H., Tanomsup, S., Teerlink, J.R., Triposkiadis, F., Troughton, R.W., Voors, A.A., Whellan, D.J., Zannad, F., and Califf, R.M. (2011). Effect of nesiritide in patients with acute decompensated heart failure. The New England journal of medicine, 365(1), 32-43. doi: 10.1056/NEJMoa1100171

214 Obrowsky, S., Chandak, P.G., Patankar, J.V., Povoden, S., Schlager, S., Kershaw, E.E., Bogner-Strauss, J.G., Hoefler, G., Levak-Frank, S., and Kratky, D. (2013). Adipose triglyceride lipase is a TG hydrolase of the small intestine and regulates intestinal PPARalpha signaling. Journal of lipid research, 54(2), 425-435. doi: 10.1194/jlr.M031716

215 Oliver, P.M., Fox, J.E., Kim, R., Rockman, H.A., Kim, H.S., Reddick, R.L., Pandey, K.N., Milgram, S.L., Smithies, O., and Maeda, N. (1997). Hypertension, cardiac hypertrophy, and sudden death in mice lacking natriuretic peptide receptor A. Proc Natl Acad Sci U S A, 94(26), 14730-14735.

216 Olofsson, C.S., Salehi, A., Holm, C., and Rorsman, P. (2004). Palmitate increases L-type Ca2+ currents and the size of the readily releasable granule pool in mouse pancreatic beta-cells. The Journal of physiology, 557(Pt 3), 935-948. doi: 10.1113/jphysiol.2004.066258

217 Ong, K.T., Mashek, M.T., Bu, S.Y., Greenberg, A.S., and Mashek, D.G. (2011). Adipose triglyceride lipase is a major hepatic lipase that regulates triacylglycerol turnover and fatty acid signaling and partitioning. Hepatology (Baltimore, Md), 53(1), 116-126. doi: 10.1002/hep.24006

218 Osorio, J.C., Stanley, W.C., Linke, A., Castellari, M., Diep, Q.N., Panchal, A.R., Hintze, T.H., Lopaschuk, G.D., and Recchia, F.A. (2002). Impaired myocardial fatty acid oxidation and reduced protein expression of retinoid X receptor-alpha in pacing-induced heart failure. Circulation, 106(5), 606-612.

219 Osuga, J., Ishibashi, S., Oka, T., Yagyu, H., Tozawa, R., Fujimoto, A., Shionoiri, F., Yahagi, N., Kraemer, F.B., Tsutsumi, O., and Yamada, N. (2000). Targeted disruption of hormone-sensitive lipase results in male sterility and adipocyte hypertrophy, but not in obesity. Proc Natl Acad Sci U S A, 97(2), 787-792.

220 Pagnon, J., Matzaris, M., Stark, R., Meex, R.C., Macaulay, S.L., Brown, W., O'Brien, P.E., Tiganis, T., and Watt, M.J. (2012). Identification and functional characterization of protein kinase A phosphorylation sites in the major lipolytic

protein, adipose triglyceride lipase. Endocrinology, 153(9), 4278-4289. doi: 10.1210/en.2012-1127

221 Pandya, K., Kim, H.S., and Smithies, O. (2006). Fibrosis, not cell size, delineates beta-myosin heavy chain reexpression during cardiac hypertrophy and normal aging in vivo. Proc Natl Acad Sci U S A, 103(45), 16864-16869. doi: 10.1073/pnas.0607700103

222 Pandya, K., and Smithies, O. (2011). beta-MyHC and cardiac hypertrophy: size does matter. Circulation research, 109(6), 609-610. doi: 10.1161/circresaha.111.252619

223 Paolisso, G., Gambardella, A., Galzerano, D., D'Amore, A., Rubino, P., Verza, M., Teasuro, P., Varricchio, M., and D'Onofrio, F. (1994). Total-body and myocardial substrate oxidation in congestive heart failure. Metabolism: clinical and experimental, 43(2), 174-179.

224 Papackova, Z., and Cahova, M. (2015). Fatty acid signaling: the new function of intracellular lipases. International journal of molecular sciences, 16(2), 3831-3855. doi: 10.3390/ijms16023831

225 Parati, G., and Esler, M. (2012). The human sympathetic nervous system: its relevance in hypertension and heart failure. Eur Heart J, 33(9), 1058-1066. doi: 10.1093/eurheartj/ehs041

226 Perdrix, L., Mansencal, N., Cocheteux, B., Chatellier, G., Bissery, A., Diebold, B., Mousseaux, E., and Abergel, E. (2011). How to calculate left ventricular mass in routine practice? An echocardiographic versus cardiac magnetic resonance study. Archives of cardiovascular diseases, 104(5), 343-351. doi: 10.1016/j.acvd.2011.04.003

227 Peters, L.L., Robledo, R.F., Bult, C.J., Churchill, G.A., Paigen, B.J., and Svenson, K.L. (2007). The mouse as a model for human biology: a resource guide for complex trait analysis. Nature reviews Genetics, 8(1), 58-69. doi: 10.1038/nrg2025

228 Peterson, K.L. (2002). Pressure overload hypertrophy and congestive heart failure. Where is the "Achilles' heel"? Journal of the American College of Cardiology, 39(4), 672-675.

229 Peterson, L.R., Herrero, P., Schechtman, K.B., Racette, S.B., Waggoner, A.D., Kisrieva-Ware, Z., Dence, C., Klein, S., Marsala, J., Meyer, T., and Gropler, R.J. (2004). Effect of obesity and insulin resistance on myocardial substrate metabolism and efficiency in young women. Circulation, 109(18), 2191-2196. doi: 10.1161/01.cir.0000127959.28627.f8

230 Petrovic, N., Walden, T.B., Shabalina, I.G., Timmons, J.A., Cannon, B., and Nedergaard, J. (2010). Chronic peroxisome proliferator-activated receptor gamma (PPARgamma) activation of epididymally derived white adipocyte cultures reveals a population of thermogenically competent, UCP1-containing

adipocytes molecularly distinct from classic brown adipocytes. The Journal of biological chemistry, 285(10), 7153-7164. doi: 10.1074/jbc.M109.053942

231 Pichler, M., Rainer, P.P., Schauer, S., and Hoefler, G. (2012). Cardiac fibrosis in human transplanted hearts is mainly driven by cells of intracardiac origin. Journal of the American College of Cardiology, 59(11), 1008-1016. doi: 10.1016/j.jacc.2011.11.036

232 Pinent, M., Hackl, H., Burkard, T.R., Prokesch, A., Papak, C., Scheideler, M., Hammerle, G., Zechner, R., Trajanoski, Z., and Strauss, J.G. (2008). Differential transcriptional modulation of biological processes in adipocyte triglyceride lipase and hormone-sensitive lipase-deficient mice. Genomics, 92(1), 26-32. doi: 10.1016/j.ygeno.2008.03.010

233 Pluim, B.M., Zwinderman, A.H., van der Laarse, A., and van der Wall, E.E. (2000). The athlete's heart. A meta-analysis of cardiac structure and function. Circulation, 101(3), 336-344.

234 Poirier, P., Giles, T.D., Bray, G.A., Hong, Y., Stern, J.S., Pi-Sunyer, F.X., and Eckel, R.H. (2006). Obesity and cardiovascular disease: pathophysiology, evaluation, and effect of weight loss. Arteriosclerosis, thrombosis, and vascular biology, 26(5), 968-976. doi: 10.1161/01.ATV.0000216787.85457.f3

235 Polak, J., Kotrc, M., Wedellova, Z., Jabor, A., Malek, I., Kautzner, J., Kazdova, L., and Melenovsky, V. (2011). Lipolytic effects of B-type natriuretic peptide 1-32 in adipose tissue of heart failure patients compared with healthy controls. Journal of the American College of Cardiology, 58(11), 1119-1125. doi: 10.1016/j.jacc.2011.05.042

236 Ponikowski, P., Voors, A.A., Anker, S.D., Bueno, H., Cleland, J.G., Coats, A.J., Falk, V., Gonzalez-Juanatey, J.R., Harjola, V.P., Jankowska, E.A., Jessup, M., Linde, C., Nihoyannopoulos, P., Parissis, J.T., Pieske, B., Riley, J.P., Rosano, G.M., Ruilope, L.M., Ruschitzka, F., Rutten, F.H., and van der Meer, P. (2016). 2016 ESC Guidelines for the diagnosis and treatment of acute and chronic heart failure: The Task Force for the diagnosis and treatment of acute and chronic heart failure of the European Society of Cardiology (ESC)Developed with the special contribution of the Heart Failure Association (HFA) of the ESC. Eur Heart J. doi: 10.1093/eurheartj/ehw128

237 Psyrogiannis, A., Kyriazopoulou, V., Symeonidis, A., Leotsinidis, M., and Vagenakis, A.G. (2003). Relative iron "overload" in offspring of patients with type 2 diabetes mellitus: a new component in the conundrum of insulin resistance syndrome? Hormones (Athens, Greece), 2(3), 161-168.

238 QIAGEN® (2007). RNeasy® Micro Handbook, Vol 2 (Austin, Texas).

239 Qiu, H., Gabrielsen, A., Agardh, H.E., Wan, M., Wetterholm, A., Wong, C.H., Hedin, U., Swedenborg, J., Hansson, G.K., Samuelsson, B., Paulsson-Berne, G., and Haeggstrom, J.Z. (2006). Expression of 5-lipoxygenase and leukotriene A4 hydrolase in human atherosclerotic lesions correlates with symptoms of plaque

instability. Proc Natl Acad Sci U S A, 103(21), 8161-8166. doi: 10.1073/pnas.0602414103

240 Randle, P.J., Garland, P.B., Hales, C.N., and Newsholme, E.A. (1963). The glucose fatty-acid cycle. Its role in insulin sensitivity and the metabolic disturbances of diabetes mellitus. Lancet (London, England), 1(7285), 785-789.

241 Rasmussen, B.B., Holmback, U.C., Volpi, E., Morio-Liondore, B., Paddon-Jones, D., and Wolfe, R.R. (2002). Malonyl coenzyme A and the regulation of functional carnitine palmitoyltransferase-1 activity and fat oxidation in human skeletal muscle. The Journal of clinical investigation, 110(11), 1687-1693. doi: 10.1172/jci15715

242 Recchia, F.A., McConnell, P.I., Bernstein, R.D., Vogel, T.R., Xu, X., and Hintze, T.H. (1998). Reduced nitric oxide production and altered myocardial metabolism during the decompensation of pacing-induced heart failure in the conscious dog. Circulation research, 83(10), 969-979.

243 Reilich, P., Horvath, R., Krause, S., Schramm, N., Turnbull, D.M., Trenell, M., Hollingsworth, K.G., Gorman, G.S., Hans, V.H., Reimann, J., MacMillan, A., Turner, L., Schollen, A., Witte, G., Czermin, B., Holinski-Feder, E., Walter, M.C., Schoser, B., and Lochmuller, H. (2011). The phenotypic spectrum of neutral lipid storage myopathy due to mutations in the PNPLA2 gene. Journal of neurology, 258(11), 1987-1997. doi: 10.1007/s00415-011-6055-4

244 Remondino, A., Rosenblatt-Velin, N., Montessuit, C., Tardy, I., Papageorgiou, I., Dorsaz, P.A., Jorge-Costa, M., and Lerch, R. (2000). Altered expression of proteins of metabolic regulation during remodeling of the left ventricle after myocardial infarction. Journal of molecular and cellular cardiology, 32(11), 2025-2034. doi: 10.1006/jmcc.2000.1234

245 Rennison, J.H., McElfresh, T.A., Chen, X., Anand, V.R., Hoit, B.D., Hoppel, C.L., and Chandler, M.P. (2009). Prolonged exposure to high dietary lipids is not associated with lipotoxicity in heart failure. Journal of molecular and cellular cardiology, 46(6), 883-890. doi: 10.1016/j.yjmcc.2009.02.019

246 Rial, E., and Gonzalez-Barroso, M.M. (2001). Physiological regulation of the transport activity in the uncoupling proteins UCP1 and UCP2. Biochimica et biophysica acta, 1504(1), 70-81.

247 Riehle, C., and Abel, E.D. (2016). Insulin Signaling and Heart Failure. Circulation research, 118(7), 1151-1169. doi: 10.1161/circresaha.116.306206

248 Riquelme, C.A., Magida, J.A., Harrison, B.C., Wall, C.E., Marr, T.G., Secor, S.M., and Leinwand, L.A. (2011). Fatty acids identified in the Burmese python promote beneficial cardiac growth. Science, 334(6055), 528-531. doi: 10.1126/science.1210558

249 Rockman, H.A., Ross, R.S., Harris, A.N., Knowlton, K.U., Steinhelper, M.E., Field, L.J., Ross, J., Jr., and Chien, K.R. (1991). Segregation of atrial-specific

and inducible expression of an atrial natriuretic factor transgene in an in vivo murine model of cardiac hypertrophy. Proc Natl Acad Sci U S A, 88(18), 8277-8281. Retrieved from http://www.ncbi.nlm.nih.gov/pubmed/1832775

250 Roman, M.J., Kizer, J.R., Best, L.G., Lee, E.T., Howard, B.V., Shara, N.M., and Devereux, R.B. (2012). Vascular biomarkers in the prediction of clinical cardiovascular disease: the Strong Heart Study. Hypertension, 59(1), 29-35. doi: 10.1161/hypertensionaha.111.181925

251 Rosen, E.D., and Spiegelman, B.M. (2006). Adipocytes as regulators of energy balance and glucose homeostasis. Nature, 444(7121), 847-853. doi: 10.1038/nature05483

252 Rousset, S., Alves-Guerra, M.C., Mozo, J., Miroux, B., Cassard-Doulcier, A.M., Bouillaud, F., and Ricquier, D. (2004). The biology of mitochondrial uncoupling proteins. Diabetes, 53 Suppl 1, S130-135.

253 Russell, L., and Forsdyke, D.R. (1991). A human putative lymphocyte G0/G1 switch gene containing a CpG-rich island encodes a small basic protein with the potential to be phosphorylated. DNA and cell biology, 10(8), 581-591.

254 Rydel, T.J., Williams, J.M., Krieger, E., Moshiri, F., Stallings, W.C., Brown, S.M., Pershing, J.C., Purcell, J.P., and Alibhai, M.F. (2003). The crystal structure, mutagenesis, and activity studies reveal that patatin is a lipid acyl hydrolase with a Ser-Asp catalytic dyad. Biochemistry, 42(22), 6696-6708. doi: 10.1021/bi027156r

255 Sarzani, R., Dessi-Fulgheri, P., Paci, V.M., Espinosa, E., and Rappelli, A. (1996). Expression of natriuretic peptide receptors in human adipose and other tissues. Journal of endocrinological investigation, 19(9), 581-585.

256 Sarzani, R., Paci, V.M., Zingaretti, C.M., Pierleoni, C., Cinti, S., Cola, G., Rappelli, A., and Dessi-Fulgheri, P. (1995). Fasting inhibits natriuretic peptides clearance receptor expression in rat adipose tissue. Journal of hypertension, 13(11), 1241-1246.

257 Schlosburg, J.E., Blankman, J.L., Long, J.Z., Nomura, D.K., Pan, B., Kinsey, S.G., Nguyen, P.T., Ramesh, D., Booker, L., Burston, J.J., Thomas, E.A., Selley, D.E., Sim-Selley, L.J., Liu, Q.S., Lichtman, A.H., and Cravatt, B.F. (2010). Chronic monoacylglycerol lipase blockade causes functional antagonism of the endocannabinoid system. Nature neuroscience, 13(9), 1113-1119. doi: 10.1038/nn.2616

258 Schlueter, N., de Sterke, A., Willmes, D.M., Spranger, J., Jordan, J., and Birkenfeld, A.L. (2014). Metabolic actions of natriuretic peptides and therapeutic potential in the metabolic syndrome. Pharmacology & therapeutics, 144(1), 12-27. doi: 10.1016/j.pharmthera.2014.04.007

259 Schmidt, R.F., and Lang, F. (2011). Physiologie des Menschen: mit Pathophysiologie (Munich, Germany: Springer-Lehrbuch).

260 Schoiswohl, G., Schweiger, M., Schreiber, R., Gorkiewicz, G., Preiss-Landl, K., Taschler, U., Zierler, K.A., Radner, F.P., Eichmann, T.O., Kienesberger, P.C., Eder, S., Lass, A., Haemmerle, G., Alsted, T.J., Kiens, B., Hoefler, G., Zechner, R., and Zimmermann, R. (2010). Adipose triglyceride lipase plays a key role in the supply of the working muscle with fatty acids. Journal of lipid research, 51(3), 490-499. doi: 10.1194/jlr.M001073

261 Schoiswohl, G., Stefanovic-Racic, M., Menke, M.N., Wills, R.C., Surlow, B.A., Basantani, M.K., Sitnick, M.T., Cai, L., Yazbeck, C.F., Stolz, D.B., Pulinilkunnil, T., O'Doherty, R.M., and Kershaw, E.E. (2015). Impact of Reduced ATGL-Mediated Adipocyte Lipolysis on Obesity-Associated Insulin Resistance and Inflammation in Male Mice. Endocrinology, 156(10), 3610-3624. doi: 10.1210/en.2015-1322

262 Schrammel, A., Mussbacher, M., Wolkart, G., Stessel, H., Pail, K., Winkler, S., Schweiger, M., Haemmerle, G., Al Zoughbi, W., Hofler, G., Lametschwandtner, A., Zechner, R., and Mayer, B. (2014). Endothelial dysfunction in adipose triglyceride lipase deficiency. Biochimica et biophysica acta, 1841(6), 906-917. doi: 10.1016/j.bbalip.2014.03.005

263 Schulze, P.C., Drosatos, K., and Goldberg, I.J. (2016). Lipid Use and Misuse by the Heart. Circulation research, 118(11), 1736-1751. doi: 10.1161/circresaha.116.306842

264 Schweiger, M., Schoiswohl, G., Lass, A., Radner, F.P., Haemmerle, G., Malli, R., Graier, W., Cornaciu, I., Oberer, M., Salvayre, R., Fischer, J., Zechner, R., and Zimmermann, R. (2008). The C-terminal region of human adipose triglyceride lipase affects enzyme activity and lipid droplet binding. The Journal of biological chemistry, 283(25), 17211-17220. doi: 10.1074/jbc.M710566200

265 Schweiger, M., Schreiber, R., Haemmerle, G., Lass, A., Fledelius, C., Jacobsen, P., Tornqvist, H., Zechner, R., and Zimmermann, R. (2006). Adipose triglyceride lipase and hormone-sensitive lipase are the major enzymes in adipose tissue triacylglycerol catabolism. The Journal of biological chemistry, 281(52), 40236-40241. doi: 10.1074/jbc.M608048200

266 Sengenes, C., Berlan, M., De Glisezinski, I., Lafontan, M., and Galitzky, J. (2000). Natriuretic peptides: a new lipolytic pathway in human adipocytes. FASEB journal : official publication of the Federation of American Societies for Experimental Biology, 14(10), 1345-1351.

267 Sengenes, C., Bouloumie, A., Hauner, H., Berlan, M., Busse, R., Lafontan, M., and Galitzky, J. (2003). Involvement of a cGMP-dependent pathway in the natriuretic peptide-mediated hormone-sensitive lipase phosphorylation in human adipocytes. The Journal of biological chemistry, 278(49), 48617-48626. doi: 10.1074/jbc.M303713200

268 Shen, J.Z., Morgan, J., Tesch, G.H., Fuller, P.J., and Young, M.J. (2014). CCL2-dependent macrophage recruitment is critical for mineralocorticoid receptor-

mediated cardiac fibrosis, inflammation, and blood pressure responses in male mice. Endocrinology, 155(3), 1057-1066. doi: 10.1210/en.2013-1772

269 Shimizu, I., Yoshida, Y., Katsuno, T., Tateno, K., Okada, S., Moriya, J., Yokoyama, M., Nojima, A., Ito, T., Zechner, R., Komuro, I., Kobayashi, Y., and Minamino, T. (2012). p53-induced adipose tissue inflammation is critically involved in the development of insulin resistance in heart failure. Cell metabolism, 15(1), 51-64. doi: 10.1016/j.cmet.2011.12.006

270 Shin, J.A., Jeong, S.I., Kim, M., Yoon, J.C., Kim, H.S., and Park, E.M. (2015). Visceral adipose tissue inflammation is associated with age-related brain changes and ischemic brain damage in aged mice. Brain, behavior, and immunity, 50, 221-231. doi: 10.1016/j.bbi.2015.07.008

271 Shmukler, M. (2004). Density of Blood. In The Physics Factbook.

272 Singh, R., Kaushik, S., Wang, Y., Xiang, Y., Novak, I., Komatsu, M., Tanaka, K., Cuervo, A.M., and Czaja, M.J. (2009). Autophagy regulates lipid metabolism. Nature, 458(7242), 1131-1135. doi: 10.1038/nature07976

273 Sitnick, M.T., Basantani, M.K., Cai, L., Schoiswohl, G., Yazbeck, C.F., Distefano, G., Ritov, V., DeLany, J.P., Schreiber, R., Stolz, D.B., Gardner, N.P., Kienesberger, P.C., Pulinilkunnil, T., Zechner, R., Goodpaster, B.H., Coen, P., and Kershaw, E.E. (2013). Skeletal muscle triacylglycerol hydrolysis does not influence metabolic complications of obesity. Diabetes, 62(10), 3350-3361. doi: 10.2337/db13-0500

274 Skavdahl, M., Steenbergen, C., Clark, J., Myers, P., Demianenko, T., Mao, L., Rockman, H.A., Korach, K.S., and Murphy, E. (2005). Estrogen receptor-beta mediates male-female differences in the development of pressure overload hypertrophy. American journal of physiology Heart and circulatory physiology, 288(2), H469-476. doi: 10.1152/ajpheart.00723.2004

275 Smorlesi, A., Frontini, A., Giordano, A., and Cinti, S. (2012). The adipose organ: white-brown adipocyte plasticity and metabolic inflammation. Obesity reviews : an official journal of the International Association for the Study of Obesity, 13 Suppl 2, 83-96. doi: 10.1111/j.1467-789X.2012.01039.x

276 Snijder, M.B., Dekker, J.M., Visser, M., Bouter, L.M., Stehouwer, C.D., Kostense, P.J., Yudkin, J.S., Heine, R.J., Nijpels, G., and Seidell, J.C. (2003). Associations of hip and thigh circumferences independent of waist circumference with the incidence of type 2 diabetes: the Hoorn Study. The American journal of clinical nutrition, 77(5), 1192-1197.

277 Song, W., Wang, H., and Wu, Q. (2015). Atrial natriuretic peptide in cardiovascular biology and disease (NPPA). Gene, 569(1), 1-6. doi: 10.1016/j.gene.2015.06.029

278 Soni, K.G., Mardones, G.A., Sougrat, R., Smirnova, E., Jackson, C.L., and Bonifacino, J.S. (2009). Coatomer-dependent protein delivery to lipid droplets. Journal of cell science, 122(Pt 11), 1834-1841. doi: 10.1242/jcs.045849

279 Souza, S.C., Chau, M.D., Yang, Q., Gauthier, M.S., Clairmont, K.B., Wu, Z., Gromada, J., and Dole, W.P. (2011). Atrial natriuretic peptide regulates lipid mobilization and oxygen consumption in human adipocytes by activating AMPK. Biochemical and biophysical research communications, 410(3), 398-403. doi: 10.1016/j.bbrc.2011.05.143

280 Spinale, F.G. (2007). Myocardial matrix remodeling and the matrix metalloproteinases: influence on cardiac form and function. Physiological reviews, 87(4), 1285-1342. doi: 10.1152/physrev.00012.2007

281 Stanley, W.C., Recchia, F.A., and Lopaschuk, G.D. (2005). Myocardial substrate metabolism in the normal and failing heart. Physiological reviews, 85(3), 1093-1129. doi: 10.1152/physrev.00006.2004

282 Strayer, D., Belcher, M., Dawson, T., Delaney, B., Fine, J., Flickinger, B., Friedman, P., Heckel, C., Hughes, J., Kincs, F., Liu, L., McBrayer, T., McCaskill, D., McNeill, G., Nugent, M., Paladini, E., Rosegrant, P., Tiffany, T., Wainwright, B., and Wilken, J. (2006). Food fats and oils. (Washington (DC): Institute of Shortening and Edible Oils).

283 Sudoh, T., Kangawa, K., Minamino, N., and Matsuo, H. (1988). A new natriuretic peptide in porcine brain. Nature, 332(6159), 78-81. doi: 10.1038/332078a0

284 Sudoh, T., Minamino, N., Kangawa, K., and Matsuo, H. (1990). C-type natriuretic peptide (CNP): a new member of natriuretic peptide family identified in porcine brain. Biochemical and biophysical research communications, 168(2), 863-870.

285 Szabo, T., Postrach, E., Mahler, A., Kung, T., Turhan, G., von Haehling, S., Anker, S.D., Boschmann, M., and Doehner, W. (2013). Increased catabolic activity in adipose tissue of patients with chronic heart failure. European journal of heart failure, 15(10), 1131-1137. doi: 10.1093/eurjhf/hft067

286 Taegtmeyer, H. (2000). Metabolism--the lost child of cardiology. Journal of the American College of Cardiology, 36(4), 1386-1388.

287 Tamura, N., Ogawa, Y., Chusho, H., Nakamura, K., Nakao, K., Suda, M., Kasahara, M., Hashimoto, R., Katsuura, G., Mukoyama, M., Itoh, H., Saito, Y., Tanaka, I., Otani, H., and Katsuki, M. (2000). Cardiac fibrosis in mice lacking brain natriuretic peptide. Proc Natl Acad Sci U S A, 97(8), 4239-4244. doi: 10.1073/pnas.070371497

288 Tanko, L.B., Bagger, Y.Z., Alexandersen, P., Larsen, P.J., and Christiansen, C. (2003). Peripheral adiposity exhibits an independent dominant antiatherogenic effect in elderly women. Circulation, 107(12), 1626-1631. doi: 10.1161/01.cir.0000057974.74060.68

289 Tardiff, J.C., Hewett, T.E., Factor, S.M., Vikstrom, K.L., Robbins, J., and Leinwand, L.A. (2000). Expression of the beta (slow)-isoform of MHC in the adult mouse heart causes dominant-negative functional effects. American journal of physiology Heart and circulatory physiology, 278(2), H412-419.

290 Tarnavski, O., McMullen, J.R., Schinke, M., Nie, Q., Kong, S., and Izumo, S. (2004). Mouse cardiac surgery: comprehensive techniques for the generation of mouse models of human diseases and their application for genomic studies. Physiological genomics, 16(3), 349-360. doi: 10.1152/physiolgenomics.00041.2003

291 Taschler, U., Radner, F.P., Heier, C., Schreiber, R., Schweiger, M., Schoiswohl, G., Preiss-Landl, K., Jaeger, D., Reiter, B., Koefeler, H.C., Wojciechowski, J., Theussl, C., Penninger, J.M., Lass, A., Haemmerle, G., Zechner, R., and Zimmermann, R. (2011). Monoglyceride lipase deficiency in mice impairs lipolysis and attenuates diet-induced insulin resistance. The Journal of biological chemistry, 286(20), 17467-17477. doi: 10.1074/jbc.M110.215434

292 Teres, S., Barcelo-Coblijn, G., Benet, M., Alvarez, R., Bressani, R., Halver, J.E., and Escriba, P.V. (2008). Oleic acid content is responsible for the reduction in blood pressure induced by olive oil. Proc Natl Acad Sci U S A, 105(37), 13811-13816. doi: 10.1073/pnas.0807500105

293 Ueland, T., Gullestad, L., Nymo, S.H., Yndestad, A., Aukrust, P., and Askevold, E.T. (2015). Inflammatory cytokines as biomarkers in heart failure. Clinica chimica acta; international journal of clinical chemistry, 443, 71-77. doi: 10.1016/j.cca.2014.09.001

294 Uriel, N., Naka, Y., Colombo, P.C., Farr, M., Pak, S.W., Cotarlan, V., Albu, J.B., Gallagher, D., Mancini, D., Ginsberg, H.N., and Jorde, U.P. (2011). Improved diabetic control in advanced heart failure patients treated with left ventricular assist devices. European journal of heart failure, 13(2), 195-199. doi: 10.1093/eurjhf/hfq204

295 Urs, S., Harrington, A., Liaw, L., and Small, D. (2006). Selective expression of an aP2/Fatty Acid Binding Protein 4-Cre transgene in non-adipogenic tissues during embryonic development. Transgenic research, 15(5), 647-653. doi: 10.1007/s11248-006-9000-z

296 van Eickels, M., Grohe, C., Cleutjens, J.P., Janssen, B.J., Wellens, H.J., and Doevendans, P.A. (2001). 17beta-estradiol attenuates the development of pressure-overload hypertrophy. Circulation, 104(12), 1419-1423.

297 Velez, M., Kohli, S., and Sabbah, H.N. (2014). Animal models of insulin resistance and heart failure. Heart failure reviews, 19(1), 1-13. doi: 10.1007/s10741-013-9387-6

298 Verdecchia, P., Carini, G., Circo, A., Dovellini, E., Giovannini, E., Lombardo, M., Solinas, P., Gorini, M., and Maggioni, A.P. (2001). Left ventricular mass and

cardiovascular morbidity in essential hypertension: the MAVI study. Journal of the American College of Cardiology, 38(7), 1829-1835.

299 Villena, J.A., Roy, S., Sarkadi-Nagy, E., Kim, K.H., and Sul, H.S. (2004). Desnutrin, an adipocyte gene encoding a novel patatin domain-containing protein, is induced by fasting and glucocorticoids: ectopic expression of desnutrin increases triglyceride hydrolysis. The Journal of biological chemistry, 279(45), 47066-47075. doi: 10.1074/jbc.M403855200

300 Wang, H., Hu, L., Dalen, K., Dorward, H., Marcinkiewicz, A., Russell, D., Gong, D., Londos, C., Yamaguchi, T., Holm, C., Rizzo, M.A., Brasaemle, D., and Sztalryd, C. (2009a). Activation of hormone-sensitive lipase requires two steps, protein phosphorylation and binding to the PAT-1 domain of lipid droplet coat proteins. The Journal of biological chemistry, 284(46), 32116-32125. doi: 10.1074/jbc.M109.006726

301 Wang, S., Soni, K.G., Semache, M., Casavant, S., Fortier, M., Pan, L., and Mitchell, G.A. (2008). Lipolysis and the integrated physiology of lipid energy metabolism. Molecular genetics and metabolism, 95(3), 117-126. doi: 10.1016/j.ymgme.2008.06.012

302 Wang, T.J., Larson, M.G., Levy, D., Benjamin, E.J., Leip, E.P., Wilson, P.W., and Vasan, R.S. (2004). Impact of obesity on plasma natriuretic peptide levels. Circulation, 109(5), 594-600. doi: 10.1161/01.cir.0000112582.16683.ea

303 Wang, X., McLennan, S.V., Allen, T.J., Tsoutsman, T., Semsarian, C., and Twigg, S.M. (2009b). Adverse effects of high glucose and free fatty acid on cardiomyocytes are mediated by connective tissue growth factor. American journal of physiology Cell physiology, 297(6), C1490-1500. doi: 10.1152/ajpcell.00049.2009

304 Wang, Z.V., Li, D.L., and Hill, J.A. (2014). Heart failure and loss of metabolic control. Journal of cardiovascular pharmacology, 63(4), 302-313. doi: 10.1097/fjc.0000000000000054

305 Wende, A.R., and Abel, E.D. (2010). Lipotoxicity in the heart. Biochimica et biophysica acta, 1801(3), 311-319. doi: 10.1016/j.bbalip.2009.09.023

306 Westerhof, N., and O'Rourke, M.F. (1995). Haemodynamic basis for the development of left ventricular failure in systolic hypertension and for its logical therapy. Journal of hypertension, 13(9), 943-952.

307 Westphal, C., Schubert, C., Prelle, K., Penkalla, A., Fliegner, D., Petrov, G., and Regitz-Zagrosek, V. (2012). Effects of estrogen, an ERalpha agonist and raloxifene on pressure overload induced cardiac hypertrophy. PLoS One, 7(12), e50802. doi: 10.1371/journal.pone.0050802

308 White, U.A., and Tchoukalova, Y.D. (2014). Sex dimorphism and depot differences in adipose tissue function. Biochimica et biophysica acta, 1842(3), 377-392. doi: 10.1016/j.bbadis.2013.05.006

309 WHO, W.H.O. (2003). Diet, nutrition and the prevention of chronic diseases. In Technical Report Series 916, WHO, ed. (Geneva), pp. p 1–104.

310 Wilson, P.A., Gardner, S.D., Lambie, N.M., Commans, S.A., and Crowther, D.J. (2006). Characterization of the human patatin-like phospholipase family. Journal of lipid research, 47(9), 1940-1949. doi: 10.1194/jlr.M600185-JLR200

311 Wu, J.W., Wang, S.P., Alvarez, F., Casavant, S., Gauthier, N., Abed, L., Soni, K.G., Yang, G., and Mitchell, G.A. (2011). Deficiency of liver adipose triglyceride lipase in mice causes progressive hepatic steatosis. Hepatology (Baltimore, Md), 54(1), 122-132. doi: 10.1002/hep.24338

312 Wu, J.W., Wang, S.P., Casavant, S., Moreau, A., Yang, G.S., and Mitchell, G.A. (2012). Fasting energy homeostasis in mice with adipose deficiency of desnutrin/adipose triglyceride lipase. Endocrinology, 153(5), 2198-2207. doi: 10.1210/en.2011-1518

313 Wu, K.C., Weiss, R.G., Thiemann, D.R., Kitagawa, K., Schmidt, A., Dalal, D., Lai, S., Bluemke, D.A., Gerstenblith, G., Marban, E., Tomaselli, G.F., and Lima, J.A. (2008). Late gadolinium enhancement by cardiovascular magnetic resonance heralds an adverse prognosis in nonischemic cardiomyopathy. Journal of the American College of Cardiology, 51(25), 2414-2421. doi: 10.1016/j.jacc.2008.03.018

314 Yang, X., Lu, X., Lombes, M., Rha, G.B., Chi, Y.I., Guerin, T.M., Smart, E.J., and Liu, J. (2010). The G(0)/G(1) switch gene 2 regulates adipose lipolysis through association with adipose triglyceride lipase. Cell metabolism, 11(3), 194-205. doi: 10.1016/j.cmet.2010.02.003

315 Yasue, H., Yoshimura, M., Sumida, H., Kikuta, K., Kugiyama, K., Jougasaki, M., Ogawa, H., Okumura, K., Mukoyama, M., and Nakao, K. (1994). Localization and mechanism of secretion of B-type natriuretic peptide in comparison with those of A-type natriuretic peptide in normal subjects and patients with heart failure. Circulation, 90(1), 195-203.

316 Yazaki, Y., Isobe, M., Takahashi, W., Kitabayashi, H., Nishiyama, O., Sekiguchi, M., and Takemura, T. (1999). Assessment of myocardial fatty acid metabolic abnormalities in patients with idiopathic dilated cardiomyopathy using 123I BMIPP SPECT: correlation with clinicopathological findings and clinical course. Heart (British Cardiac Society), 81(2), 153-159.

317 Yoshimura, M., Yasue, H., Okumura, K., Ogawa, H., Jougasaki, M., Mukoyama, M., Nakao, K., and Imura, H. (1993). Different secretion patterns of atrial natriuretic peptide and brain natriuretic peptide in patients with congestive heart failure. Circulation, 87(2), 464-469.

318 Young, S.G., and Zechner, R. (2013). Biochemistry and pathophysiology of intravascular and intracellular lipolysis. Genes & development, 27(5), 459-484. doi: 10.1101/gad.209296.112

319 Zaphiriou, A., Robb, S., Murray-Thomas, T., Mendez, G., Fox, K., McDonagh, T., Hardman, S.M., Dargie, H.J., and Cowie, M.R. (2005). The diagnostic accuracy of plasma BNP and NTproBNP in patients referred from primary care with suspected heart failure: results of the UK natriuretic peptide study. European journal of heart failure, 7(4), 537-541. doi: 10.1016/j.ejheart.2005.01.022

320 Zechner, R., Zimmermann, R., Eichmann, T.O., Kohlwein, S.D., Haemmerle, G., Lass, A., and Madeo, F. (2012). FAT SIGNALS--lipases and lipolysis in lipid metabolism and signaling. Cell metabolism, 15(3), 279-291. doi: 10.1016/j.cmet.2011.12.018

321 Zhabyeyev, P., Gandhi, M., Mori, J., Basu, R., Kassiri, Z., Clanachan, A., Lopaschuk, G.D., and Oudit, G.Y. (2013). Pressure-overload-induced heart failure induces a selective reduction in glucose oxidation at physiological afterload. Cardiovascular research, 97(4), 676-685. doi: 10.1093/cvr/cvs424

322 Zhang, J., Wang, Y., Gao, Z., Yun, Z., and Ye, J. (2012). Hypoxia-inducible factor 1 activation from adipose protein 2-cre mediated knockout of von Hippel-Lindau gene leads to embryonic lethality. Clinical and experimental pharmacology & physiology, 39(2), 145-150. doi: 10.1111/j.1440-1681.2011.05656.x

323 Zhao, Y.F., Feng, D.D., and Chen, C. (2006). Contribution of adipocyte-derived factors to beta-cell dysfunction in diabetes. The international journal of biochemistry & cell biology, 38(5-6), 804-819. doi: 10.1016/j.biocel.2005.11.008

324 Zhou, L., Huang, H., Yuan, C.L., Keung, W., Lopaschuk, G.D., and Stanley, W.C. (2008). Metabolic response to an acute jump in cardiac workload: effects on malonyl-CoA, mechanical efficiency, and fatty acid oxidation. American journal of physiology Heart and circulatory physiology, 294(2), H954-960. doi: 10.1152/ajpheart.00557.2007

325 Zimmermann, R., Strauss, J.G., Haemmerle, G., Schoiswohl, G., Birner-Gruenberger, R., Riederer, M., Lass, A., Neuberger, G., Eisenhaber, F., Hermetter, A., and Zechner, R. (2004). Fat mobilization in adipose tissue is promoted by adipose triglyceride lipase. Science, 306(5700), 1383-1386. doi: 10.1126/science.1100747

326 Zugck, C. (2013). Versorgungsrealität in Deutschland: Wird die Herzfrequenz bei chronischer systolischer Herzinsuffizienz ausreichend gesenkt?, DGK, ed. (Düsseldorf: DEUTSCHE GESELLSCHAFT FÜR KARDIOLOGIE – HERZ- UND KREISLAUFFORSCHUNG e.V. German Cardiac Society), pp. 2.

8 Affidavit

“I, Janek Salatzki, certify under penalty of perjury by my own signature that I have submitted the thesis on the topic ***“Influence of Adipose tissue-specific Adipose Triglyceride Lipase on the Development of Heart Failure”*** I wrote this thesis independently and without assistance from third parties, I used no other aids than the listed sources and resources.

All points based literally or in spirit on publications or presentations of other authors are, as such, in proper citations (see "uniform requirements for manuscripts (URM)" the ICMJE www.icmje.org) indicated. The sections on methodology (in particular practical work, laboratory requirements, statistical processing) and results (in particular images, graphics and tables) correspond to the URM (s.o) and are answered by me. My interest in any publications to this dissertation correspond to those that are specified in the following joint declaration with the responsible person and supervisor. All publications resulting from this thesis and which I am author correspond to the URM (see above) and I am solely responsible.

The importance of this affidavit and the criminal consequences of a false affidavit (section 156,161 of the Criminal Code) are known to me and I understand the rights and responsibilities stated therein.”

6 January 2018 Signature

9 Declaration of any eventual publications

Janek Salatzki had the following share in the following publications:

Grune J, Benz V, Brix S, **Salatzki J**, Blumrich A, Höft B, Klopfleisch R, Foryst-Ludwig A, Kolkhof P, Kintscher U. Steroidal and Nonsteroidal Mineralocorticoid Receptor Antagonists Cause Differential Cardiac Gene Expression in Pressure Overload-Induced Cardiac Hypertrophy. *J Cardiovasc Pharmacol.* 2016 May;67(5):402-11. doi: 10.1097/FJC.0000000000000366.

Contribution in detail (please briefly explain): Performing animal experiments

Foryst-Ludwig A, Kreissl MC, Benz V, Brix S, Smeir E, Ban Z, Januszewicz E, **Salatzki J**, Grune J, Schwanstecher AK, Blumrich A, Schirbel A, Klopfleisch R, Rothe M, Blume K, Halle M, Wolfarth B, Kershaw EE, Kintscher U. Adipose Tissue Lipolysis Promotes Exercise-Induced Cardiac Hypertrophy Involving the Lipokine C16:1n7-Palmitoleate. *J Biol Chem.* 2015 Sep 25;290(39):23603-15.

Contribution in detail (please briefly explain): Performing animal experiments

Signature, date and stamp of the supervising University teacher

_____

Signature of the doctoral candidate

_____

10 Curriculum Vitae

“Mein Lebenslauf wird aus datenschutzrechtlichen Gründen in der elektronischen Version meiner Arbeit nicht veröffentlicht.“

11 List of Publications

Publications in Peer-Reviewed Journals

MacIsaac RL, **Salatzki J**, Higgins R, Walters MR, Padmanabhan S, Dominiczak AF, Touyz RM, Dawson J. Allopurinol and Cardiovascular Outcomes in Adults With Hypertension. *Hypertension*. 2016;67:535-540, published online before print January 25 2016

Grune J, Benz V, Brix S, **Salatzki J**, Blumrich A, Höft B, Klopfleisch R, Foryst-Ludwig A, Kolkhof P, Kintscher U. Steroidal and Nonsteroidal Mineralocorticoid Receptor Antagonists Cause Differential Cardiac Gene Expression in Pressure Overload-Induced Cardiac Hypertrophy. *J Cardiovasc Pharmacol.* 2016 May;67(5):402-11. doi: 10.1097/FJC.0000000000000366.

Foryst-Ludwig A, Kreissl MC, Benz V, Brix S, Smeir E, Ban Z, Januszewicz E, **Salatzki J**, Grune J, Schwanstecher AK, Blumrich A, Schirbel A, Klopfleisch R, Rothe M, Blume K, Halle M, Wolfarth B, Kershaw EE, Kintscher U. Adipose Tissue Lipolysis Promotes Exercise-Induced Cardiac Hypertrophy Involving the Lipokine C16:1n7-Palmitoleate. *J Biol Chem.* 2015 Sep 25;290(39):23603-15.

Oral Presentations at Scientific Conferences

05/2015 Diabetes Congress 2015, Berlin, Germany

Poster Presentations at Scientific Conferences

03/2016 German Cardiac Society (DGK), Mannheim, Germany
08/2015 Summer School on Endocrinology, Bregenz, Austria
12/2014 German Hypertension Society (DHL), Berlin, Germany
09/2014 High Blood Pressure Research (HBPR), San Francisco, USA
07/2014 Frontiers in Cardiovascular Biology (FCVB), Barcelona, Spain
05/2013 German Society for Research of Arteriosclerosis (DGFA), Gießen, Germany

Berlin, 6 January 2018

12 Danksagung

An dieser Stelle danke ich ganz besonders Herrn Professor Dr. Ulrich Kintscher. Er hat mir die Möglichkeit gegeben zu diesem sehr spannenden Projekt während meines Medizinstudiums zu promovieren. Die anregenden Diskussionen und seine herausragende fachliche Expertise haben mir sehr geholfen. Er hat es mir zudem ermöglicht, Ergebnisse dieser Arbeit auf internationalen und nationalen Kongressen vorzustellen. Dafür bin ich sehr dankbar.

Ein außerordentlichen Dank geht an Frau PD Dr. Anna Foryst-Ludwig, für Ihre hervorragende Einarbeitung in die Thematik, die exzellente Betreuung bei der Versuchsplanung, ihre Geduld bei den Versuchen, die vielen kritischen Diskussionen zu den Ergebnissen und die moralische Unterstützung über die gesamte Zeit. Beim Anfertigen von Postern und Vorträgen hat Sie mich ebenfalls unterstützt und mir ein fundiertes Feedback bei der Erstellung dieser Arbeit gegeben. Ich habe eine wunderbare Betreuung erfahren dürfen!

Mein besonderer Dank gilt Frau Beata Höft und Frau Christiane Sprang für ihre sehr professionelle Unterstützung bei den TAC-Versuchen, metabolischen Untersuchungen und in vitro Experimenten. Durch ihre Hilfe, Organisation und labortechnische Erfahrung waren viele Versuche leichter durchzuführen und zum Teil erst möglich.

An dieser Stelle möchte ich meinen besonderen Dank an folgende Mitglieder der AG Kintscher ausdrücken: Frau Dr. Verena Benz, Frau Dr. Jana Grune, Frau Sarah Brix, Frau Zsofia Ban, Frau Annelie Blumrich, Frau Dr. Elzbieta Januszewicz und Herrn Patrick Schmerler. Vielen Dank an euch alle für die Unterstützung bei den Experimenten. Ihr habt mich motiviert, habt mit mir diskutiert und mich stets unterstützt. Besonders möchte ich mich für die sehr angenehme Atmosphäre im CCR und im Doktorandenraum bedanken. Vielen Dank für die schönen Erinnerungen an die gemeinsamen Kongressteilnahmen, Staffelläufe und Geburtstagsfeiern. Es war eine schöne und freudige Zeit mit euch!

Weiterhin gilt mein Dank Frau Dr. Daniela Fliegner und Frau Vanessa Riese, die viel Geduld beim Erlernen der TAC und Echokardiographie mit mir hatten.

Vielen Dank an Herrn Professor Dr. Robert Klopfleisch für seine fachliche Expertise und Unterstützung bei den histologischen Untersuchungen sowie Herrn Dr. Michael Rothe von der Firma Lipidomix GmbH für das FA profiling.

Weiterhin möchte ich unseren Kooperationspartnern danken für die Unterstützung bei

der Anfertigung einer gemeinsamen Publikation. Folgende Personen möchte ich namentlich nennen: Herr Dr. Kajetan Bentele und Herr Dr. Dieter Beule im Berlin Institute of Health (BIH), Core Unit Bioinformatics, Frau Professor Dr. Erin Kershaw an der University of Pittsburgh, Herrn Dr. Christian Klose und Herr Dr. Michal Surma von der Firma Lipotype GmbH aus Dresden. Ein besonderer Dank geht an Herrn Professor Dr. Nikolaus Marx an der Uniklinik RWTH Aachen.

Mein größter Dank geht an meine lieben Eltern, welche mich bei meinen Vorhaben immer voll und ganz unterstützen.